

<b>Impact Factor:</b>	<b>ISRA (India) = 6.317</b>	<b>SIS (USA) = 0.912</b>	<b>ICV (Poland) = 6.630</b>
	<b>ISI (Dubai, UAE) = 1.582</b>	<b>РИНЦ (Russia) = 3.939</b>	<b>PIF (India) = 1.940</b>
	<b>GIF (Australia) = 0.564</b>	<b>ESJI (KZ) = 8.771</b>	<b>IBI (India) = 4.260</b>
	<b>JIF = 1.500</b>	<b>SJIF (Morocco) = 7.184</b>	<b>OAJI (USA) = 0.350</b>

SOI: [1.1/TAS](#) DOI: [10.15863/TAS](#)

**International Scientific Journal  
Theoretical & Applied Science**

p-ISSN: 2308-4944 (print) e-ISSN: 2409-0085 (online)

Year: 2022 Issue: 04 Volume: 108

Published: 16.04.2022 <http://T-Science.org>

Issue



Article



**Denis Chemezov**

Vladimir Industrial College

M.Sc.Eng., Corresponding Member of International Academy of Theoretical and Applied Sciences, Lecturer, Russian Federation

<https://orcid.org/0000-0002-2747-552X>

[vic-science@yandex.ru](mailto:vic-science@yandex.ru)

**Agannes Arzikyan**

Vladimir Industrial College

Student, Russian Federation

**Alyona Kozlova**

Vladimir Industrial College

Student, Russian Federation

**Viktoriya Korolyova**

Vladimir Industrial College

Student, Russian Federation

**Dmitriy Satarin**

Vladimir Industrial College

Student, Russian Federation

**Dmitriy Sevrikov**

Vladimir Industrial College

Student, Russian Federation

**Nikolay Kornev**

Vladimir Industrial College

Student, Russian Federation

## REFERENCE DATA OF PRESSURE DISTRIBUTION ON THE SURFACES OF AIRFOILS HAVING THE NAMES BEGINNING WITH THE LETTER G (THE THIRD PART)

**Abstract:** The results of the computer calculation of air flow around the airfoils having the names beginning with the letter G (continuation) are presented in the article. The contours of pressure distribution on the surfaces of the airfoils at the angles of attack of 0, 15 and -15 degrees in conditions of the subsonic airplane flight speed were obtained.

**Key words:** the airfoil, the angle of attack, pressure, the surface.

**Language:** English

**Citation:** Chemezov, D., et al. (2022). Reference data of pressure distribution on the surfaces of airfoils having the names beginning with the letter G (the third part). *ISJ Theoretical & Applied Science*, 04 (108), 401-484.

**Soi:** <http://s-o-i.org/1.1/TAS-04-108-52>    **Doi:** <https://dx.doi.org/10.15863/TAS.2022.04.108.52>

**Scopus ASCC:** 1507.

## Impact Factor:

<b>ISRA (India)</b>	<b>= 6.317</b>	<b>SIS (USA)</b>	<b>= 0.912</b>	<b>ICV (Poland)</b>	<b>= 6.630</b>
<b>ISI (Dubai, UAE)</b>	<b>= 1.582</b>	<b>РИНЦ (Russia)</b>	<b>= 3.939</b>	<b>PIF (India)</b>	<b>= 1.940</b>
<b>GIF (Australia)</b>	<b>= 0.564</b>	<b>ESJI (KZ)</b>	<b>= 8.771</b>	<b>IBI (India)</b>	<b>= 4.260</b>
<b>JIF</b>	<b>= 1.500</b>	<b>SJIF (Morocco)</b>	<b>= 7.184</b>	<b>OAJI (USA)</b>	<b>= 0.350</b>

### Introduction

Creating reference materials that determine the most accurate pressure distribution on the airfoils surfaces is an actual task of the airplane aerodynamics.

### Materials and methods

The study of air flow around the airfoils was carried out in a two-dimensional formulation by means of the computer calculation in the *Comsol Multiphysics* program. The airfoils in the cross section were taken as objects of research [1-21]. In this work,

the airfoils having the names beginning with the letter *G* were adopted. Air flow around the airfoils was carried out at the angles of attack ( $\alpha$ ) of 0, 15 and -15 degrees. Flight speed of the airplane in each case was subsonic. The airplane flight in the atmosphere was carried out under normal weather conditions. The geometric characteristics of the studied airfoils are presented in the Table 1. The geometric shapes of the airfoils in the cross section are presented in the Table 2.

**Table 1. The geometric characteristics of the airfoils.**

Airfoil name	Max. thickness	Max. camber	Leading edge radius	Trailing edge thickness
<i>GOE 529</i>	9.7% at 30.0% of the chord	5.78% at 40.0% of the chord	0.9959%	0.0%
<i>GOE 530</i>	12.89% at 30.0% of the chord	5.08% at 30.0% of the chord	2.3863%	0.0%
<i>GOE 531</i>	13.77% at 19.9% of the chord	14.68% at 49.7% of the chord	3.234%	0.0%
<i>GOE 532</i>	12.5% at 30.0% of the chord	4.84% at 40.0% of the chord	2.007%	0.0%
<i>GOE 533</i>	13.7% at 30.0% of the chord	4.68% at 40.0% of the chord	1.7598%	0.0%
<i>GOE 534</i>	14.1% at 20.1% of the chord	5.21% at 40.0% of the chord	2.6543%	0.0%
<i>GOE 535</i>	16.05% at 20.0% of the chord	5.75% at 50.0% of the chord	3.3279%	0.0%
<i>GOE 54</i>	6.48% at 15.0% of the chord	3.48% at 20.0% of the chord	1.2012%	0.35%
<i>GOE 546</i>	10.4% at 30.0% of the chord	3.57% at 50.0% of the chord	1.0971%	0.0%
<i>GOE 547</i>	10.5% at 30.1% of the chord	4.01% at 50.0% of the chord	1.0282%	0.0%
<i>GOE 548</i>	11.9% at 40.0% of the chord	2.3% at 50.0% of the chord	0.8502%	0.0%
<i>GOE 549</i>	13.85% at 30.0% of the chord	4.68% at 40.0% of the chord	1.0286%	0.0%
<i>GOE 55</i>	6.16% at 15.0% of the chord	2.04% at 20.0% of the chord	1.144%	0.75%
<i>GOE 550</i>	12.95% at 20.0% of the chord	4.28% at 50.0% of the chord	1.5808%	0.0%
<i>GOE 553</i>	13.67% at 30.1% of the chord	4.65% at 40.1% of the chord	1.7941%	0.0%
<i>GOE 559</i>	11.15% at 30.0% of the chord	3.42% at 30.0% of the chord	0.6332%	0.0%
<i>GOE 561</i>	24.94% at 30.0% of the chord	10.24% at 30.0% of the chord	4.5157%	0.0%
<i>GOE 562</i>	14.1% at 30.0% of the chord	6.25% at 30.0% of the chord	1.2279%	0.0%
<i>GOE 563</i>	8.89% at 30.1% of the chord	2.24% at 50.1% of the chord	0.9821%	0.0%
<i>GOE 564</i>	8.2% at 30.0% of the chord	2.67% at 40.0% of the chord	0.8999%	0.0%
<i>GOE 565</i>	8.4% at 30.0% of the chord	2.79% at 50.0% of the chord	0.896%	0.0%
<i>GOE 566</i>	8.65% at 30.0% of the chord	2.55% at 40.0% of the chord	0.9352%	0.0%
<i>GOE 567</i>	14.73% at 30.1% of the chord	5.25% at 50.0% of the chord	1.6871%	0.0%
<i>GOE 57</i>	6.28% at 20.0% of the chord	5.12% at 40.0% of the chord	0.8223%	0.17%
<i>GOE 570</i>	33.7% at 30.0% of the chord	9.68% at 40.0% of the chord	4.8724%	0.0%
<i>GOE 571</i>	24.89% at 30.1% of the chord	9.82% at 30.1% of the chord	3.7648%	0.0%
<i>GOE 572</i>	18.59% at 30.0% of the chord	8.32% at 30.0% of the chord	1.5409%	0.0%
<i>GOE 573</i>	14.1% at 30.0% of the chord	6.48% at 30.0% of the chord	1.2283%	0.0%
<i>GOE 574</i>	10.25% at 30.0% of the chord	4.92% at 30.0% of the chord	0.7081%	0.0%
<i>GOE 575</i>	13.34% at 30.1% of the chord	3.6% at 40.0% of the chord	1.9633%	0.0%
<i>GOE 584</i>	12.7% at 30.0% of the chord	4.95% at 40.0% of the chord	2.057%	0.0%
<i>GOE 585</i>	8.2% at 20.0% of the chord	3.36% at 40.0% of the chord	0.9755%	0.0%
<i>GOE 587</i>	5.8% at 40.0% of the chord	2.96% at 30.0% of the chord	0.5925%	0.0%
<i>GOE 590</i>	5.7% at 30.0% of the chord	4.01% at 30.0% of the chord	0.5821%	0.0%
<i>GOE 591</i>	11.2% at 30.0% of the chord	5.05% at 40.0% of the chord	1.0931%	0.0%
<i>GOE 592</i>	14.25% at 30.0% of the chord	7.49% at 40.0% of the chord	2.3719%	0.0%
<i>GOE 593</i>	11.9% at 30.0% of the chord	4.05% at 40.0% of the chord	1.347%	0.0%
<i>GOE 595</i>	9.55% at 30.0% of the chord	3.02% at 40.0% of the chord	0.7657%	0.0%
<i>GOE 596</i>	9.75% at 30.0% of the chord	4.03% at 40.0% of the chord	1.1826%	0.0%
<i>GOE 598</i>	6.54% at 40.1% of the chord	0.97% at 50.1% of the chord	0.7279%	0.2%
<i>GOE 599</i>	9.97% at 30.2% of the chord	1.52% at 60.1% of the chord	0.8791%	0.35%
<i>GOE 5K</i>	3.7% at 50.0% of the chord	1.53% at 50.0% of the chord	1.6315%	0.0%
<i>GOE 600</i>	13.08% at 30.4% of the chord	1.87% at 50.3% of the chord	1.1948%	0.5%
<i>GOE 601</i>	16.04% at 30.6% of the chord	2.45% at 50.5% of the chord	1.9082%	0.0%
<i>GOE 602</i>	9.95% at 30.0% of the chord	3.48% at 40.0% of the chord	0.8036%	0.0%
<i>GOE 602 MOD,</i>	9.6% at 30.0% of the chord	3.8% at 50.0% of the chord	0.7897%	0.0%
<i>GOE 604</i>	17.75% at 30.2% of the chord	5.35% at 30.2% of the chord	2.262%	0.0%
<i>GOE 610 B</i>	7.79% at 40.0% of the chord	5.3% at 40.0% of the chord	0.9705%	0.0%
<i>GOE 610-B MOD,</i>	7.7% at 30.0% of the chord	5.68% at 40.0% of the chord	0.7301%	0.8%
<i>GOE 611</i>	12.9% at 30.0% of the chord	5.81% at 40.0% of the chord	1.0989%	0.65%
<i>GOE 612</i>	14.98% at 30.1% of the chord	5.0% at 50.1% of the chord	2.1885%	0.0%

**Impact Factor:**

<b>ISRA (India)</b>	<b>= 6.317</b>	<b>SIS (USA)</b>	<b>= 0.912</b>	<b>ICV (Poland)</b>	<b>= 6.630</b>
<b>ISI (Dubai, UAE)</b>	<b>= 1.582</b>	<b>РИНЦ (Russia)</b>	<b>= 3.939</b>	<b>PIF (India)</b>	<b>= 1.940</b>
<b>GIF (Australia)</b>	<b>= 0.564</b>	<b>ESJI (KZ)</b>	<b>= 8.771</b>	<b>IBI (India)</b>	<b>= 4.260</b>
<b>JIF</b>	<b>= 1.500</b>	<b>SJIF (Morocco)</b>	<b>= 7.184</b>	<b>OAJI (USA)</b>	<b>= 0.350</b>

<i>GOE 613</i>	10.3% at 30.0% of the chord	4.1% at 40.0% of the chord	0.9794%	0.0%
<i>GOE 614</i>	18.69% at 30.2% of the chord	6.17% at 40.1% of the chord	2.4776%	0.0%
<i>GOE 615</i>	13.64% at 30.0% of the chord	5.59% at 40.0% of the chord	1.9056%	0.0%
<i>GOE 617</i>	13.85% at 30.0% of the chord	2.17% at 30.0% of the chord	1.5752%	0.0%
<i>GOE 619</i>	13.77% at 20.2% of the chord	4.53% at 50.0% of the chord	1.7645%	0.0%
<i>GOE 620</i>	17.5% at 30.0% of the chord	5.9% at 50.0% of the chord	2.6777%	0.0%
<i>GOE 621</i>	14.98% at 30.1% of the chord	5.0% at 50.1% of the chord	2.1885%	0.0%
<i>GOE 622</i>	8.0% at 30.0% of the chord	2.46% at 40.0% of the chord	0.7301%	0.2%
<i>GOE 623</i>	12.0% at 30.0% of the chord	3.9% at 40.0% of the chord	1.2372%	0.3%
<i>GOE 624</i>	16.0% at 30.0% of the chord	5.3% at 40.0% of the chord	2.2599%	0.5%
<i>GOE 625</i>	20.0% at 30.0% of the chord	6.22% at 40.0% of the chord	3.0637%	0.65%
<i>GOE 626</i>	16.58% at 20.4% of the chord	5.07% at 50.1% of the chord	2.5427%	0.0%
<i>GOE 627</i>	15.75% at 30.0% of the chord	4.07% at 30.0% of the chord	2.0355%	0.0%
<i>GOE 628</i>	16.72% at 20.2% of the chord	5.63% at 40.1% of the chord	2.4925%	0.0%
<i>GOE 629</i>	13.61% at 30.3% of the chord	2.77% at 40.2% of the chord	1.8553%	0.0%
<i>GOE 63</i>	8.25% at 20.0% of the chord	6.69% at 40.0% of the chord	1.6296%	0.7%
<i>GOE 630</i>	12.54% at 30.0% of the chord	7.66% at 40.0% of the chord	1.6226%	0.0%
<i>GOE 632</i>	14.0% at 30.0% of the chord	3.92% at 40.0% of the chord	1.648%	0.0%
<i>GOE 633</i>	13.76% at 20.1% of the chord	3.94% at 40.1% of the chord	1.999%	0.0%
<i>GOE 645</i>	15.47% at 20.2% of the chord	4.81% at 40.1% of the chord	1.9928%	0.0%
<i>GOE 646</i>	18.26% at 30.4% of the chord	4.46% at 50.2% of the chord	3.0229%	0.0%
<i>GOE 647</i>	16.26% at 20.1% of the chord	5.32% at 40.1% of the chord	2.2269%	0.0%
<i>GOE 648</i>	15.13% at 30.2% of the chord	3.9% at 40.2% of the chord	2.0529%	0.0%
<i>GOE 650</i>	13.42% at 20.2% of the chord	4.41% at 50.0% of the chord	1.9734%	0.0%
<i>GOE 652</i>	17.05% at 20.0% of the chord	9.25% at 50.0% of the chord	4.4602%	0.0%
<i>GOE 654</i>	14.5% at 30.0% of the chord	5.2% at 40.0% of the chord	1.6695%	0.0%
<i>GOE 655</i>	13.9% at 30.0% of the chord	4.39% at 40.0% of the chord	1.6224%	0.0%
<i>GOE 670</i>	9.0% at 30.0% of the chord	3.39% at 40.0% of the chord	1.071%	0.0%
<i>GOE 673</i>	10.79% at 30.1% of the chord	2.75% at 50.1% of the chord	0.6887%	0.4%
<i>GOE 675</i>	14.88% at 30.1% of the chord	5.87% at 40.0% of the chord	2.5819%	0.35%
<i>GOE 676 (= M 12)</i>	11.9% at 30.0% of the chord	2.04% at 30.0% of the chord	1.234%	0.3%
<i>GOE 677 (= M 6)</i>	11.95% at 30.0% of the chord	2.29% at 30.0% of the chord	1.2613%	0.4%
<i>GOE 679</i>	18.18% at 30.3% of the chord	4.52% at 40.3% of the chord	3.2925%	0.0%
<i>GOE 681</i>	16.77% at 30.3% of the chord	4.34% at 40.2% of the chord	3.0604%	0.0%
<i>GOE 682</i>	10.65% at 30.0% of the chord	4.33% at 40.0% of the chord	1.2466%	0.0%
<i>GOE 683</i>	19.9% at 30.0% of the chord	2.95% at 30.0% of the chord	2.9142%	0.0%
<i>GOE 685</i>	13.08% at 20.2% of the chord	4.19% at 50.0% of the chord	1.7666%	0.0%
<i>GOE 692</i>	16.1% at 30.0% of the chord	5.1% at 40.0% of the chord	2.267%	0.5%
<i>GOE 693</i>	12.0% at 30.0% of the chord	3.7% at 40.0% of the chord	1.3447%	0.5%
<i>GOE 6K</i>	7.5% at 50.0% of the chord	3.1% at 50.0% of the chord	1.4652%	0.0%
<i>GOE 701</i>	12.44% at 30.1% of the chord	4.87% at 40.0% of the chord	1.6385%	0.0%
<i>GOE 702</i>	16.67% at 20.2% of the chord	5.1% at 40.1% of the chord	2.8796%	0.0%
<i>GOE 703</i>	19.4% at 30.0% of the chord	2.3% at 30.0% of the chord	3.2413%	0.0%
<i>GOE 704</i>	12.94% at 30.1% of the chord	2.13% at 40.1% of the chord	1.2923%	0.55%
<i>GOE 711</i>	14.85% at 30.0% of the chord	6.52% at 40.0% of the chord	1.3998%	1.4%
<i>GOE 723</i>	11.55% at 30.1% of the chord	4.48% at 50.0% of the chord	1.5289%	0.0%
<i>GOE 735</i>	20.1% at 30.0% of the chord	4.38% at 30.0% of the chord	3.0629%	0.0%
<i>GOE 738</i>	15.44% at 30.0% of the chord	2.12% at 30.0% of the chord	2.2738%	0.0%
<i>GOE 741</i>	15.33% at 30.0% of the chord	4.82% at 30.0% of the chord	2.5909%	0.0%
<i>GOE 744</i>	14.48% at 20.0% of the chord	7.02% at 30.0% of the chord	2.6801%	0.0%
<i>GOE 746</i>	9.75% at 30.0% of the chord	5.04% at 30.0% of the chord	0.9139%	0.0%
<i>GOE 758</i>	13.85% at 30.0% of the chord	4.68% at 40.0% of the chord	1.3988%	0.0%
<i>GOE 766</i>	12.01% at 25.0% of the chord	1.48% at 20.0% of the chord	1.8243%	0.0%
<i>GOE 767</i>	12.0% at 20.0% of the chord	1.5% at 20.0% of the chord	2.2866%	0.0%
<i>GOE 769</i>	13.82% at 20.0% of the chord	4.79% at 30.0% of the chord	3.0482%	0.0%
<i>GOE 770</i>	20.99% at 30.0% of the chord	4.04% at 30.0% of the chord	3.2057%	0.26%
<i>GOE 775</i>	21.0% at 30.0% of the chord	0.22% at 100.0% of the chord	4.2502%	0.44%
<i>GOE 776</i>	25.0% at 30.0% of the chord	0.26% at 100.0% of the chord	6.0556%	0.52%
<i>GOE 777</i>	22.0% at 30.0% of the chord	5.96% at 30.0% of the chord	3.5259%	0.26%
<i>GOE 780</i>	12.0% at 50.0% of the chord	1.0% at 40.0% of the chord	0.741%	0.0%
<i>GOE 79 (PFALZ 11)</i>	6.17% at 15.0% of the chord	5.99% at 30.0% of the chord	1.3785%	0.56%
<i>GOE 795</i>	8.01% at 30.9% of the chord	2.45% at 43.5% of the chord	0.5783%	0.0%
<i>GOE 795 smoothed</i>	8.03% at 30.9% of the chord	2.44% at 43.5% of the chord	0.5041%	0.0%
<i>GOE 796</i>	12.0% at 30.0% of the chord	3.69% at 40.0% of the chord	0.893%	0.4%
<i>GOE 797</i>	16.0% at 30.0% of the chord	5.02% at 40.0% of the chord	2.3175%	0.8%
<i>GOE 798</i>	20.0% at 30.0% of the chord	6.18% at 40.0% of the chord	3.6137%	0.75%
<i>GOE 7K</i>	11.0% at 50.0% of the chord	4.54% at 50.0% of the chord	1.4168%	0.0%
<i>GOE 801 (MVA 301)</i>	9.8% at 30.0% of the chord	6.18% at 40.0% of the chord	1.4086%	0.4%
<i>GOE 802</i>	9.8% at 30.0% of the chord	6.18% at 40.0% of the chord	1.4086%	0.4%
<i>GOE 802 A</i>	9.8% at 30.0% of the chord	6.18% at 40.0% of the chord	1.4086%	0.4%

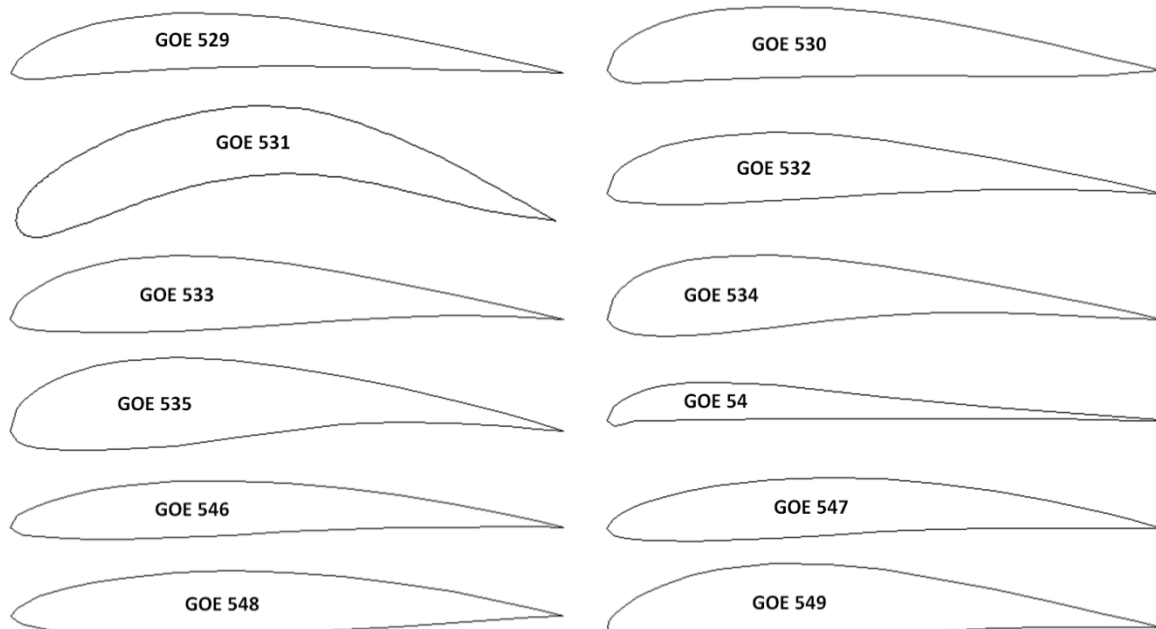
<b>Impact Factor:</b>	<b>ISRA (India) = 6.317</b>	<b>SIS (USA) = 0.912</b>	<b>ICV (Poland) = 6.630</b>
	<b>ISI (Dubai, UAE) = 1.582</b>	<b>РИНЦ (Russia) = 3.939</b>	<b>PIF (India) = 1.940</b>
	<b>GIF (Australia) = 0.564</b>	<b>ESJI (KZ) = 8.771</b>	<b>IBI (India) = 4.260</b>
	<b>JIF = 1.500</b>	<b>SJIF (Morocco) = 7.184</b>	<b>OAJI (USA) = 0.350</b>

<i>GOE 802 B</i>	9.8% at 30.0% of the chord	6.18% at 40.0% of the chord	1.4086%	0.4%
<i>GOE 803 (HACKLINGER)</i>	6.3% at 15.0% of the chord	6.67% at 40.0% of the chord	1.0304%	0.3%
<i>GOE 804 (EA 8)</i>	6.0% at 30.0% of the chord	6.25% at 50.0% of the chord	1.2926%	0.0%
<i>GOE 81</i>	7.43% at 30.0% of the chord	6.3% at 30.0% of the chord	1.0949%	0.27%
<i>GOE 8K</i>	14.85% at 50.0% of the chord	6.13% at 50.0% of the chord	1.6286%	0.0%
<i>GOE 92</i>	8.77% at 30.0% of the chord	5.55% at 30.0% of the chord	0.7373%	0.16%
<i>GOE 9K</i>	2.45% at 50.0% of the chord	0.9% at 60.0% of the chord	1.696%	0.0%
<i>Goldberg G 5</i>	9.49% at 20.0% of the chord	6.88% at 30.0% of the chord	1.532%	0.0%
<i>Goldberg Zipper</i>	9.28% at 30.0% of the chord	6.87% at 40.0% of the chord	1.2337%	0.0%
<i>GOLDBRG6</i>	7.1% at 20.0% of the chord	7.85% at 30.0% of the chord	1.5161%	0.3%
<i>GOO602</i>	10.0% at 30.0% of the chord	2.6% at 0.0% of the chord	0.9596%	0.0%
<i>GOO620M</i>	10.0% at 30.0% of the chord	5.29% at 40.0% of the chord	0.8311%	0.0%
<i>Gottingen 6K</i>	7.5% at 50.0% of the chord	3.1% at 50.0% of the chord	-0.0061%	0.0%
<i>Gottingen 7K</i>	11.0% at 50.0% of the chord	4.54% at 50.0% of the chord	0.2343%	0.0%
<i>Gottingen 8K</i>	14.85% at 50.0% of the chord	6.13% at 50.0% of the chord	0.7591%	0.0%
<i>Grant G10</i>	9.75% at 15.0% of the chord	5.74% at 40.0% of the chord	1.3614%	0.0%
<i>Grant X</i>	13.4% at 20.0% of the chord	5.5% at 30.0% of the chord	1.5875%	0.0%
<i>Grant X-10</i>	9.4% at 20.0% of the chord	3.93% at 40.0% of the chord	0.9466%	0.1%
<i>Grant X-8</i>	11.73% at 20.0% of the chord	4.9% at 40.0% of the chord	1.2909%	0.1%
<i>Grant X-9</i>	10.57% at 20.0% of the chord	4.42% at 40.0% of the chord	1.7342%	0.1%
<i>GRANTG9</i>	10.83% at 15.0% of the chord	6.41% at 30.0% of the chord	1.619%	0.0%
<i>GRANTX12</i>	7.8% at 20.0% of the chord	3.3% at 35.0% of the chord	0.7345%	0.08%
<i>GRANTX14</i>	6.7% at 20.0% of the chord	2.81% at 35.0% of the chord	0.6415%	0.06%
<i>GRANTX16</i>	5.8% at 20.0% of the chord	2.44% at 35.0% of the chord	0.608%	0.06%
<i>Griffith 30% thick symmetrical suction airfoil</i>	30.57% at 49.3% of the chord	0.0% at 0.0% of the chord	3.3846%	0.2%
<i>GRUMMAN K-2</i>	10.28% at 40.8% of the chord	2.45% at 89.6% of the chord	2.9221%	0.1%
<i>GRUMMAN K-3</i>	17.31% at 33.4% of the chord	1.35% at 71.9% of the chord	4.8841%	0.7641%

**Note:**

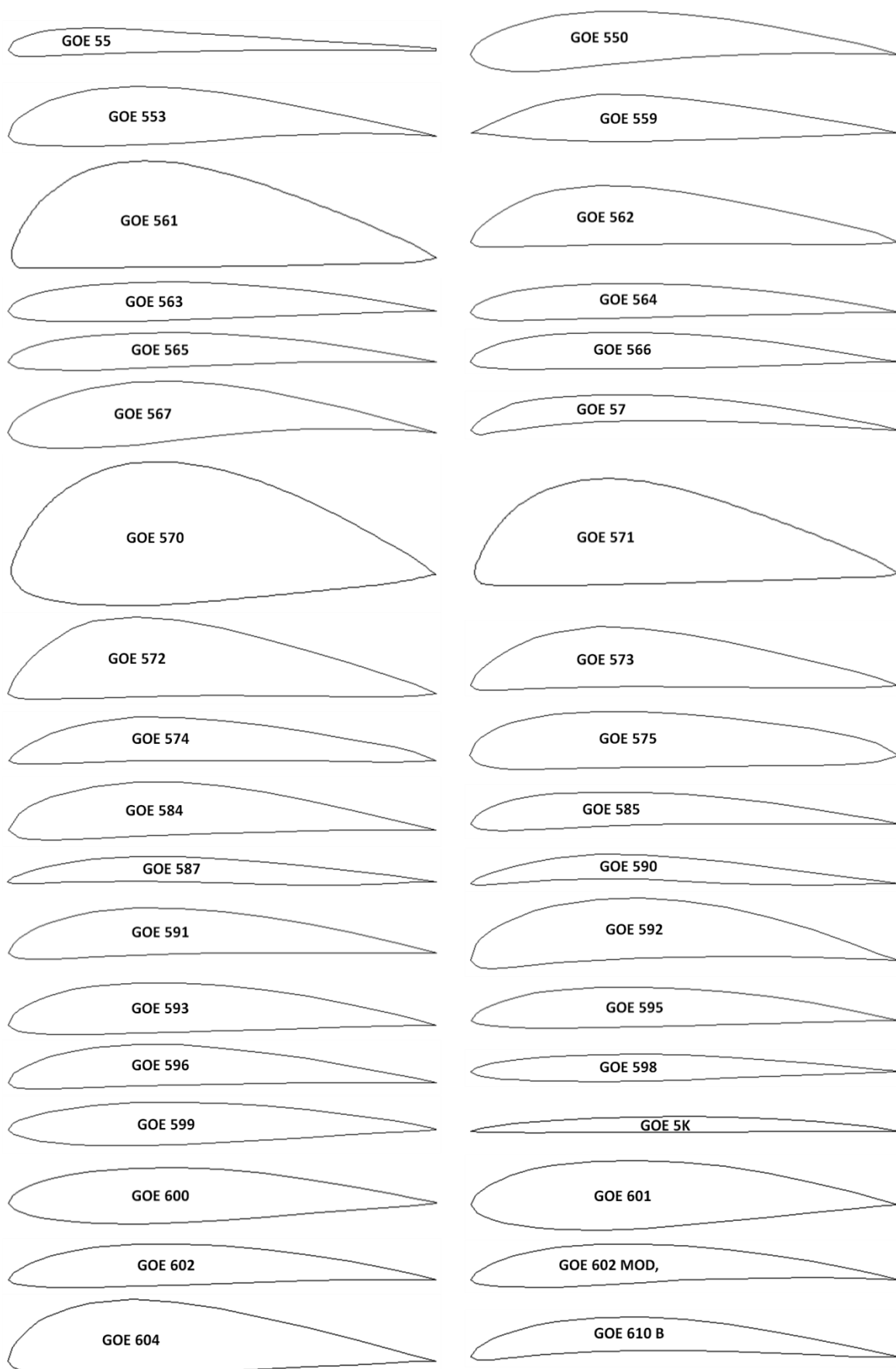
*Goldberg G 5* (C. Goldberg (USA));  
*Goldberg Zipper* (C. Goldberg (USA));  
*Grant G10* (C.H. Grant (USA));  
*Grant X* (C.H. Grant (USA));  
*Grant X-10* (C.H. Grant (USA));  
*Grant X-8* (C.H. Grant (USA));  
*Grant X-9* (C.H. Grant (USA));  
*GRUMMAN K-2* (Grumman K-2 transonic airfoil (GAC .80-.53-10.3)).

**Table 2. The geometric shapes of the airfoils in the cross section.**



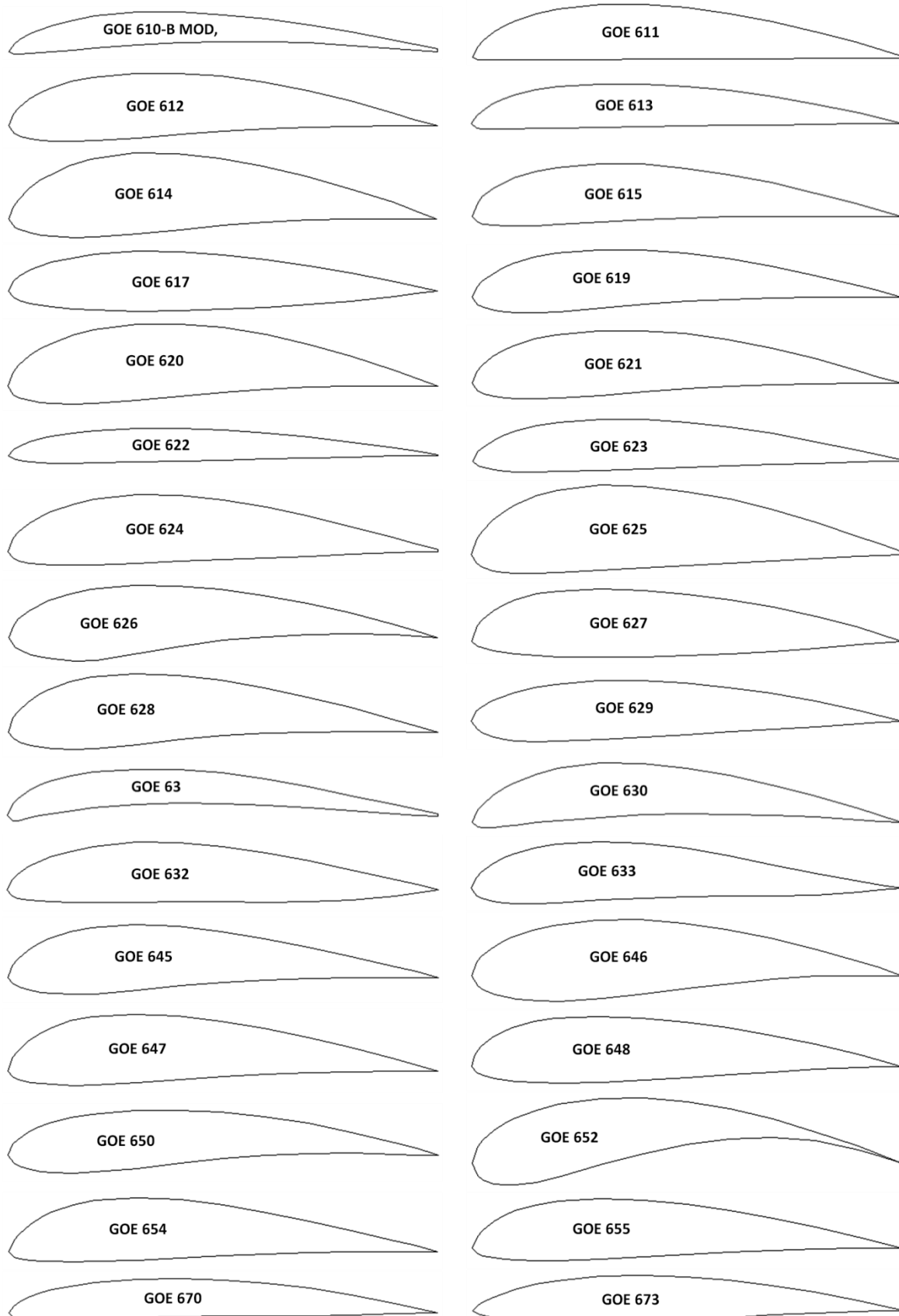
## Impact Factor:

ISRA (India)	= 6.317	SIS (USA)	= 0.912	ICV (Poland)	= 6.630
ISI (Dubai, UAE)	= 1.582	РИНЦ (Russia)	= 3.939	PIF (India)	= 1.940
GIF (Australia)	= 0.564	ESJI (KZ)	= 8.771	IBI (India)	= 4.260
JIF	= 1.500	SJIF (Morocco)	= 7.184	OAJI (USA)	= 0.350



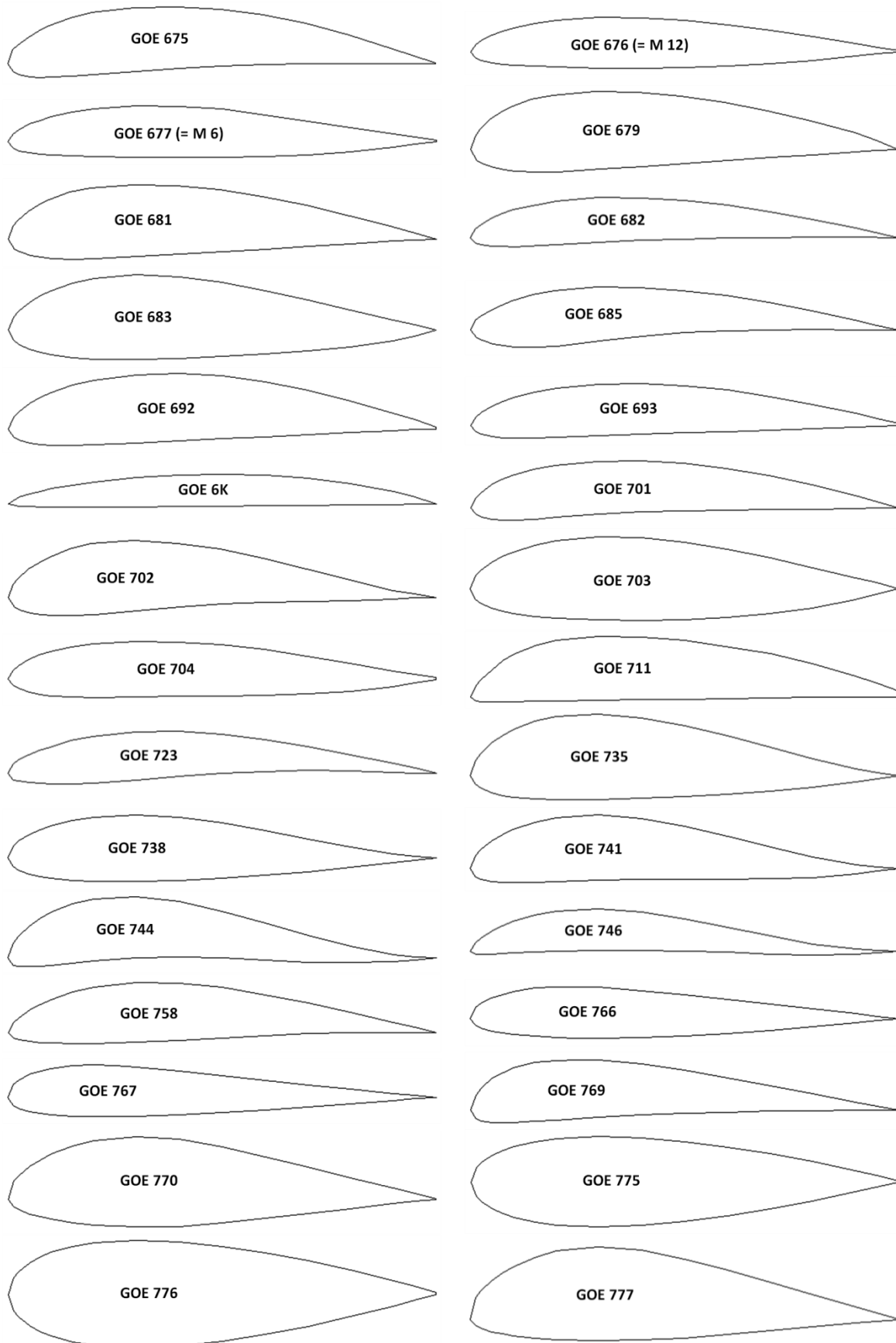
## Impact Factor:

ISRA (India)	= 6.317	SIS (USA)	= 0.912	ICV (Poland)	= 6.630
ISI (Dubai, UAE)	= 1.582	РИНЦ (Russia)	= 3.939	PIF (India)	= 1.940
GIF (Australia)	= 0.564	ESJI (KZ)	= 8.771	IBI (India)	= 4.260
JIF	= 1.500	SJIF (Morocco)	= 7.184	OAJI (USA)	= 0.350



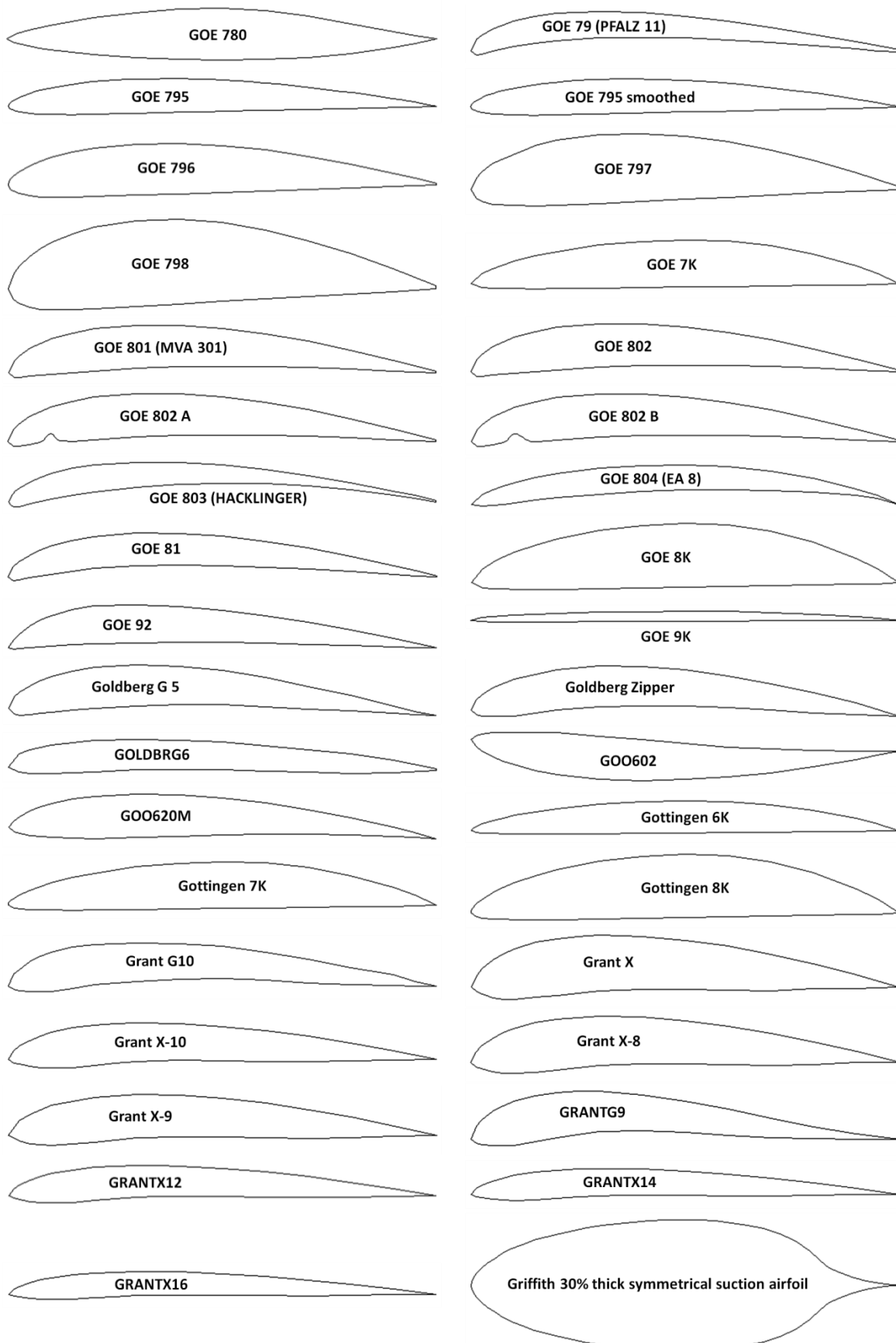
## Impact Factor:

<b>ISRA</b> (India) = <b>6.317</b>	<b>SIS</b> (USA) = <b>0.912</b>	<b>ICV</b> (Poland) = <b>6.630</b>
<b>ISI</b> (Dubai, UAE) = <b>1.582</b>	<b>РИНЦ</b> (Russia) = <b>3.939</b>	<b>PIF</b> (India) = <b>1.940</b>
<b>GIF</b> (Australia) = <b>0.564</b>	<b>ESJI</b> (KZ) = <b>8.771</b>	<b>IBI</b> (India) = <b>4.260</b>
<b>JIF</b> = <b>1.500</b>	<b>SJIF</b> (Morocco) = <b>7.184</b>	<b>OAJI</b> (USA) = <b>0.350</b>



## Impact Factor:

ISRA (India)	= 6.317	SIS (USA)	= 0.912	ICV (Poland)	= 6.630
ISI (Dubai, UAE)	= 1.582	РИНЦ (Russia)	= 3.939	PIF (India)	= 1.940
GIF (Australia)	= 0.564	ESJI (KZ)	= 8.771	IBI (India)	= 4.260
JIF	= 1.500	SJIF (Morocco)	= 7.184	OAJI (USA)	= 0.350



<b>ISRA (India)</b>	<b>= 6.317</b>	<b>SIS (USA)</b>	<b>= 0.912</b>	<b>ICV (Poland)</b>	<b>= 6.630</b>
<b>ISI (Dubai, UAE)</b>	<b>= 1.582</b>	<b>РИНЦ (Russia)</b>	<b>= 3.939</b>	<b>PIF (India)</b>	<b>= 1.940</b>
<b>GIF (Australia)</b>	<b>= 0.564</b>	<b>ESJI (KZ)</b>	<b>= 8.771</b>	<b>IBI (India)</b>	<b>= 4.260</b>
<b>JIF</b>	<b>= 1.500</b>	<b>SJIF (Morocco)</b>	<b>= 7.184</b>	<b>OAJI (USA)</b>	<b>= 0.350</b>



### Results and discussion

The calculated pressure contours on the surfaces of the airfoils at the different angles of attack are presented in the Figs. 1-148. The calculated values on the scale can be represented as the basic values when comparing the pressure drop under conditions of changing the angle of attack of the airfoils.

In this work, 148 airfoils of the GOE, Gottingen, Grant, etc. series were studied. Mostly asymmetrical airfoils in the cross section are presented, but there are also symmetrical airfoils ones (for example, GOE 598, GOE 599, GOE 776 and Griffith 30% thick symmetrical suction airfoil).

Analyzing the results of the study, it was found that during horizontal flight of the airplane with the wing profile of the Griffith 30% thick symmetrical

suction, the drag is 6.92 kPa, which is the maximum value compared to the other wing profiles. The minimum drag (6.42 kPa) is observed on the leading edge of the GOE 9K airfoil. Thus, the difference in positive pressures acting on the leading edge of the considered airfoils is 0.5 kPa.

For the some airfoils (GOE 590, GOE 673, and GOE 804 (EA 8)) high negative pressure on the leading edge occurs at the angle of attack of 15 degrees. Pressure on the leading edge of the airfoils (for example, GOE 548, GOE 533 and GOE 530) does not exceed -100 kPa at the negative angles of attack. The highest drag is determined for the GOE 804 (EA 8) airfoil. The lowest drag is determined for the GOE 559 airfoil.

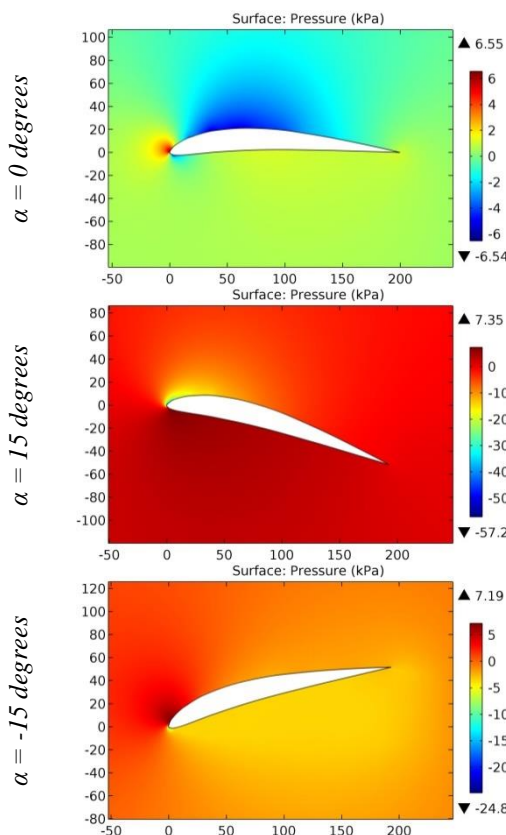
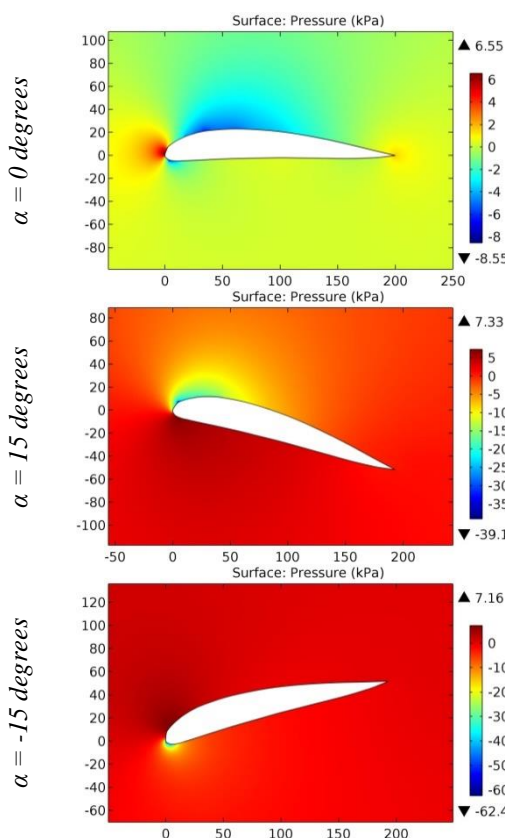
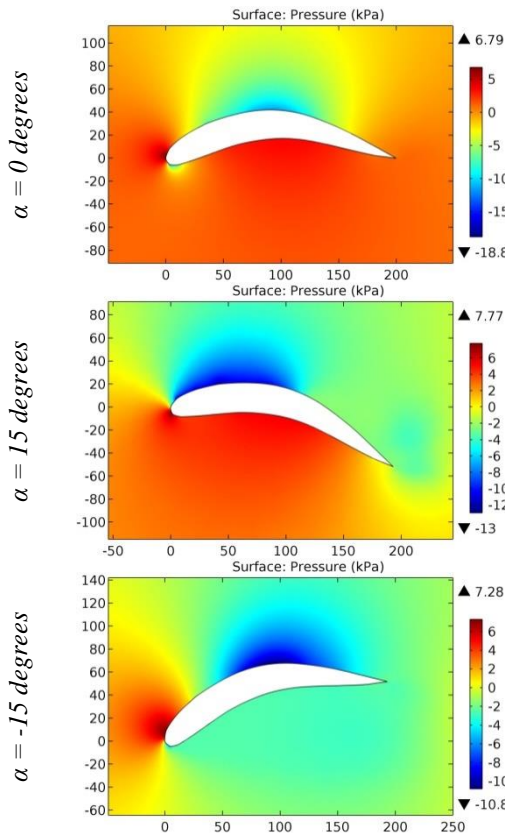


Figure 1. The pressure contours on the surfaces of the GOE 529 airfoil.



**Figure 2.** The pressure contours on the surfaces of the GOE 530 airfoil.



**Figure 3.** The pressure contours on the surfaces of the GOE 531 airfoil.

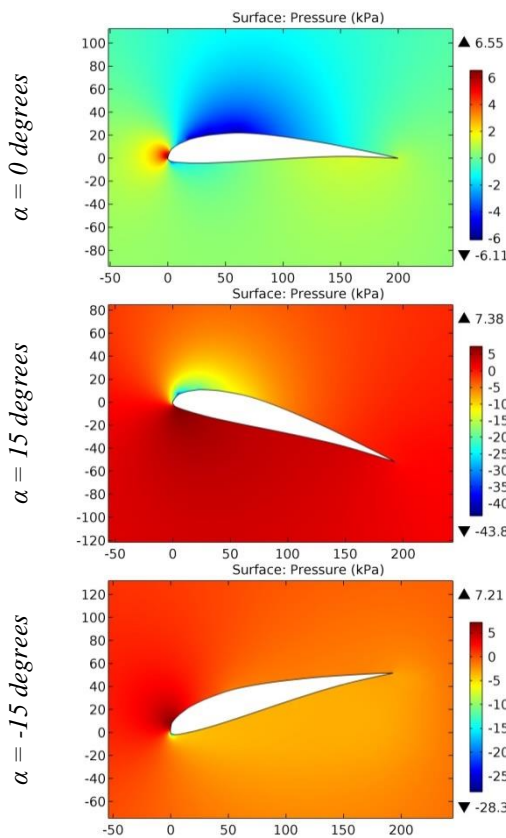


**Figure 4.** The pressure contours on the surfaces of the GOE 532 airfoil.

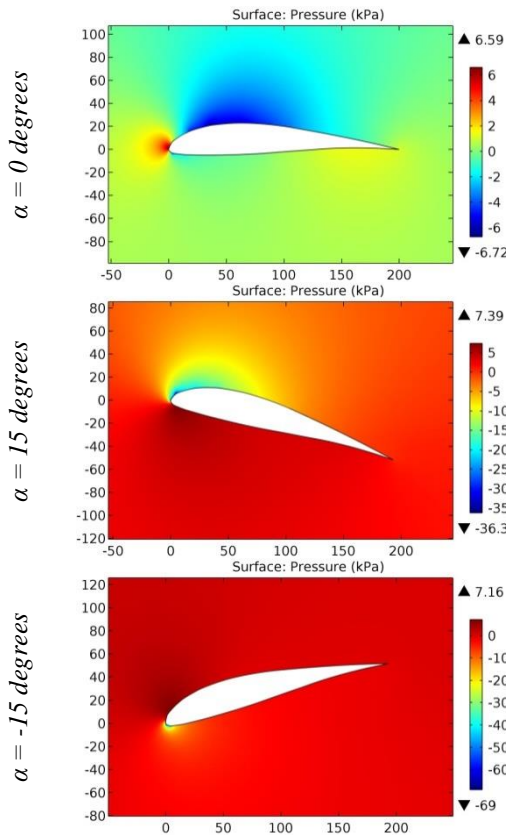


**Figure 5.** The pressure contours on the surfaces of the GOE 533 airfoil.

ISRA (India) = 6.317	SIS (USA) = 0.912	ICV (Poland) = 6.630
ISI (Dubai, UAE) = 1.582	РИНЦ (Russia) = 3.939	PIF (India) = 1.940
GIF (Australia) = 0.564	ESJI (KZ) = 8.771	IBI (India) = 4.260
JIF = 1.500	SJIF (Morocco) = 7.184	OAJI (USA) = 0.350

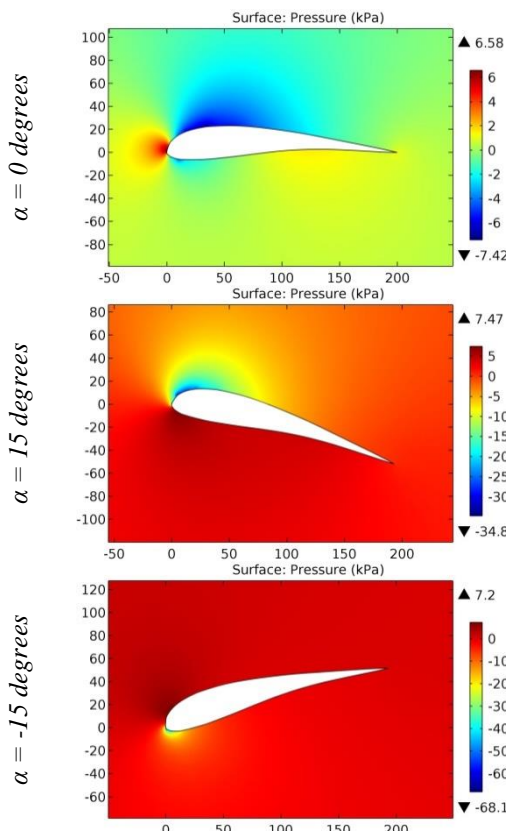


Figure 6. The pressure contours on the surfaces of the GOE 534 airfoil.

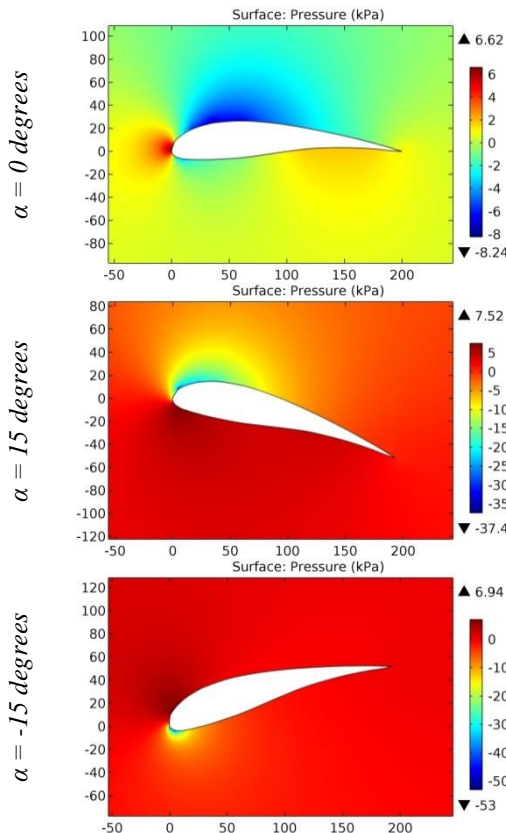
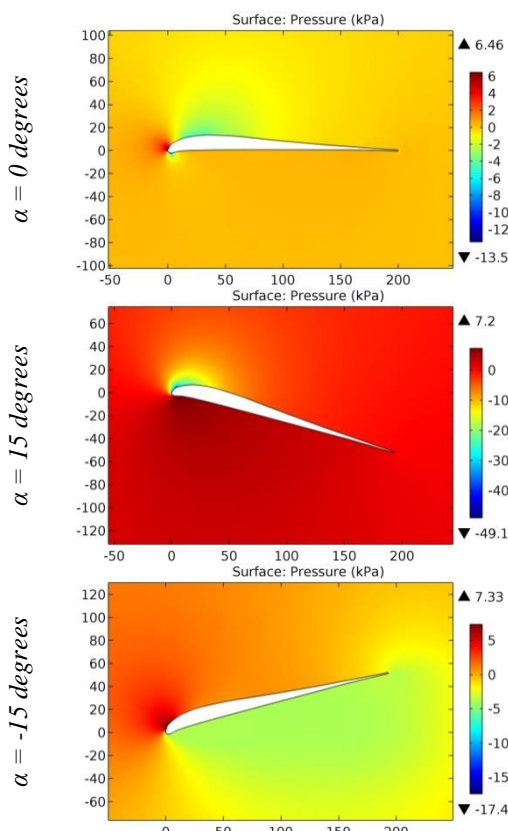
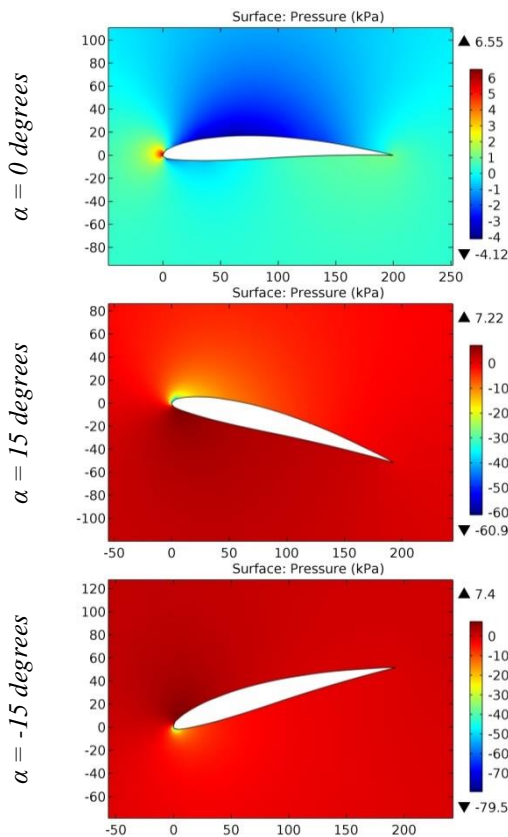


Figure 7. The pressure contours on the surfaces of the GOE 535 airfoil.

ISRA (India) = 6.317	SIS (USA) = 0.912	ICV (Poland) = 6.630
ISI (Dubai, UAE) = 1.582	РИНЦ (Russia) = 3.939	PIF (India) = 1.940
GIF (Australia) = 0.564	ESJI (KZ) = 8.771	IBI (India) = 4.260
JIF = 1.500	SJIF (Morocco) = 7.184	OAJI (USA) = 0.350



**Figure 8.** The pressure contours on the surfaces of the GOE 54 airfoil.



**Figure 9.** The pressure contours on the surfaces of the GOE 546 airfoil.

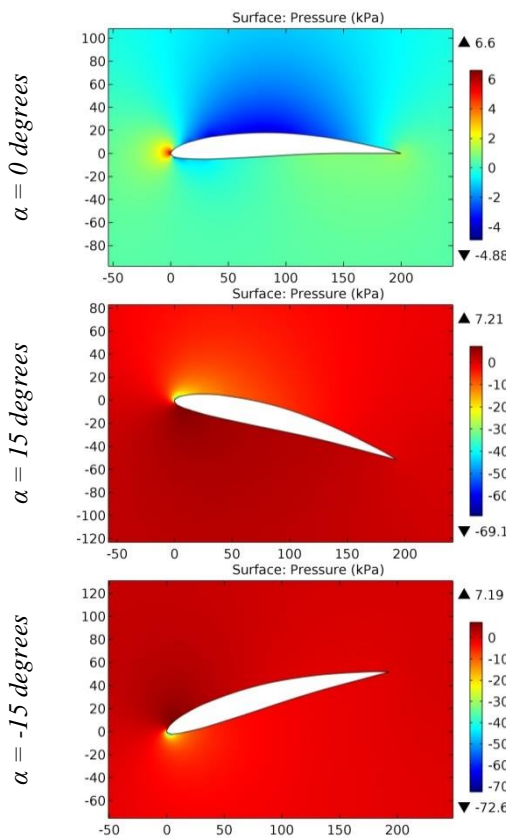


**Figure 10.** The pressure contours on the surfaces of the GOE 547 airfoil.

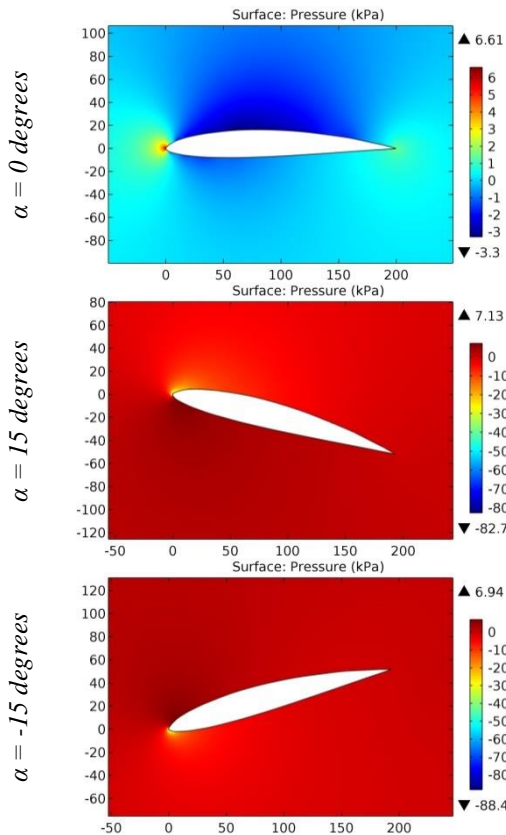


**Figure 11.** The pressure contours on the surfaces of the GOE 548 airfoil.

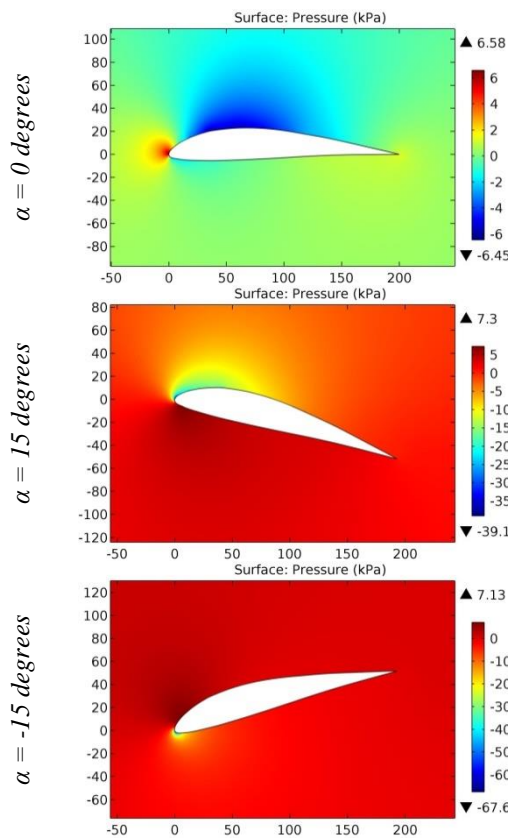


**Figure 12.** The pressure contours on the surfaces of the GOE 549 airfoil.

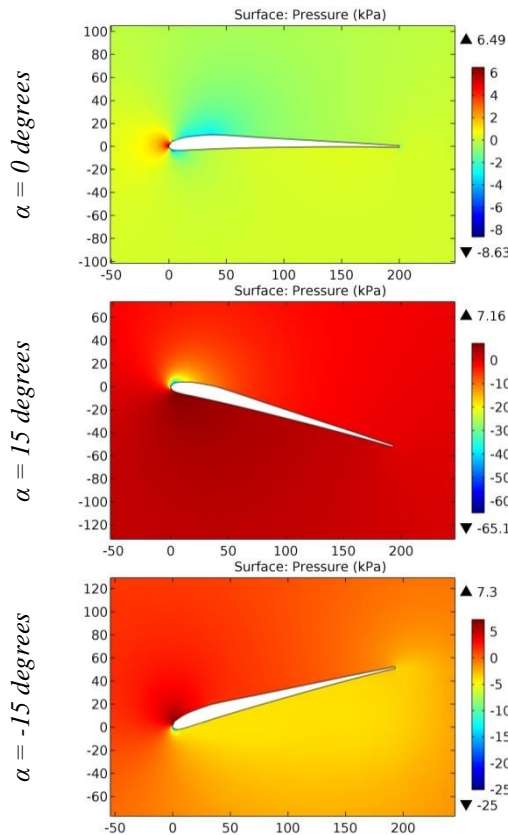


**Figure 13.** The pressure contours on the surfaces of the GOE 55 airfoil.

## Impact Factor:

<b>ISRA (India)</b>	= <b>6.317</b>	<b>SIS (USA)</b>	= <b>0.912</b>	<b>ICV (Poland)</b>	= <b>6.630</b>
<b>ISI (Dubai, UAE)</b>	= <b>1.582</b>	<b>РИНЦ (Russia)</b>	= <b>3.939</b>	<b>PIF (India)</b>	= <b>1.940</b>
<b>GIF (Australia)</b>	= <b>0.564</b>	<b>ESJI (KZ)</b>	= <b>8.771</b>	<b>IBI (India)</b>	= <b>4.260</b>
<b>JIF</b>	= <b>1.500</b>	<b>SJIF (Morocco)</b>	= <b>7.184</b>	<b>OAJI (USA)</b>	= <b>0.350</b>

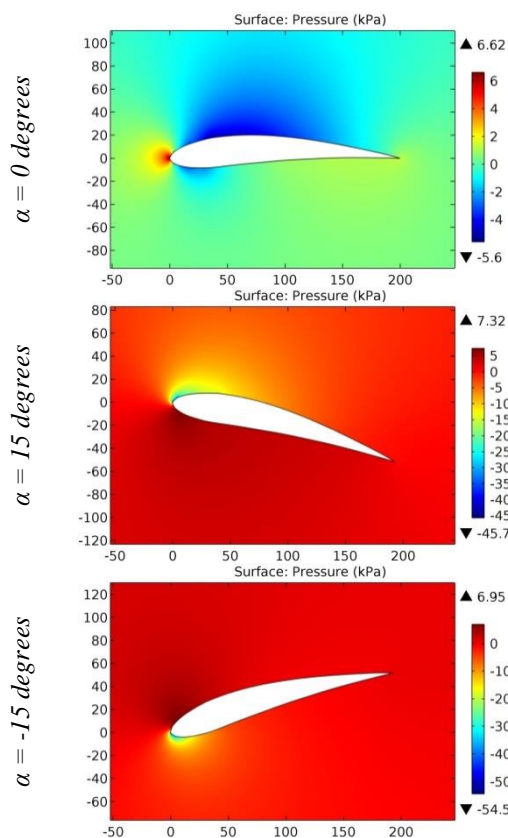


Figure 14. The pressure contours on the surfaces of the GOE 550 airfoil.

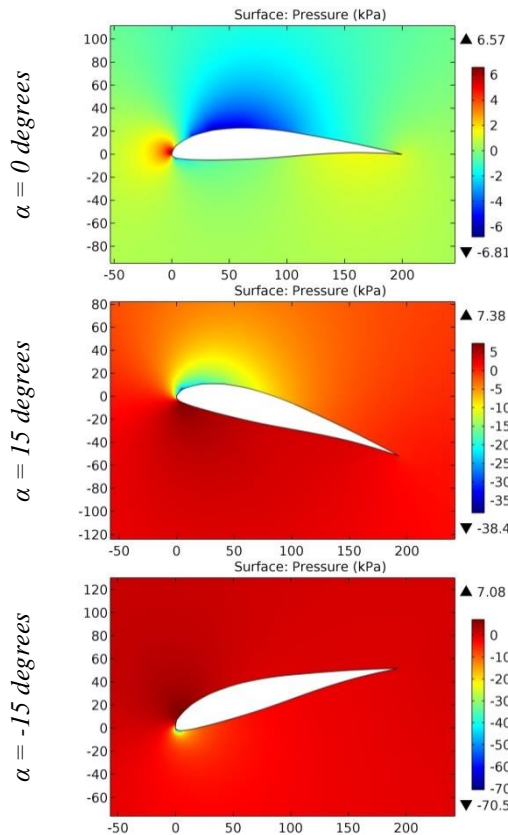
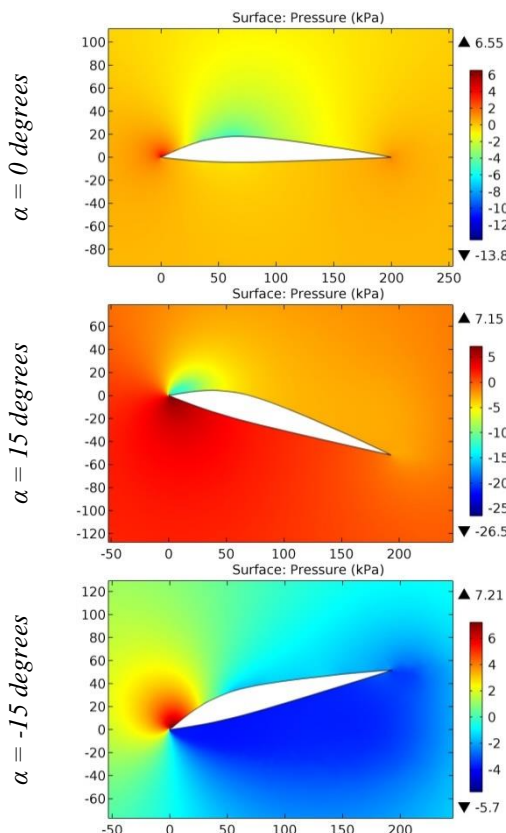
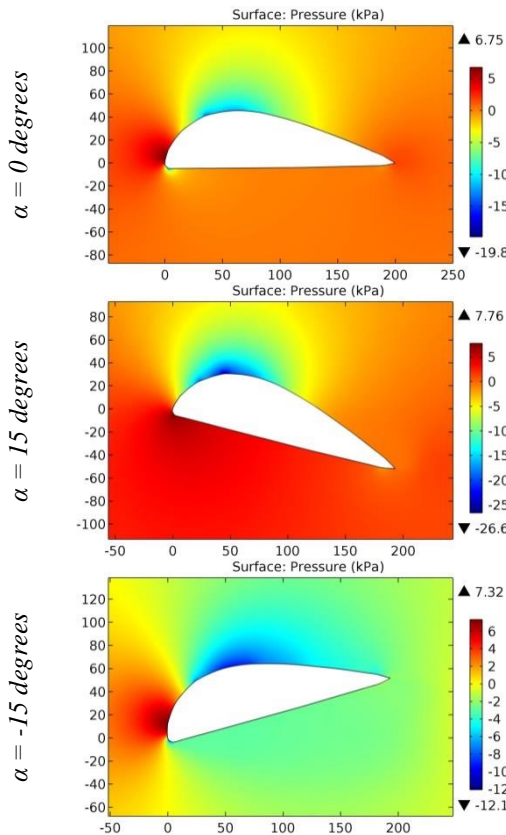


Figure 15. The pressure contours on the surfaces of the GOE 553 airfoil.



**Figure 16.** The pressure contours on the surfaces of the GOE 559 airfoil.



**Figure 17.** The pressure contours on the surfaces of the GOE 561 airfoil.

ISRA (India) = <b>6.317</b>	SIS (USA) = <b>0.912</b>	ICV (Poland) = <b>6.630</b>
ISI (Dubai, UAE) = <b>1.582</b>	РИНЦ (Russia) = <b>3.939</b>	PIF (India) = <b>1.940</b>
GIF (Australia) = <b>0.564</b>	ESJI (KZ) = <b>8.771</b>	IBI (India) = <b>4.260</b>
JIF = <b>1.500</b>	SJIF (Morocco) = <b>7.184</b>	OAJI (USA) = <b>0.350</b>

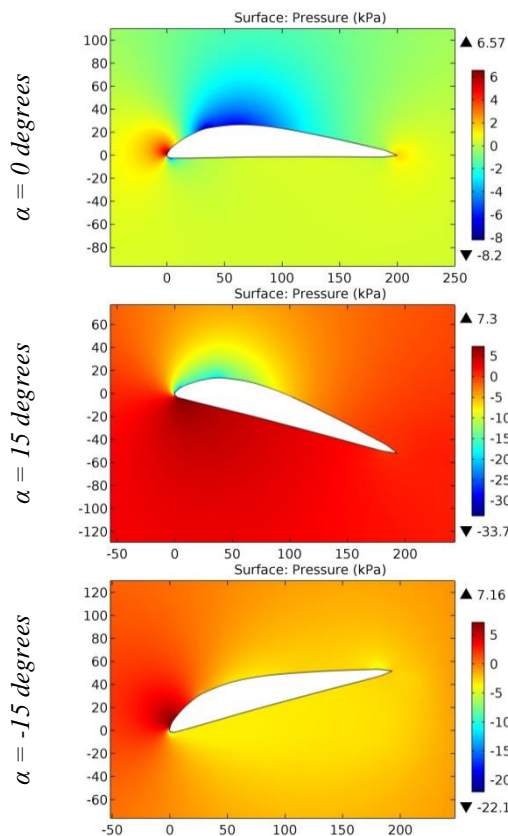


**Figure 18.** The pressure contours on the surfaces of the GOE 562 airfoil.

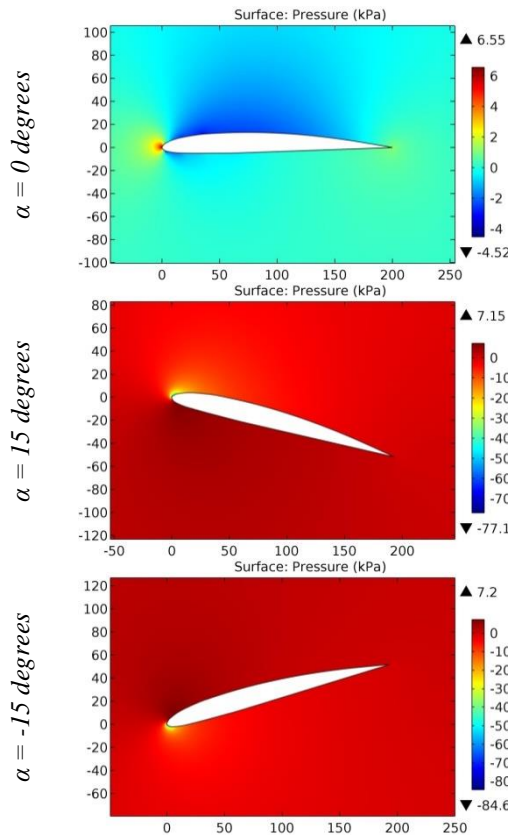


**Figure 19.** The pressure contours on the surfaces of the GOE 563 airfoil.

ISRA (India)	= 6.317	SIS (USA)	= 0.912	ICV (Poland)	= 6.630
ISI (Dubai, UAE)	= 1.582	РИНЦ (Russia)	= 3.939	PIF (India)	= 1.940
GIF (Australia)	= 0.564	ESJI (KZ)	= 8.771	IBI (India)	= 4.260
JIF	= 1.500	SJIF (Morocco)	= 7.184	OAJI (USA)	= 0.350

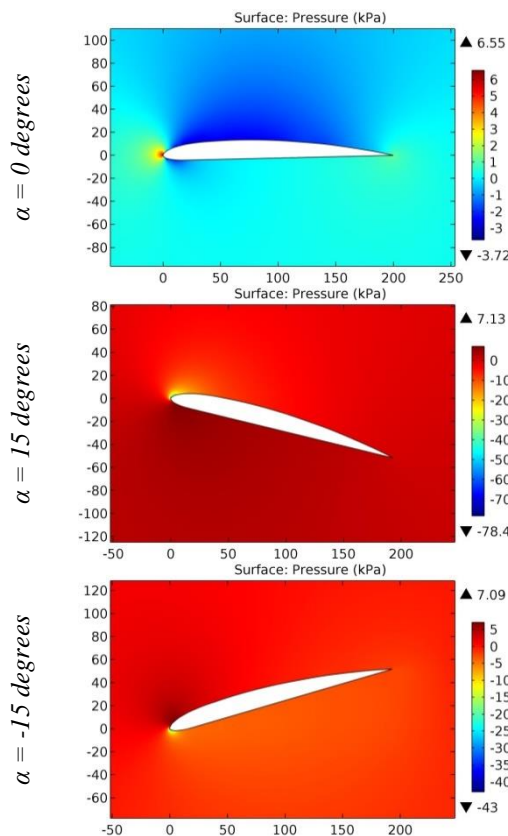


Figure 20. The pressure contours on the surfaces of the GOE 564 airfoil.

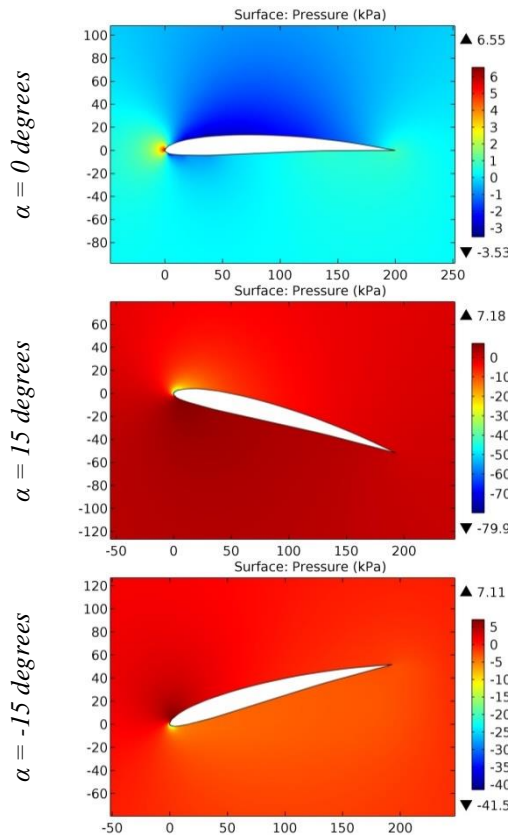


Figure 21. The pressure contours on the surfaces of the GOE 565 airfoil.

## Impact Factor:

<b>ISRA (India)</b>	= <b>6.317</b>	<b>SIS (USA)</b>	= <b>0.912</b>	<b>ICV (Poland)</b>	= <b>6.630</b>
<b>ISI (Dubai, UAE)</b>	= <b>1.582</b>	<b>РИНЦ (Russia)</b>	= <b>3.939</b>	<b>PIF (India)</b>	= <b>1.940</b>
<b>GIF (Australia)</b>	= <b>0.564</b>	<b>ESJI (KZ)</b>	= <b>8.771</b>	<b>IBI (India)</b>	= <b>4.260</b>
<b>JIF</b>	= <b>1.500</b>	<b>SJIF (Morocco)</b>	= <b>7.184</b>	<b>OAJI (USA)</b>	= <b>0.350</b>

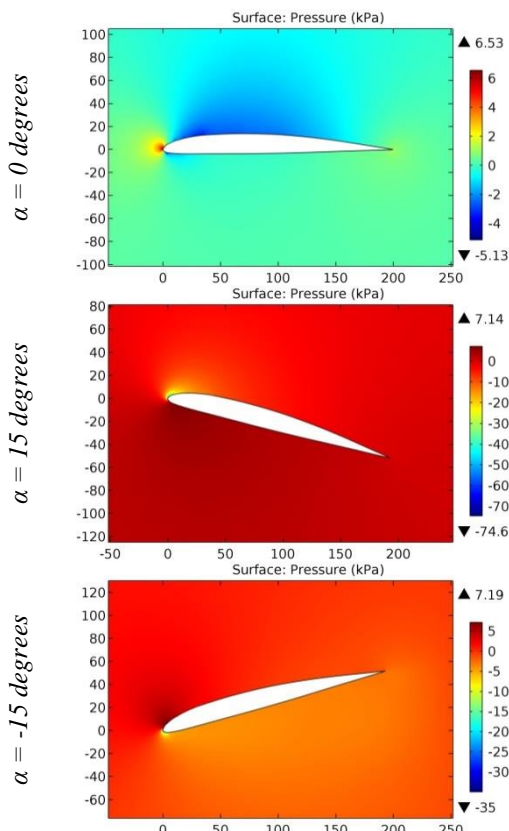


Figure 22. The pressure contours on the surfaces of the GOE 566 airfoil.

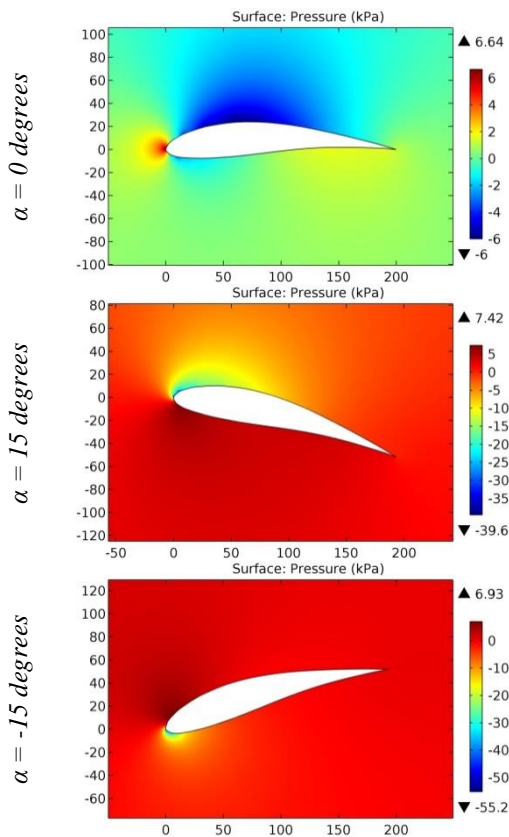
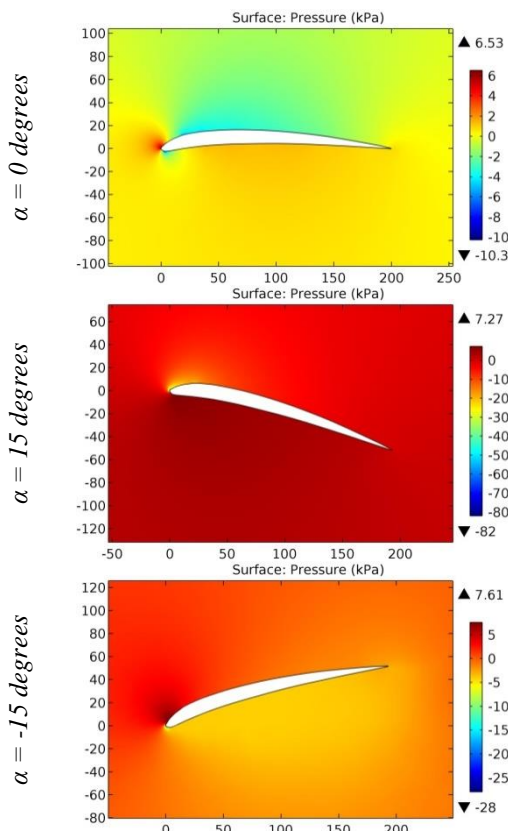
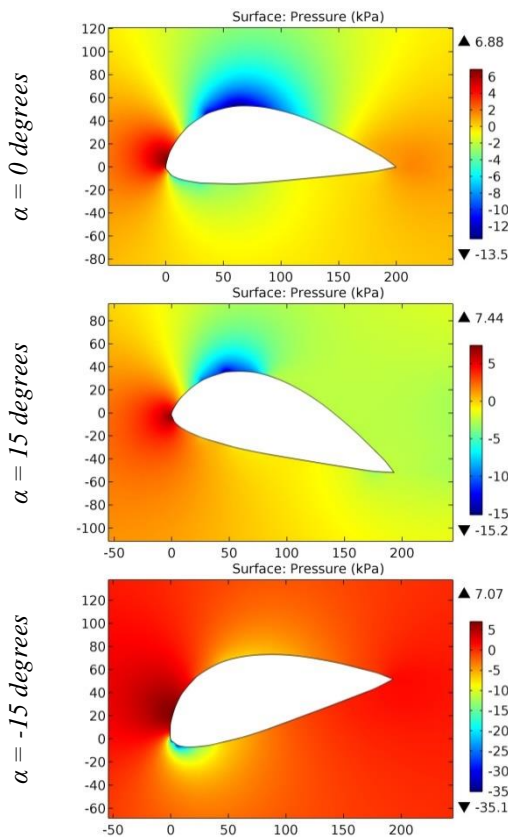


Figure 23. The pressure contours on the surfaces of the GOE 567 airfoil.



**Figure 24.** The pressure contours on the surfaces of the GOE 57 airfoil.



**Figure 25.** The pressure contours on the surfaces of the GOE 570 airfoil.

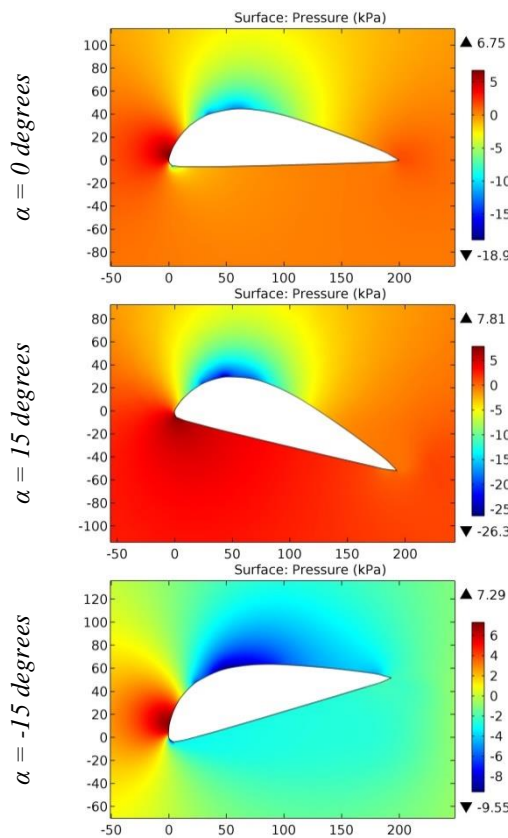


**Figure 26.** The pressure contours on the surfaces of the GOE 571 airfoil.

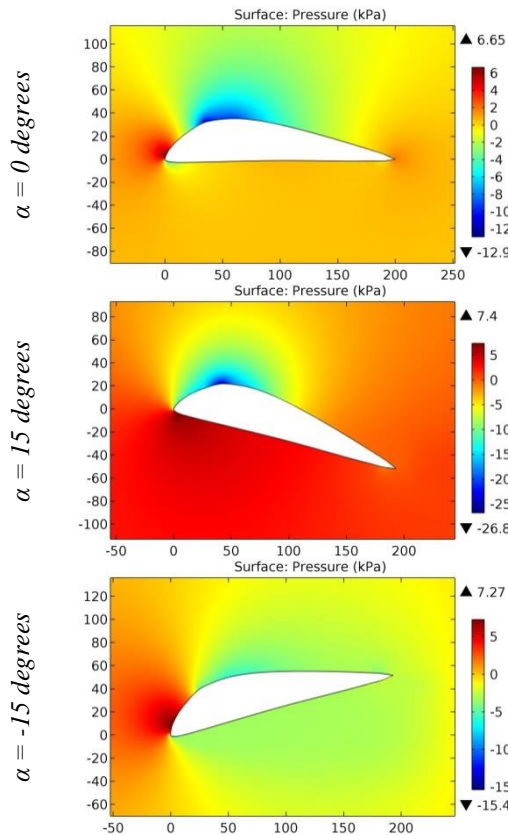


**Figure 27.** The pressure contours on the surfaces of the GOE 572 airfoil.

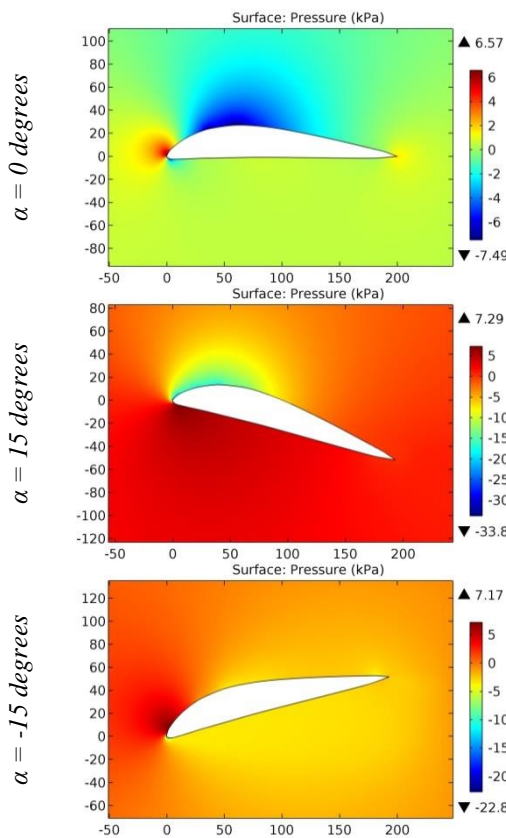


**Figure 28.** The pressure contours on the surfaces of the GOE 573 airfoil.

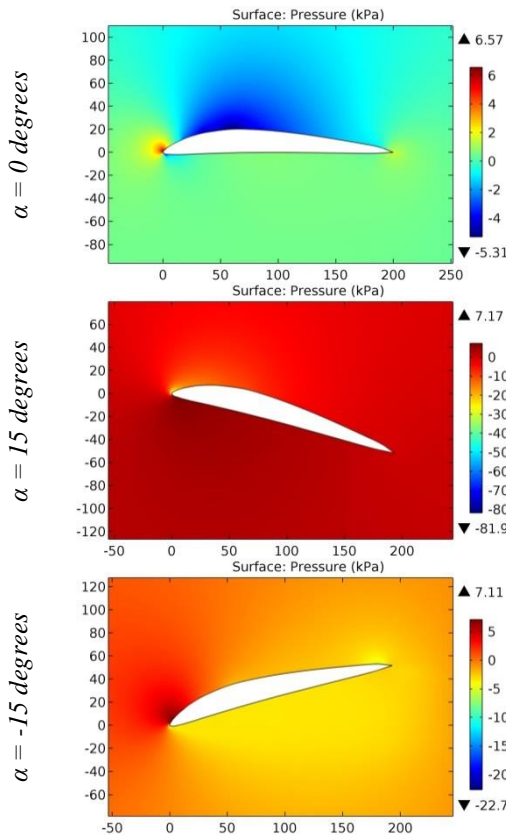


**Figure 29.** The pressure contours on the surfaces of the GOE 574 airfoil.

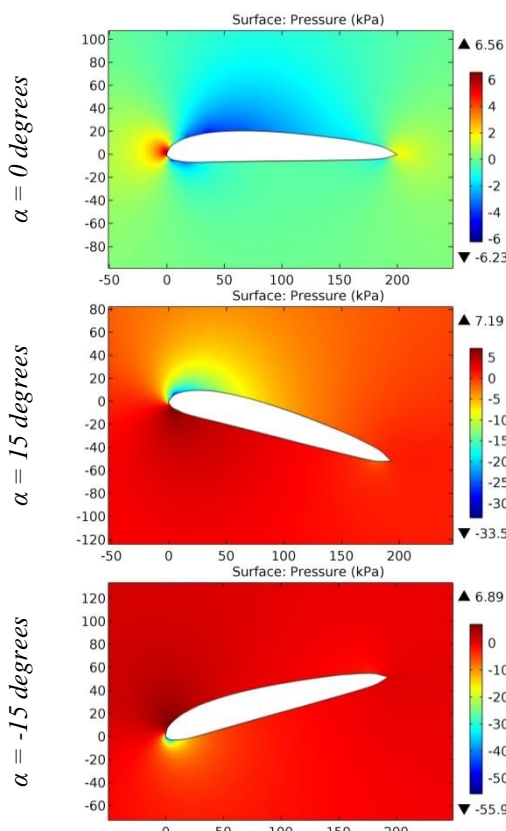


**Figure 30.** The pressure contours on the surfaces of the GOE 575 airfoil.

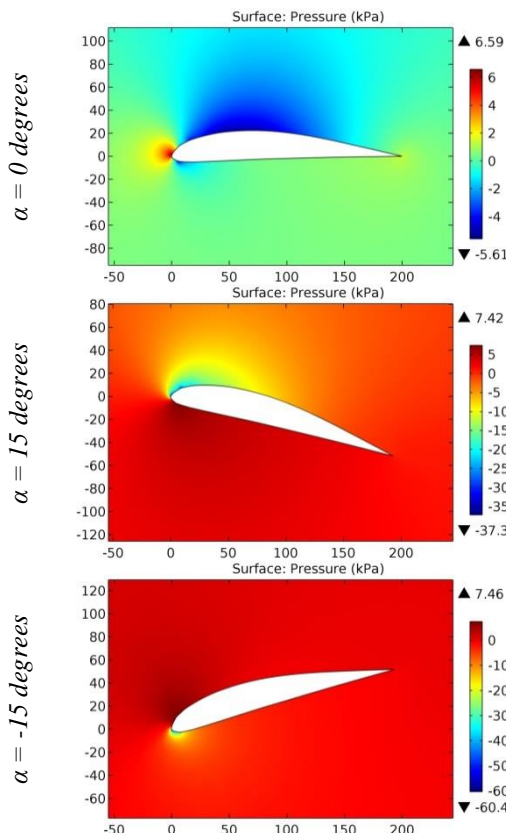


**Figure 31.** The pressure contours on the surfaces of the GOE 584 airfoil.

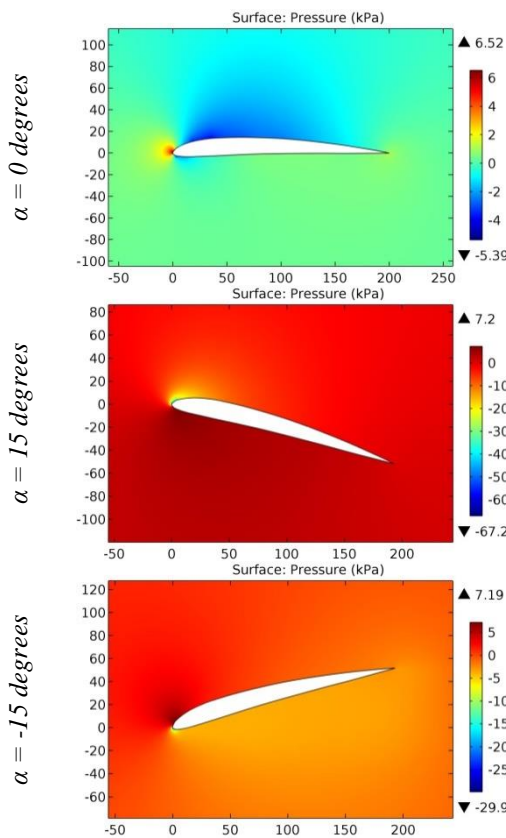


**Figure 32.** The pressure contours on the surfaces of the GOE 585 airfoil.

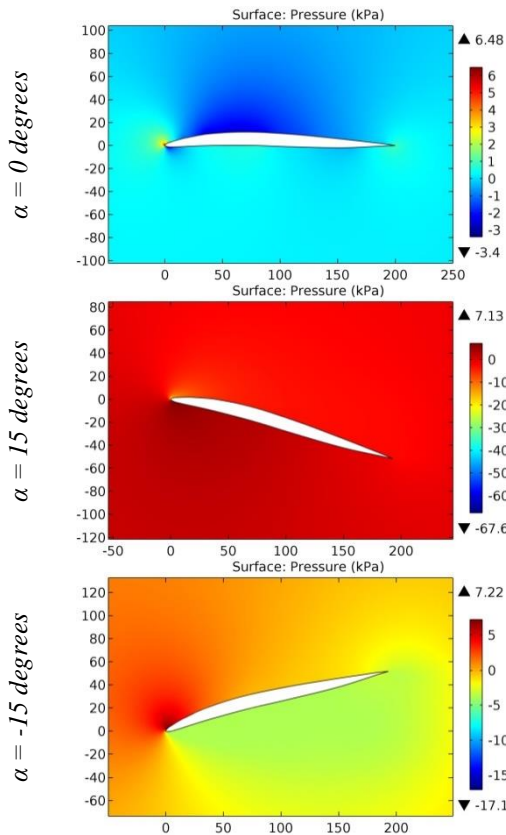


**Figure 33.** The pressure contours on the surfaces of the GOE 587 airfoil.

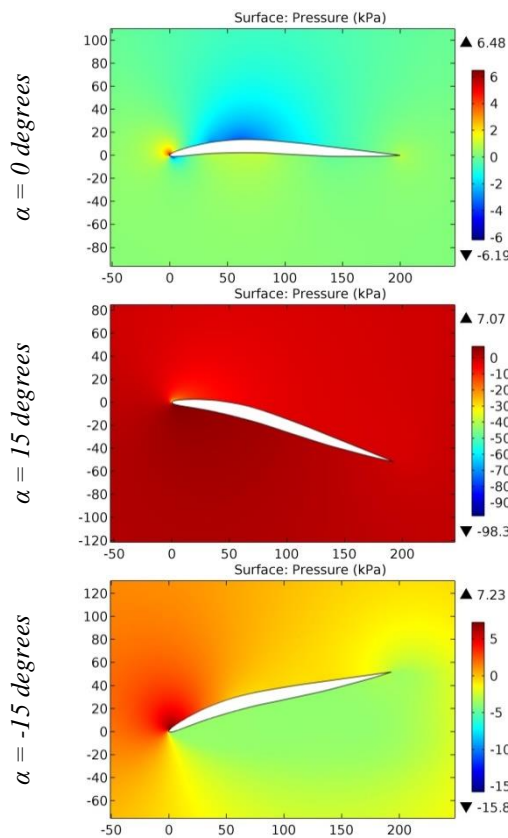


Figure 34. The pressure contours on the surfaces of the GOE 590 airfoil.

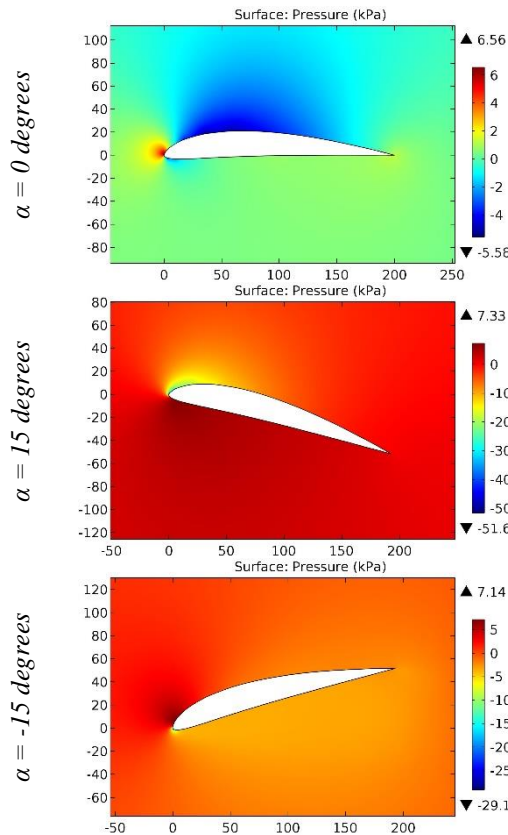
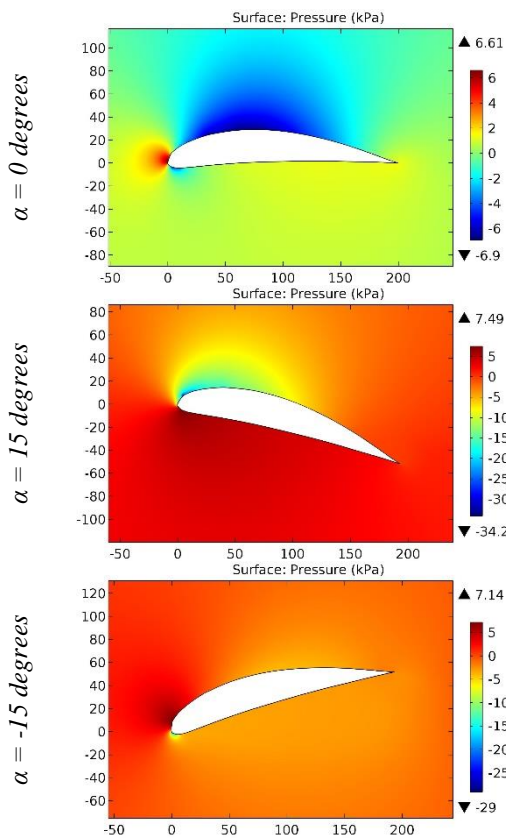
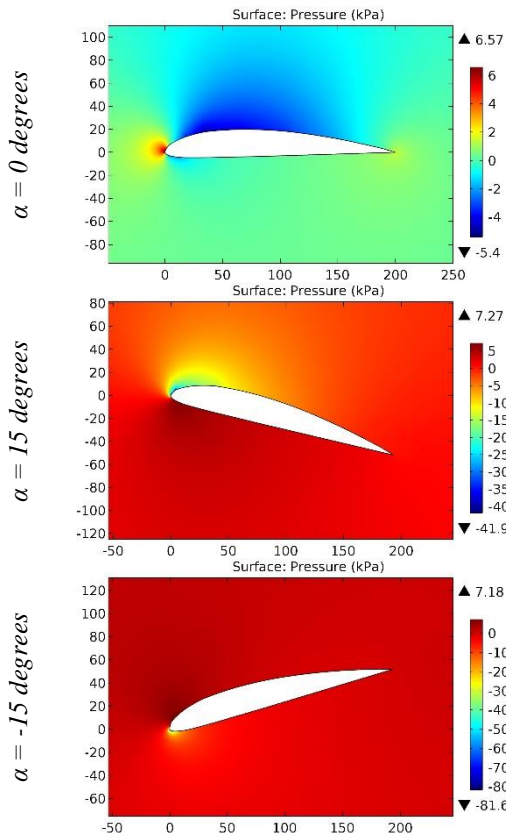


Figure 35. The pressure contours on the surfaces of the GOE 591 airfoil.

ISRA (India)	= 6.317	SIS (USA)	= 0.912	ICV (Poland)	= 6.630
ISI (Dubai, UAE)	= 1.582	РИНЦ (Russia)	= 3.939	PIF (India)	= 1.940
GIF (Australia)	= 0.564	ESJI (KZ)	= 8.771	IBI (India)	= 4.260
JIF	= 1.500	SJIF (Morocco)	= 7.184	OAJI (USA)	= 0.350



**Figure 36.** The pressure contours on the surfaces of the GOE 592 airfoil.



**Figure 37.** The pressure contours on the surfaces of the GOE 593 airfoil.

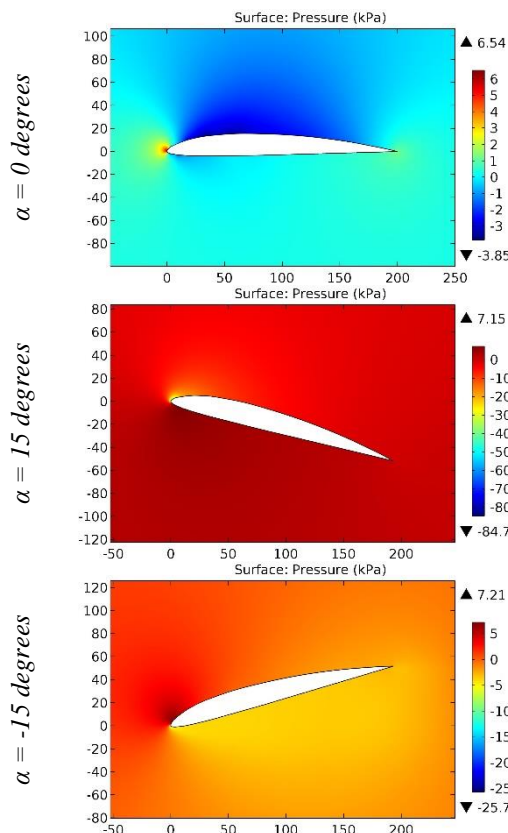


**Figure 38.** The pressure contours on the surfaces of the GOE 595 airfoil.

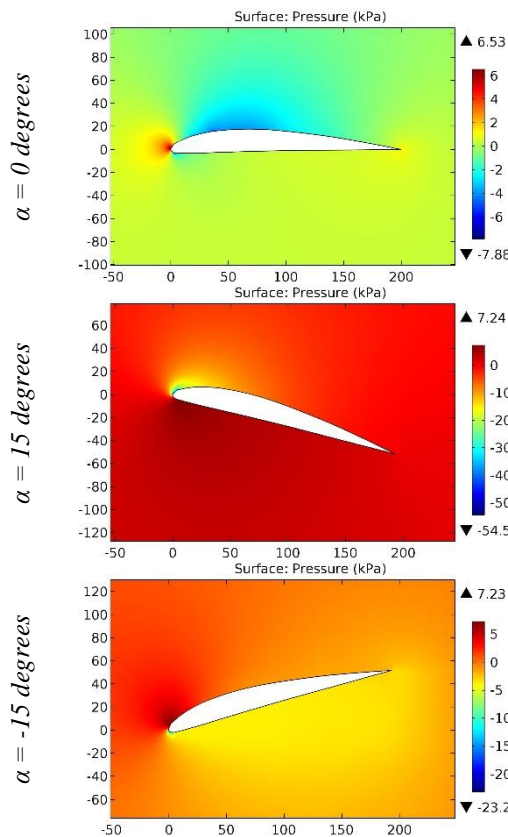


**Figure 39.** The pressure contours on the surfaces of the GOE 596 airfoil.

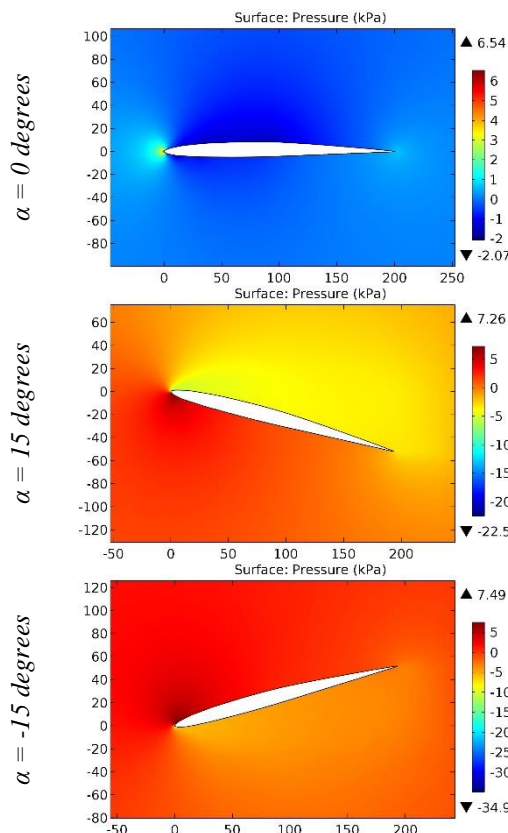


**Figure 40.** The pressure contours on the surfaces of the GOE 598 airfoil.

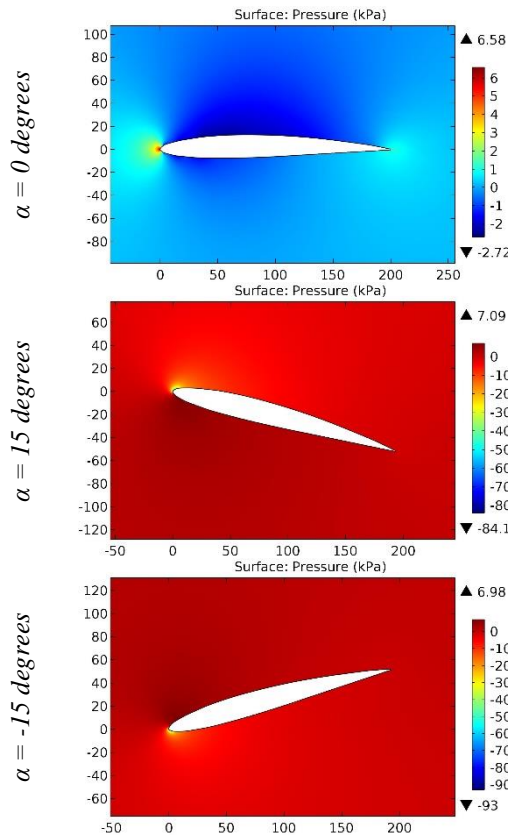


**Figure 41.** The pressure contours on the surfaces of the GOE 599 airfoil.

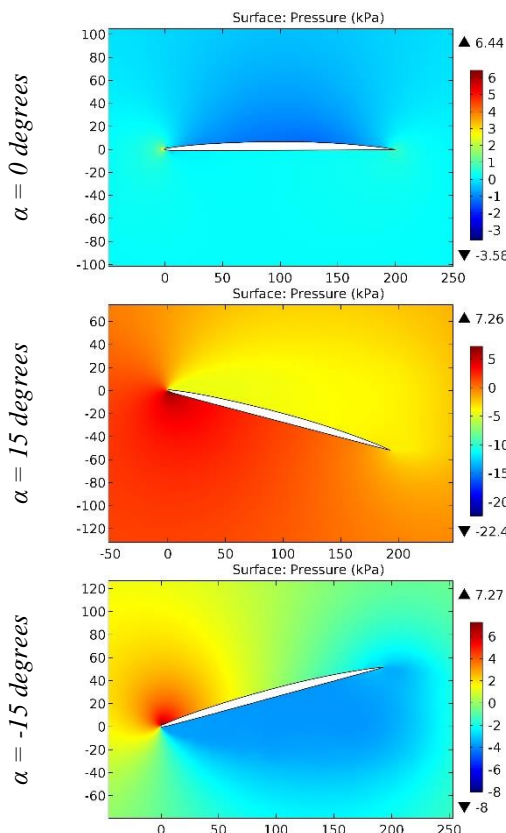


**Figure 42.** The pressure contours on the surfaces of the GOE 5K airfoil.

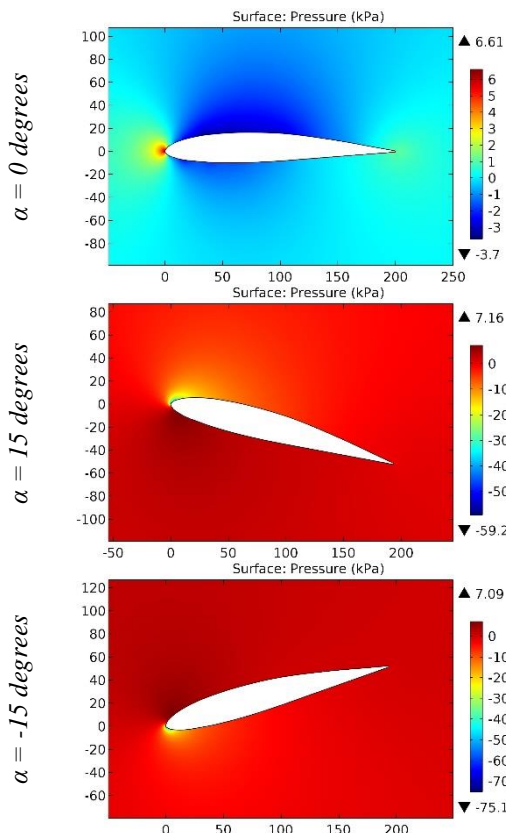


**Figure 43.** The pressure contours on the surfaces of the GOE 600 airfoil.

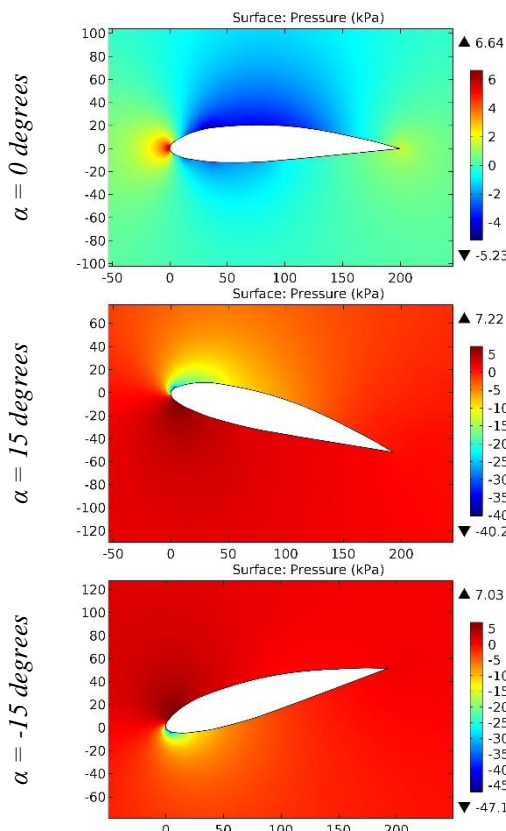


**Figure 44.** The pressure contours on the surfaces of the GOE 601 airfoil.

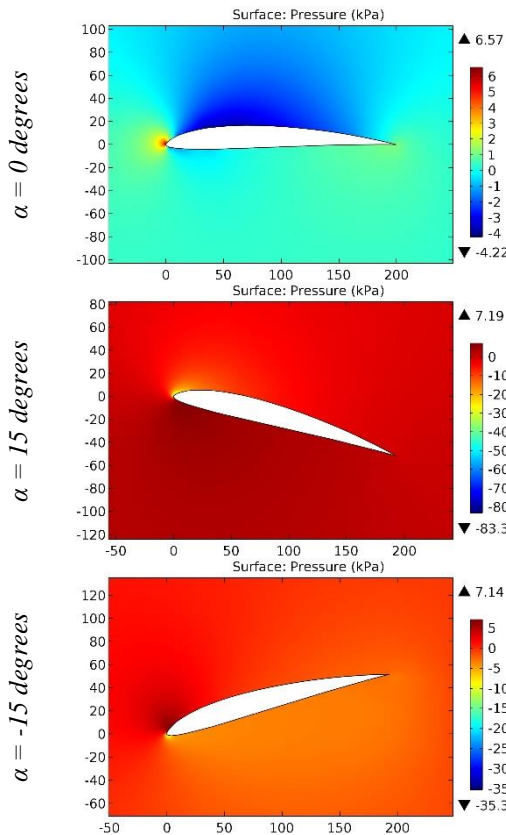


**Figure 45.** The pressure contours on the surfaces of the GOE 602 airfoil.

## Impact Factor:

<b>ISRA (India)</b>	= <b>6.317</b>	<b>SIS (USA)</b>	= <b>0.912</b>	<b>ICV (Poland)</b>	= <b>6.630</b>
<b>ISI (Dubai, UAE)</b>	= <b>1.582</b>	<b>РИНЦ (Russia)</b>	= <b>3.939</b>	<b>PIF (India)</b>	= <b>1.940</b>
<b>GIF (Australia)</b>	= <b>0.564</b>	<b>ESJI (KZ)</b>	= <b>8.771</b>	<b>IBI (India)</b>	= <b>4.260</b>
<b>JIF</b>	= <b>1.500</b>	<b>SJIF (Morocco)</b>	= <b>7.184</b>	<b>OAJI (USA)</b>	= <b>0.350</b>

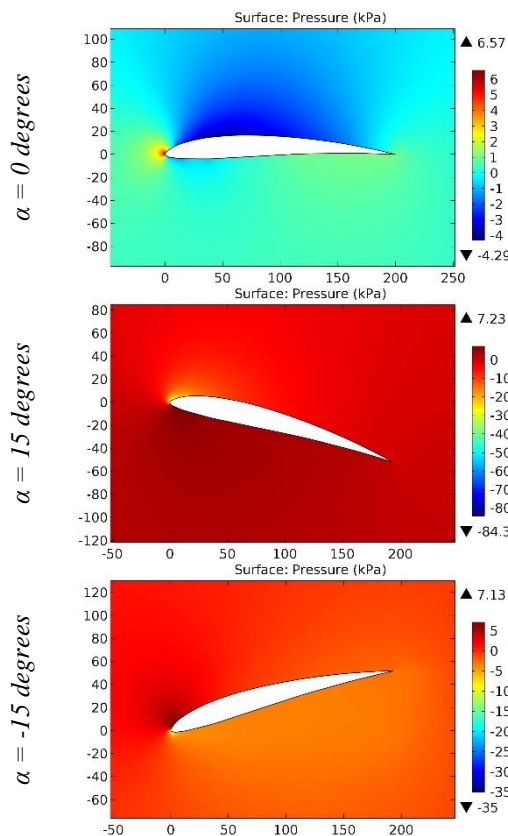


Figure 46. The pressure contours on the surfaces of the GOE 602 MOD, airfoil.

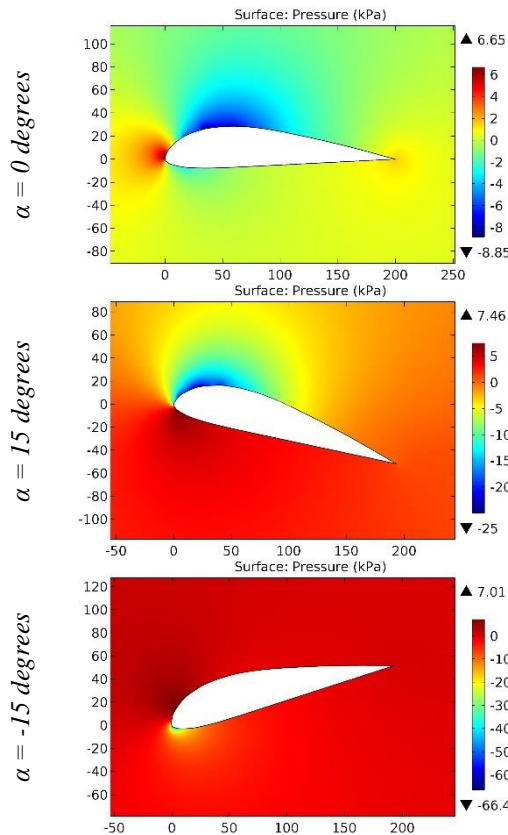
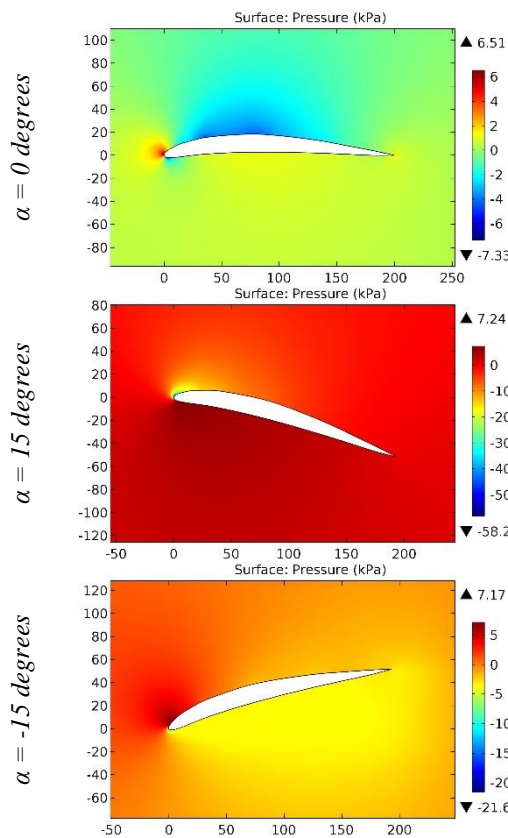
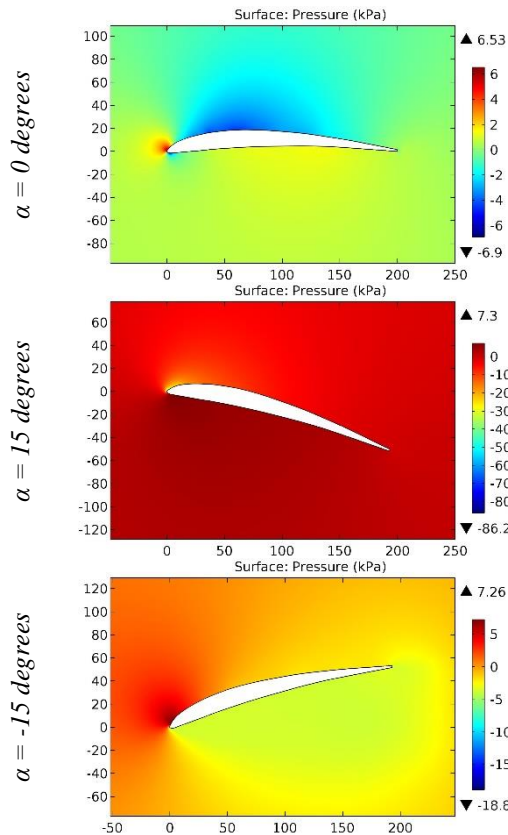


Figure 47. The pressure contours on the surfaces of the GOE 604 airfoil.



**Figure 48.** The pressure contours on the surfaces of the GOE 610 B airfoil.



**Figure 49.** The pressure contours on the surfaces of the GOE 610-B MOD, airfoil.

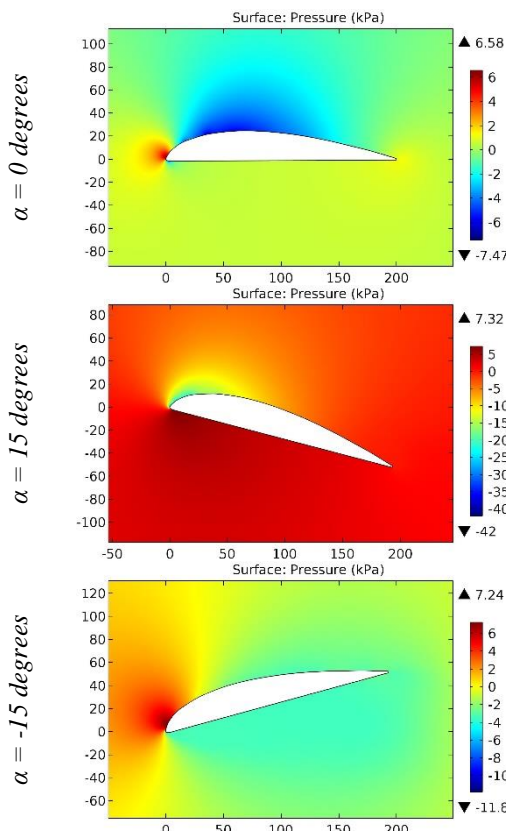


**Figure 50.** The pressure contours on the surfaces of the GOE 611 airfoil.

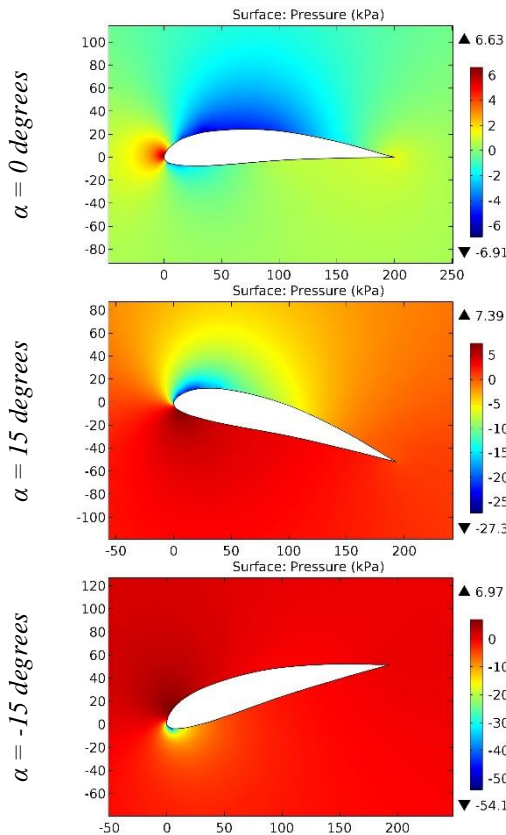


**Figure 51.** The pressure contours on the surfaces of the GOE 612 airfoil.

ISRA (India)	= 6.317	SIS (USA)	= 0.912	ICV (Poland)	= 6.630
ISI (Dubai, UAE)	= 1.582	РИНЦ (Russia)	= 3.939	PIF (India)	= 1.940
GIF (Australia)	= 0.564	ESJI (KZ)	= 8.771	IBI (India)	= 4.260
JIF	= 1.500	SJIF (Morocco)	= 7.184	OAJI (USA)	= 0.350

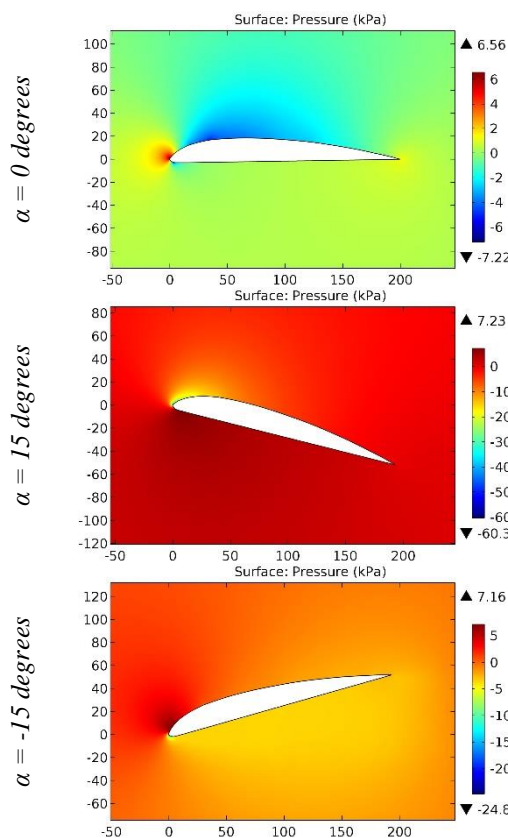


**Figure 52.** The pressure contours on the surfaces of the GOE 613 airfoil.

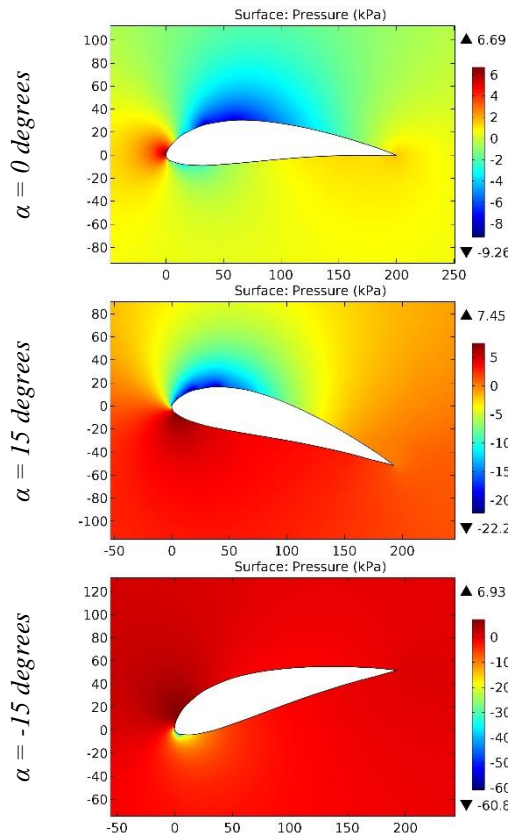


**Figure 53.** The pressure contours on the surfaces of the GOE 614 airfoil.

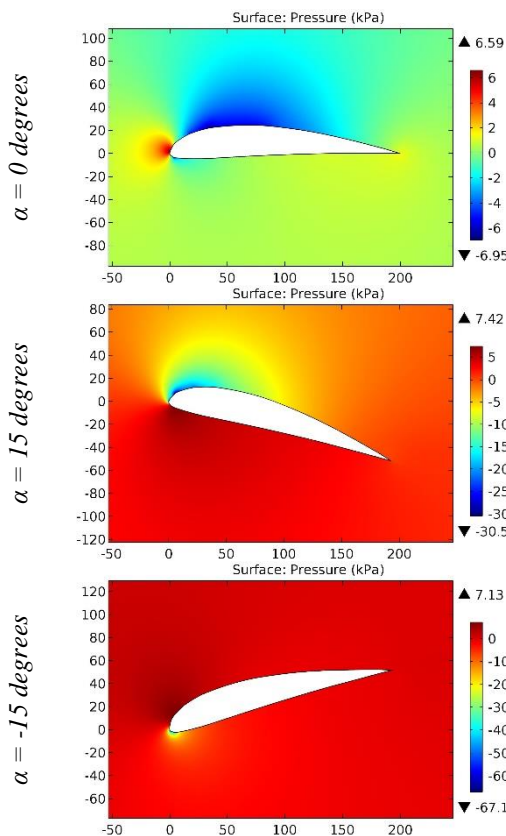


**Figure 54.** The pressure contours on the surfaces of the GOE 615 airfoil.

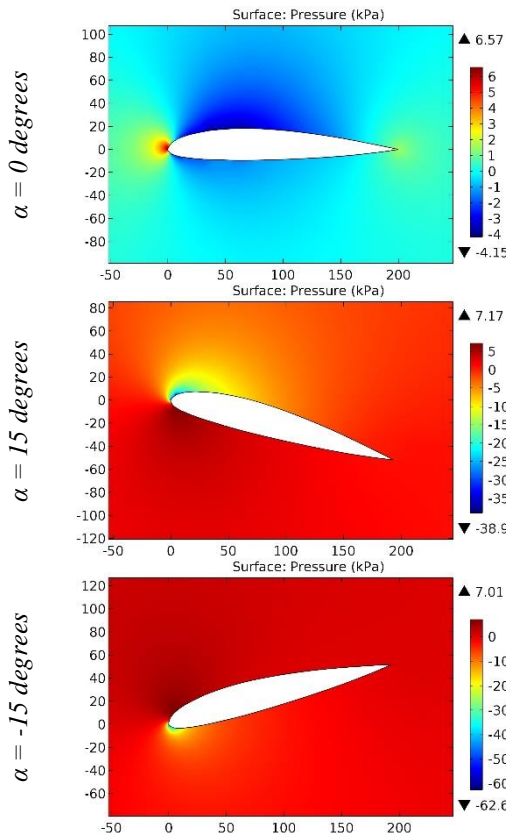


**Figure 55.** The pressure contours on the surfaces of the GOE 617 airfoil.

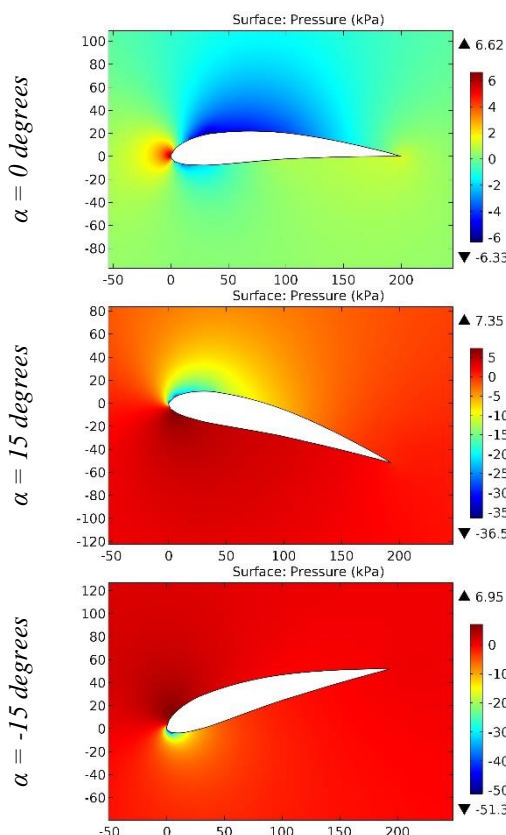


**Figure 56.** The pressure contours on the surfaces of the GOE 619 airfoil.

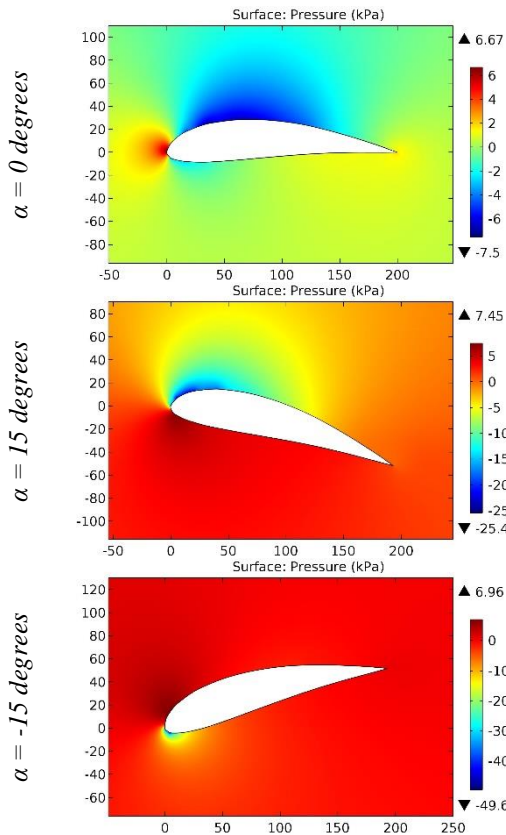


**Figure 57.** The pressure contours on the surfaces of the GOE 620 airfoil.

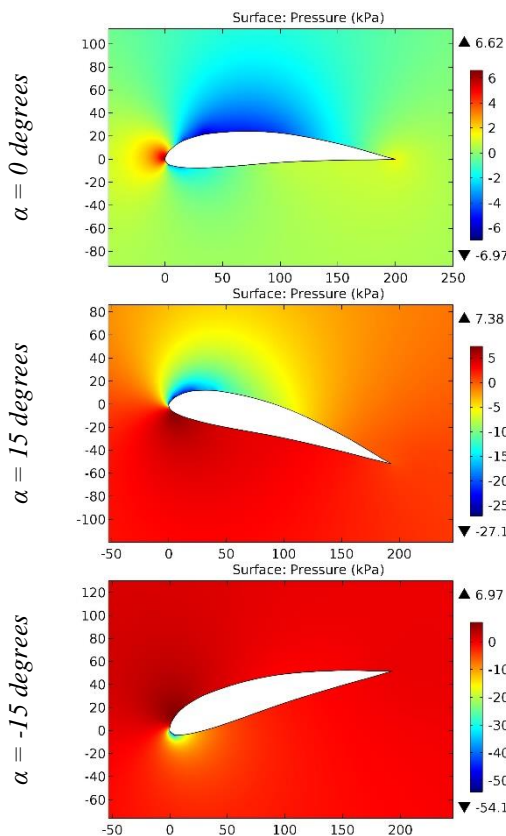


**Figure 58.** The pressure contours on the surfaces of the GOE 621 airfoil.

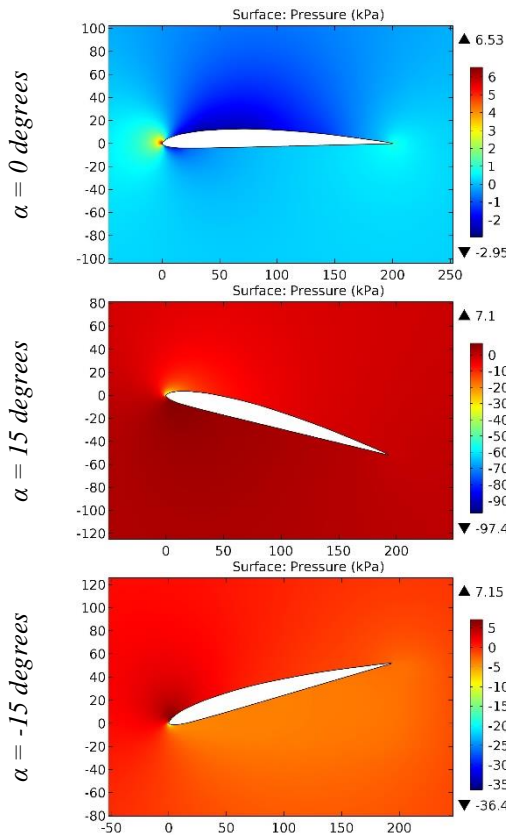


**Figure 59.** The pressure contours on the surfaces of the GOE 622 airfoil.

ISRA (India)	= 6.317	SIS (USA)	= 0.912	ICV (Poland)	= 6.630
ISI (Dubai, UAE)	= 1.582	РИНЦ (Russia)	= 3.939	PIF (India)	= 1.940
GIF (Australia)	= 0.564	ESJI (KZ)	= 8.771	IBI (India)	= 4.260
JIF	= 1.500	SJIF (Morocco)	= 7.184	OAJI (USA)	= 0.350

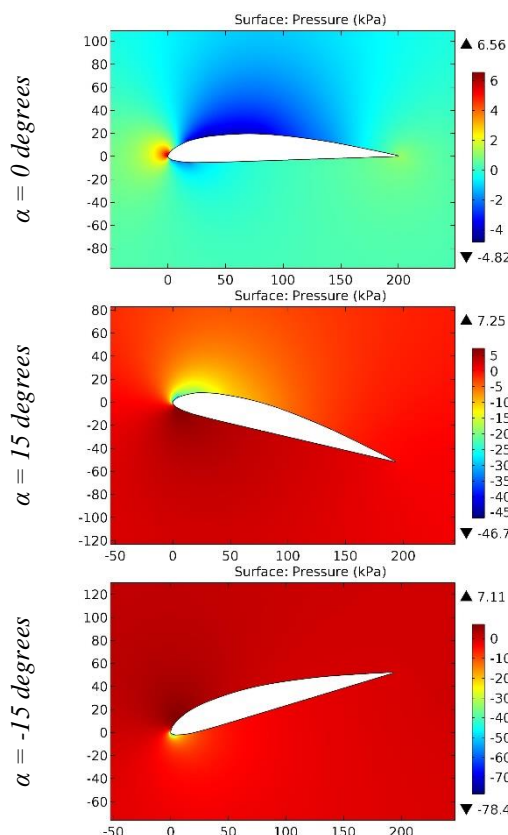


**Figure 60.** The pressure contours on the surfaces of the GOE 623 airfoil.

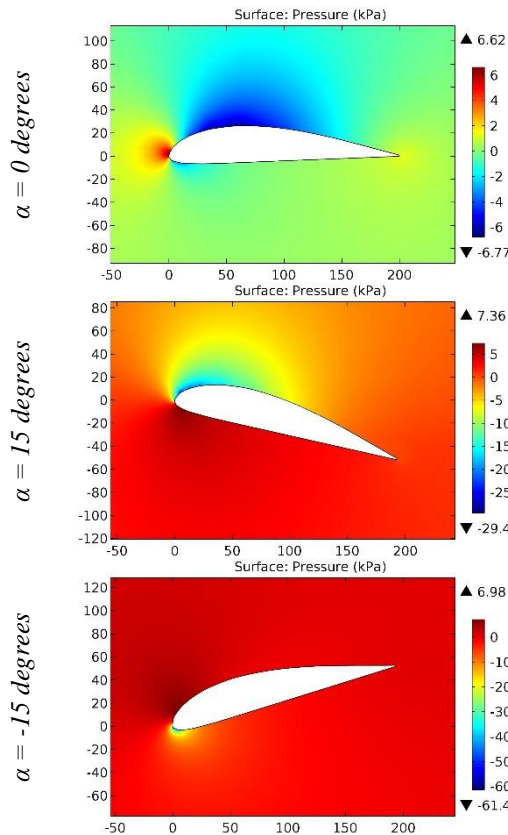


**Figure 61.** The pressure contours on the surfaces of the GOE 624 airfoil.

ISRA (India)	= 6.317	SIS (USA)	= 0.912	ICV (Poland)	= 6.630
ISI (Dubai, UAE)	= 1.582	РИНЦ (Russia)	= 3.939	PIF (India)	= 1.940
GIF (Australia)	= 0.564	ESJI (KZ)	= 8.771	IBI (India)	= 4.260
JIF	= 1.500	SJIF (Morocco)	= 7.184	OAJI (USA)	= 0.350

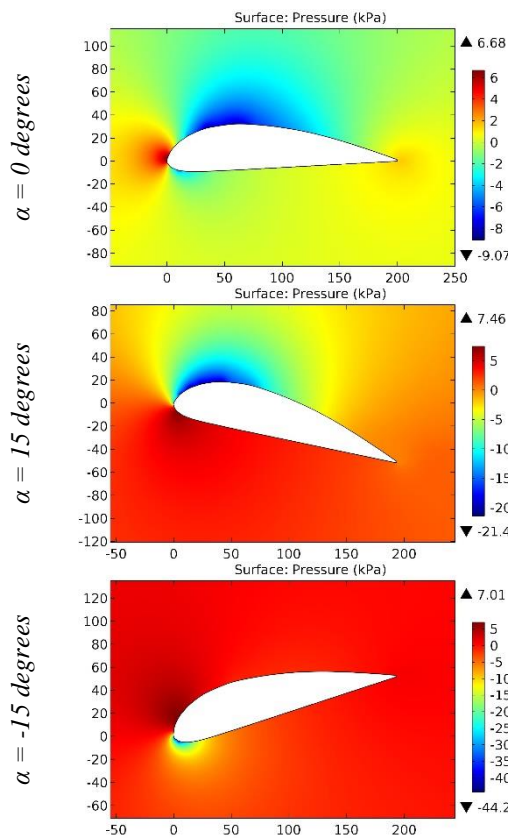


**Figure 62.** The pressure contours on the surfaces of the GOE 625 airfoil.

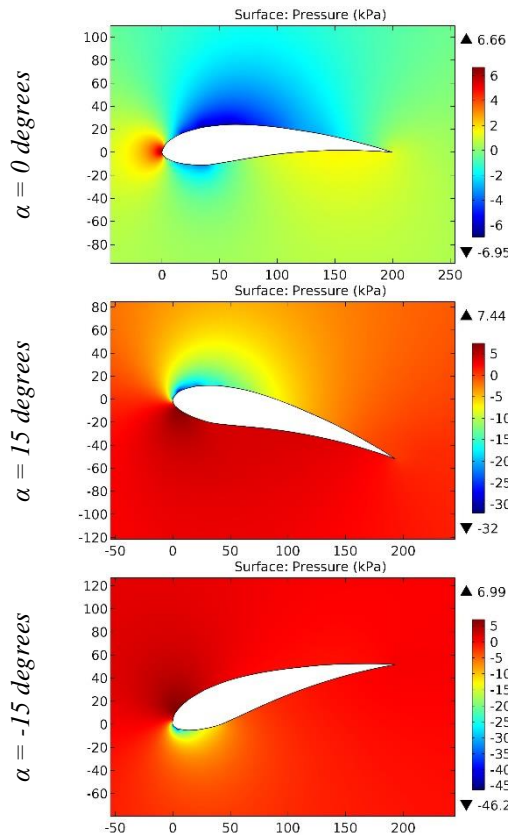


**Figure 63.** The pressure contours on the surfaces of the GOE 626 airfoil.

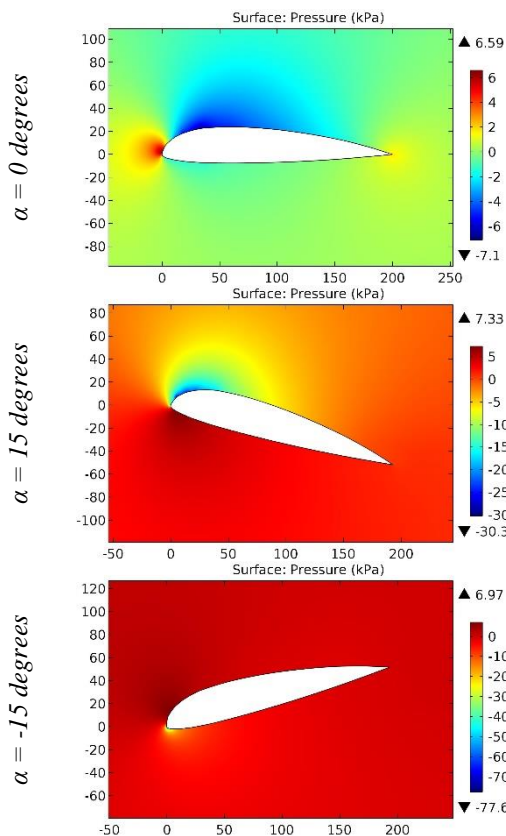


**Figure 64.** The pressure contours on the surfaces of the GOE 627 airfoil.

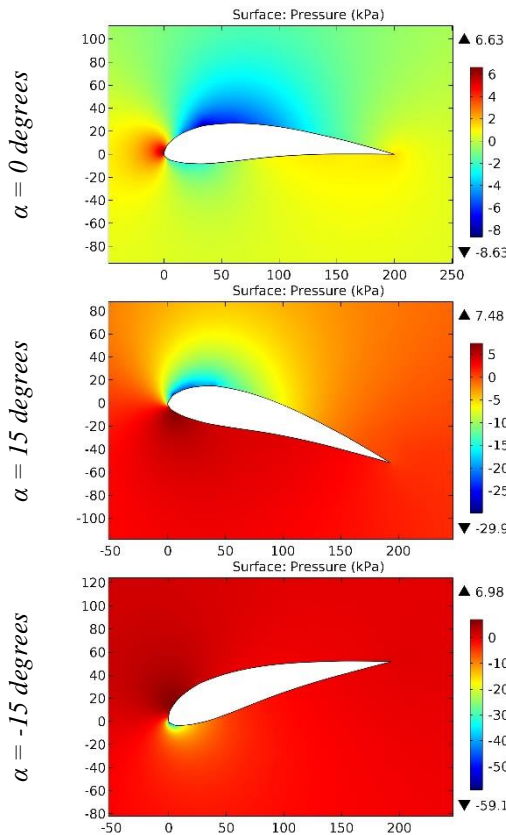


**Figure 65.** The pressure contours on the surfaces of the GOE 628 airfoil.

ISRA (India)	= 6.317	SIS (USA)	= 0.912	ICV (Poland)	= 6.630
ISI (Dubai, UAE)	= 1.582	РИНЦ (Russia)	= 3.939	PIF (India)	= 1.940
GIF (Australia)	= 0.564	ESJI (KZ)	= 8.771	IBI (India)	= 4.260
JIF	= 1.500	SJIF (Morocco)	= 7.184	OAJI (USA)	= 0.350

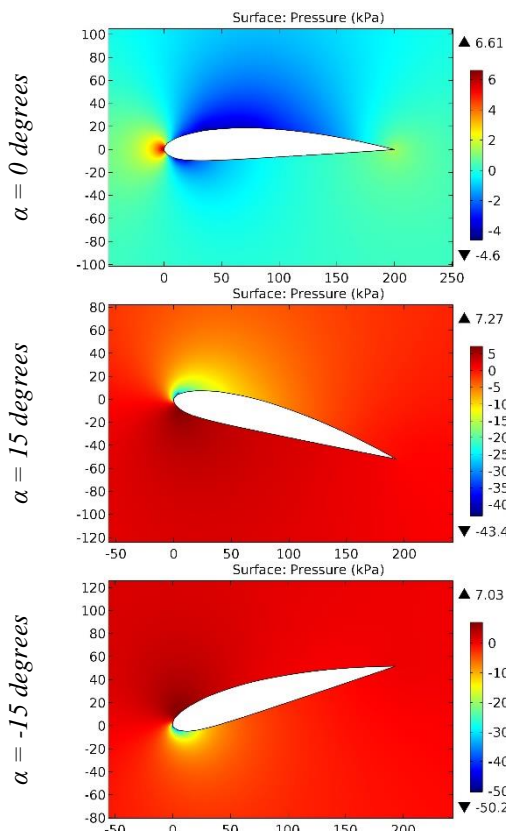


**Figure 66.** The pressure contours on the surfaces of the GOE 629 airfoil.

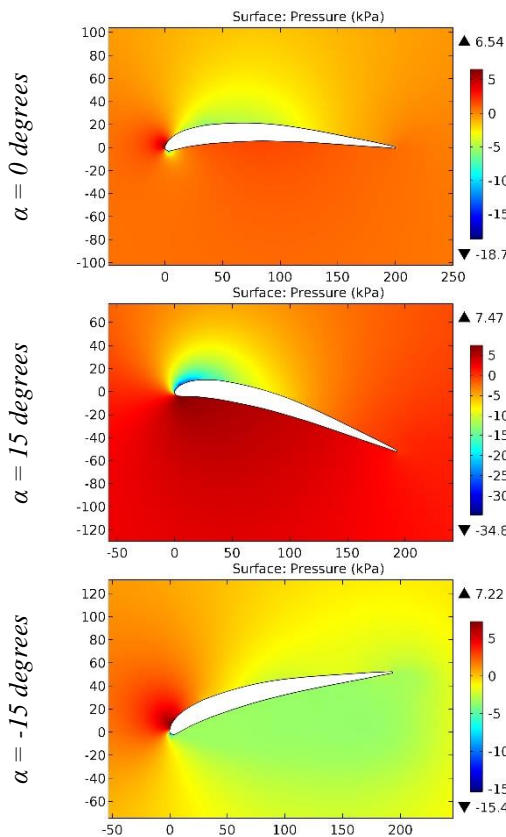


**Figure 67.** The pressure contours on the surfaces of the GOE 63 airfoil.

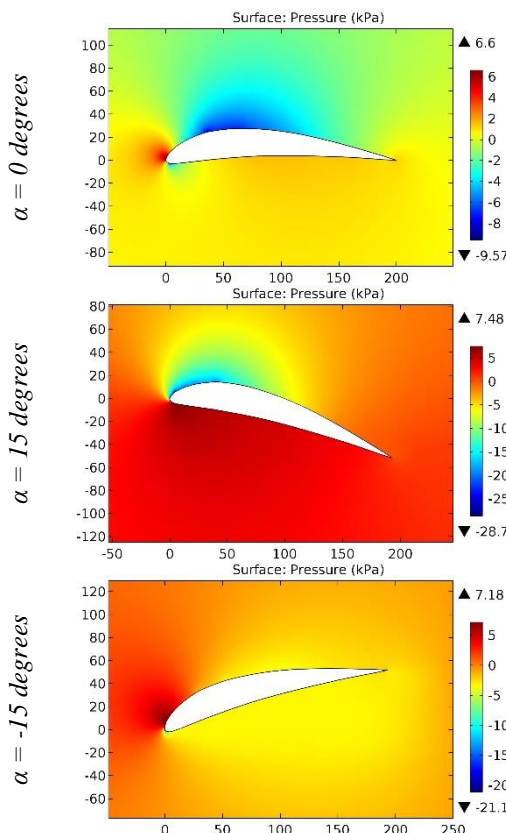


**Figure 68.** The pressure contours on the surfaces of the GOE 630 airfoil.

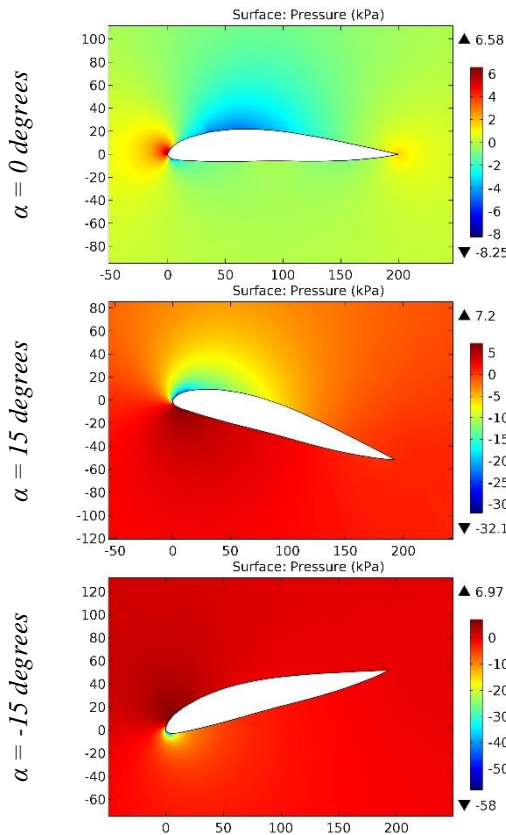


**Figure 69.** The pressure contours on the surfaces of the GOE 632 airfoil.

ISRA (India)	= 6.317	SIS (USA)	= 0.912	ICV (Poland)	= 6.630
ISI (Dubai, UAE)	= 1.582	РИНЦ (Russia)	= 3.939	PIF (India)	= 1.940
GIF (Australia)	= 0.564	ESJI (KZ)	= 8.771	IBI (India)	= 4.260
JIF	= 1.500	SJIF (Morocco)	= 7.184	OAJI (USA)	= 0.350

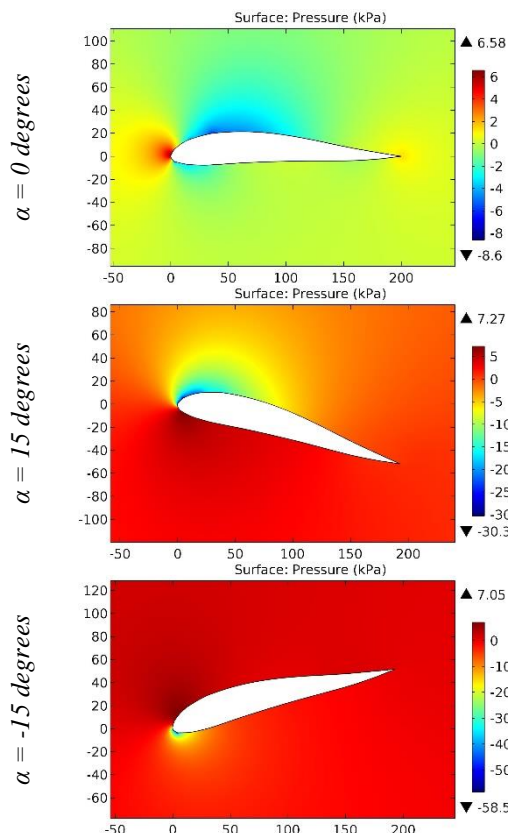


**Figure 70.** The pressure contours on the surfaces of the GOE 633 airfoil.

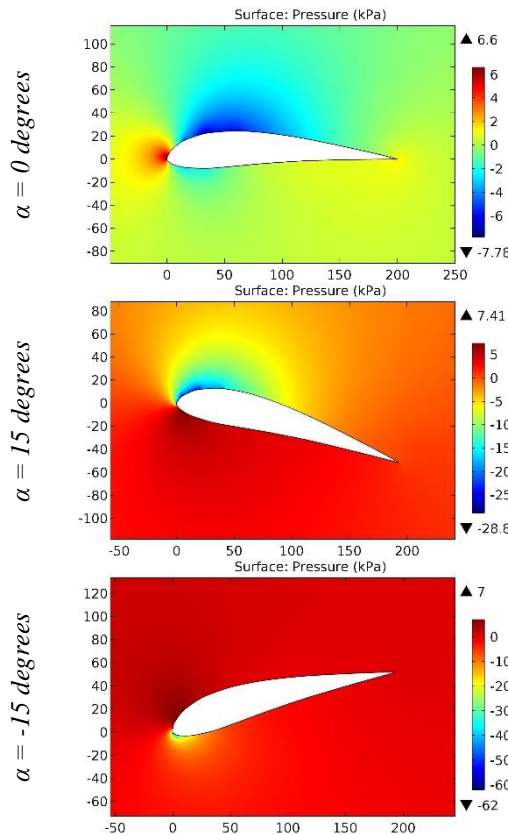


**Figure 71.** The pressure contours on the surfaces of the GOE 645 airfoil.

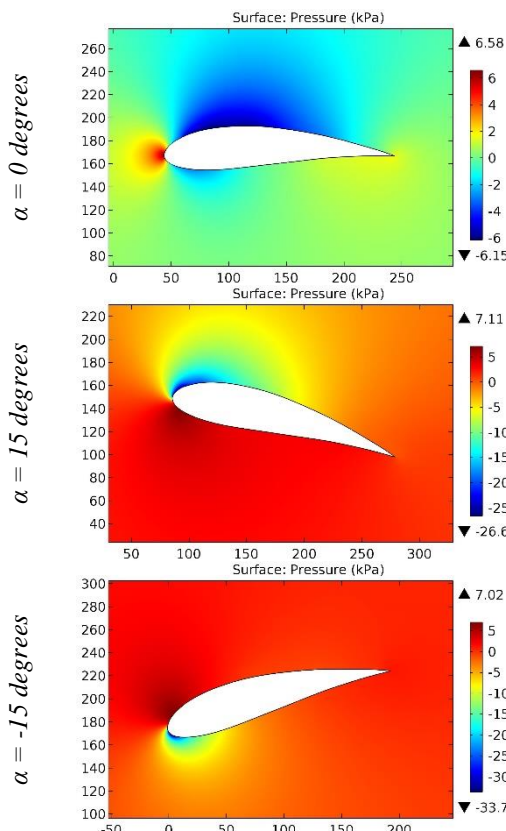


Figure 72. The pressure contours on the surfaces of the GOE 646 airfoil.

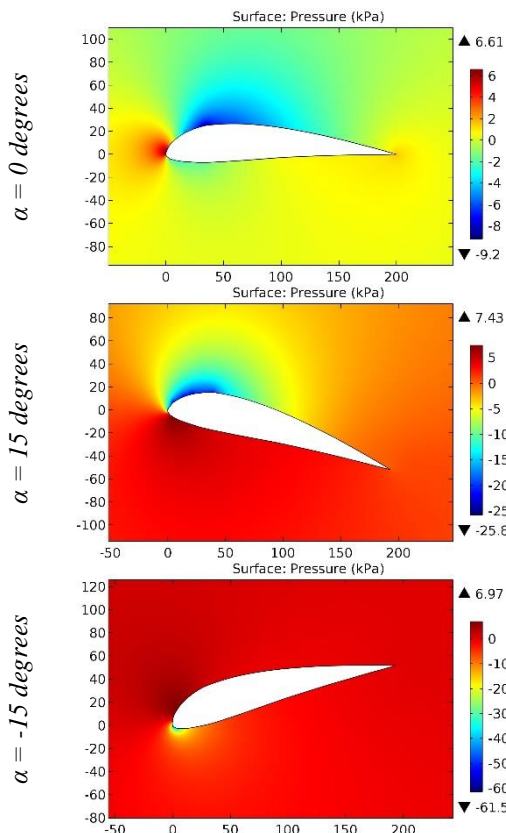
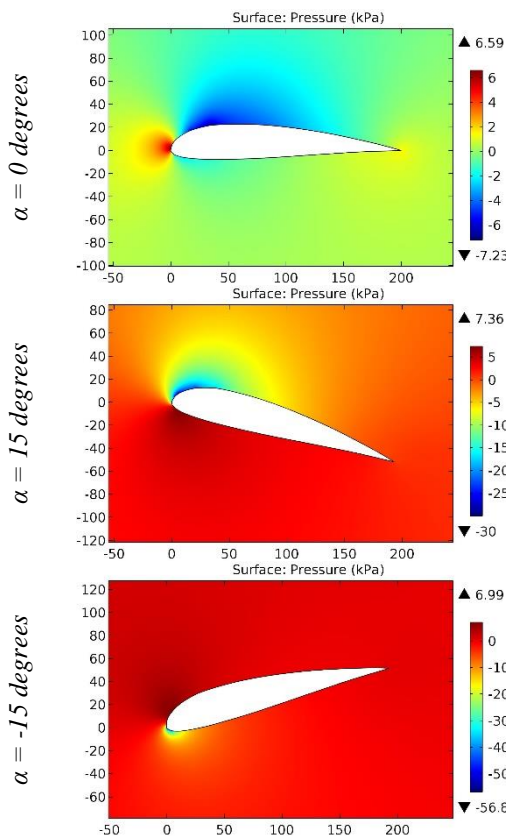
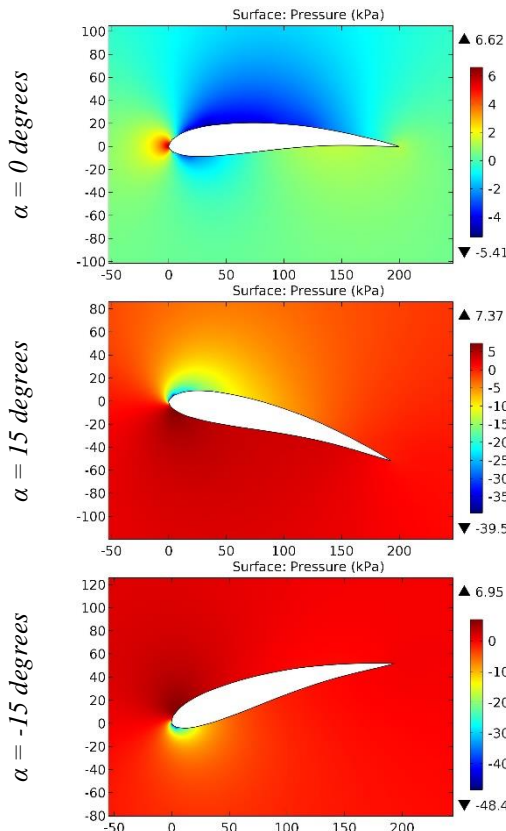


Figure 73. The pressure contours on the surfaces of the GOE 647 airfoil.



**Figure 74.** The pressure contours on the surfaces of the GOE 648 airfoil.



**Figure 75.** The pressure contours on the surfaces of the GOE 650 airfoil.

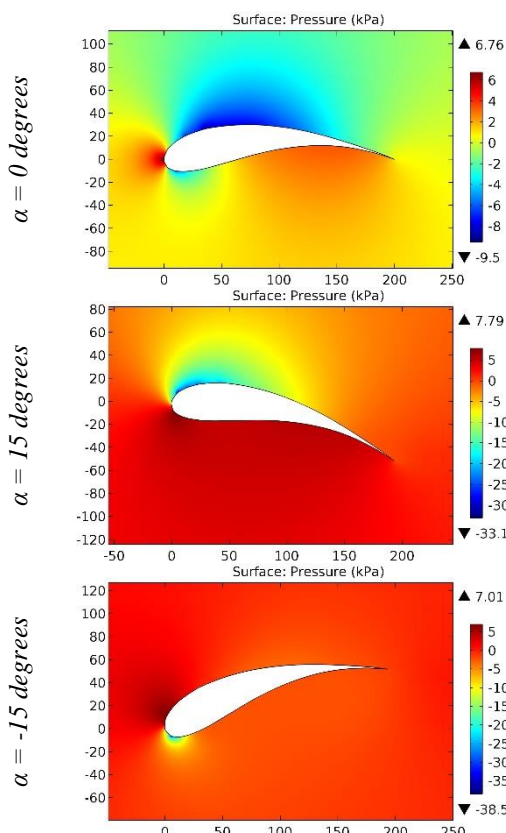


**Figure 76.** The pressure contours on the surfaces of the GOE 652 airfoil.

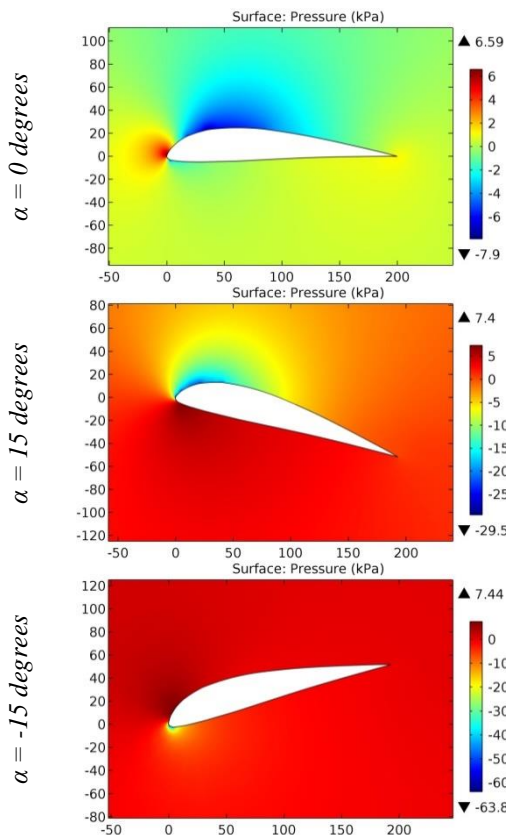


**Figure 77.** The pressure contours on the surfaces of the GOE 654 airfoil.

**Impact Factor:**

ISRA (India)	= 6.317	SIS (USA)	= 0.912	ICV (Poland)	= 6.630
ISI (Dubai, UAE)	= 1.582	РИНЦ (Russia)	= 3.939	PIF (India)	= 1.940
GIF (Australia)	= 0.564	ESJI (KZ)	= 8.771	IBI (India)	= 4.260
JIF	= 1.500	SJIF (Morocco)	= 7.184	OAJI (USA)	= 0.350

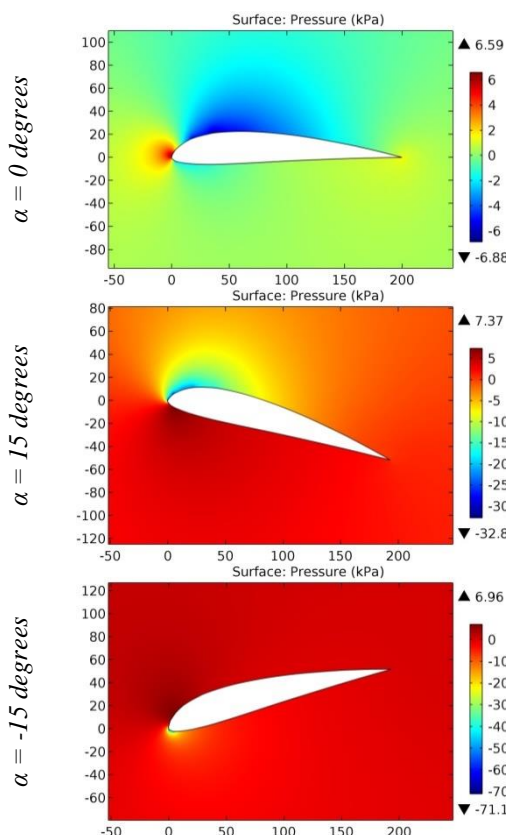


Figure 78. The pressure contours on the surfaces of the GOE 655 airfoil.

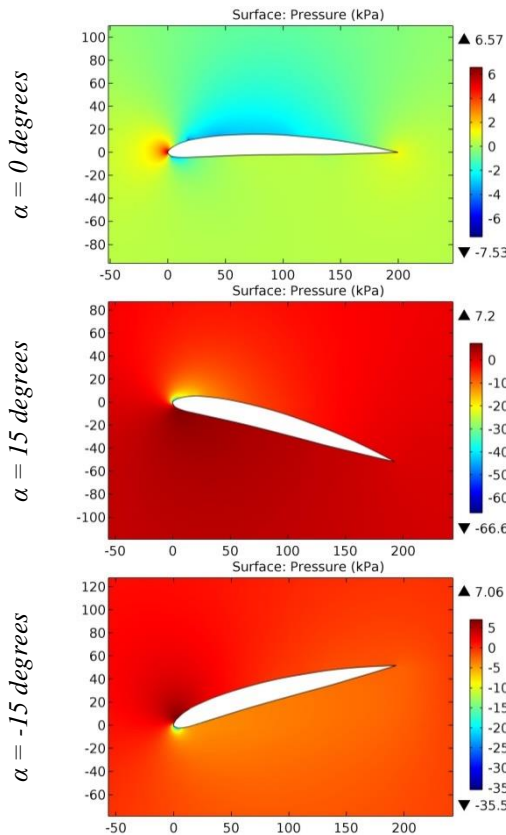
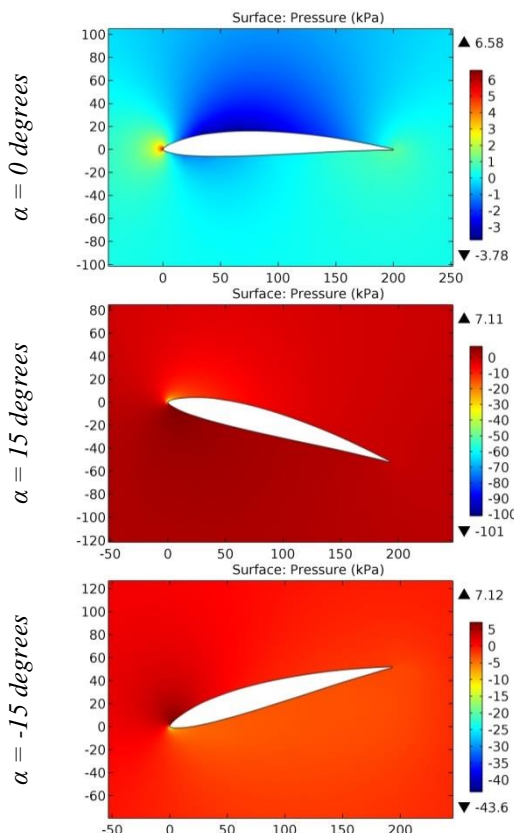
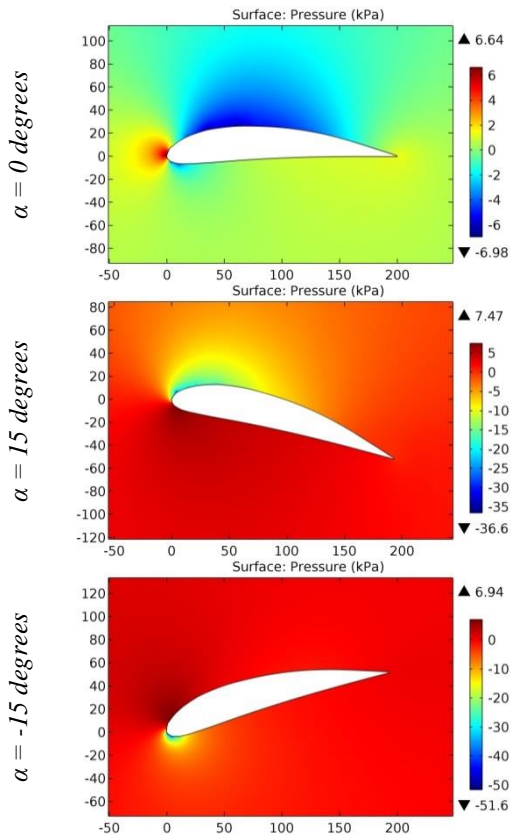


Figure 79. The pressure contours on the surfaces of the GOE 670 airfoil.



**Figure 80.** The pressure contours on the surfaces of the GOE 673 airfoil.



**Figure 81.** The pressure contours on the surfaces of the GOE 675 airfoil.

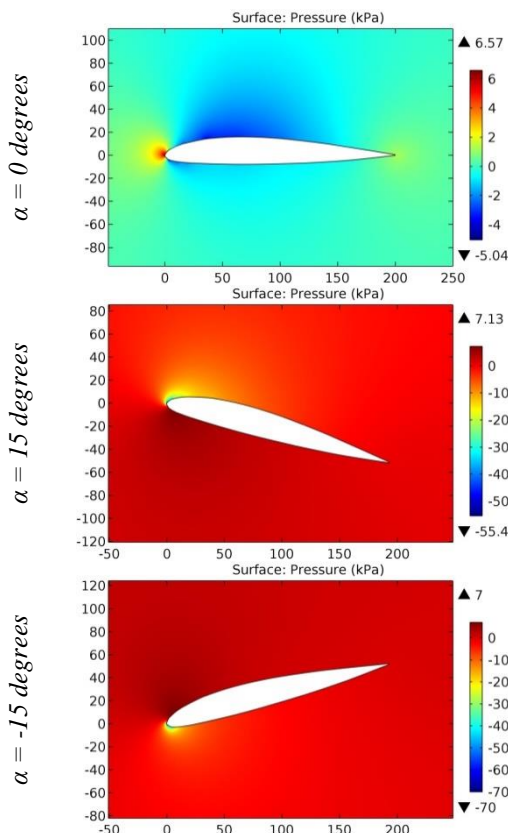


**Figure 82.** The pressure contours on the surfaces of the GOE 676 (= M 12) airfoil.

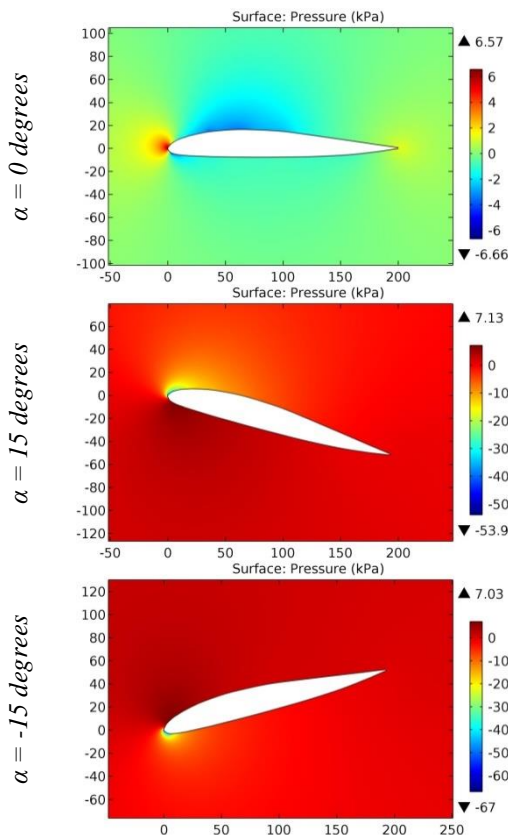


**Figure 83.** The pressure contours on the surfaces of the GOE 677 (= M 6) airfoil.

ISRA (India) = 6.317	SIS (USA) = 0.912	ICV (Poland) = 6.630
ISI (Dubai, UAE) = 1.582	РИНЦ (Russia) = 3.939	PIF (India) = 1.940
GIF (Australia) = 0.564	ESJI (KZ) = 8.771	IBI (India) = 4.260
JIF = 1.500	SJIF (Morocco) = 7.184	OAJI (USA) = 0.350

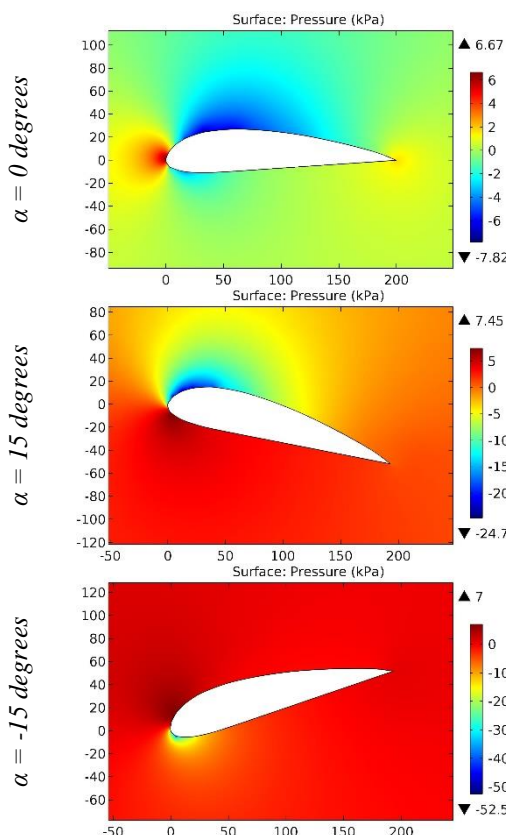


Figure 84. The pressure contours on the surfaces of the GOE 679 airfoil.

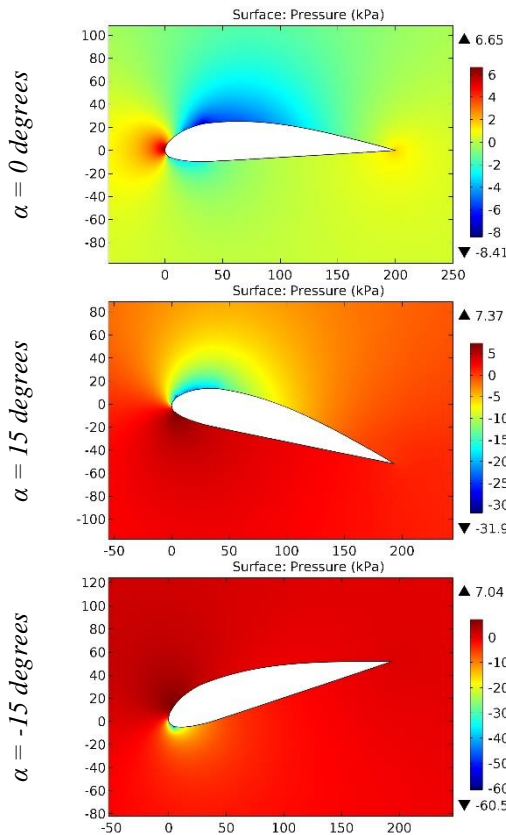
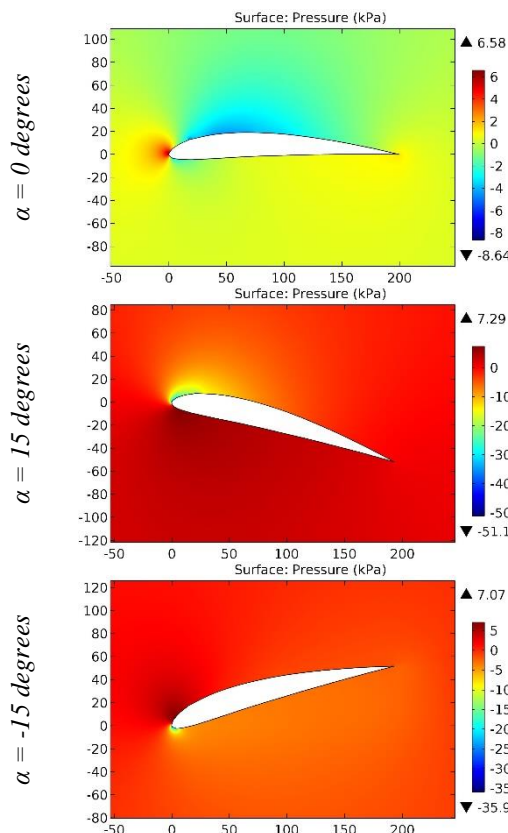
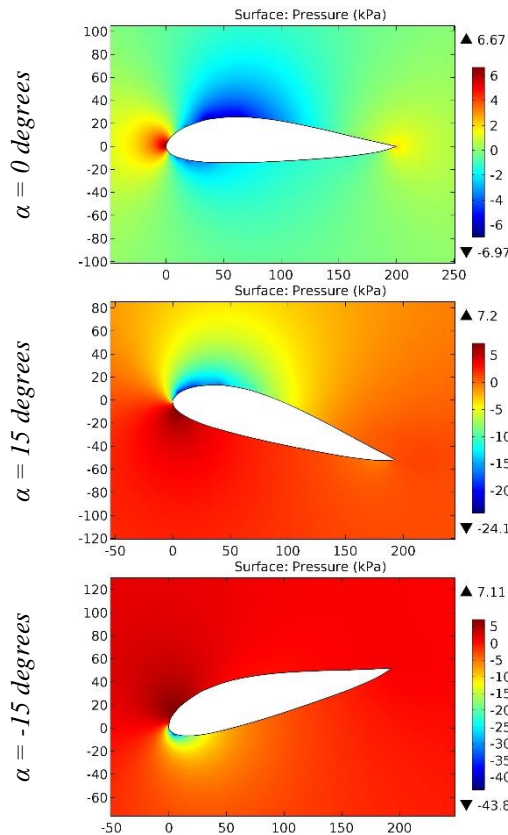


Figure 85. The pressure contours on the surfaces of the GOE 681 airfoil.

ISRA (India)	= 6.317	SIS (USA)	= 0.912	ICV (Poland)	= 6.630
ISI (Dubai, UAE)	= 1.582	РИНЦ (Russia)	= 3.939	PIF (India)	= 1.940
GIF (Australia)	= 0.564	ESJI (KZ)	= 8.771	IBI (India)	= 4.260
JIF	= 1.500	SJIF (Morocco)	= 7.184	OAJI (USA)	= 0.350



**Figure 86.** The pressure contours on the surfaces of the GOE 682 airfoil.



**Figure 87.** The pressure contours on the surfaces of the GOE 683 airfoil.

ISRA (India)	= 6.317	SIS (USA)	= 0.912	ICV (Poland)	= 6.630
ISI (Dubai, UAE)	= 1.582	РИНЦ (Russia)	= 3.939	PIF (India)	= 1.940
GIF (Australia)	= 0.564	ESJI (KZ)	= 8.771	IBI (India)	= 4.260
JIF	= 1.500	SJIF (Morocco)	= 7.184	OAJI (USA)	= 0.350

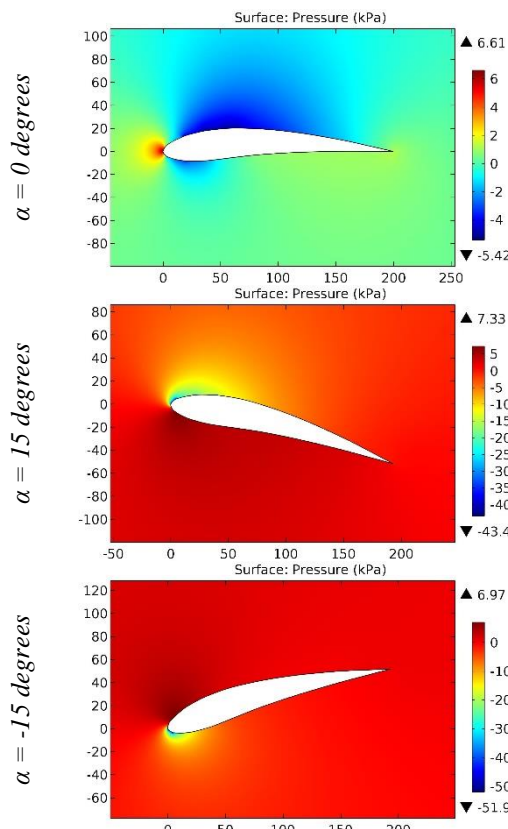


**Figure 88.** The pressure contours on the surfaces of the GOE 685 airfoil.

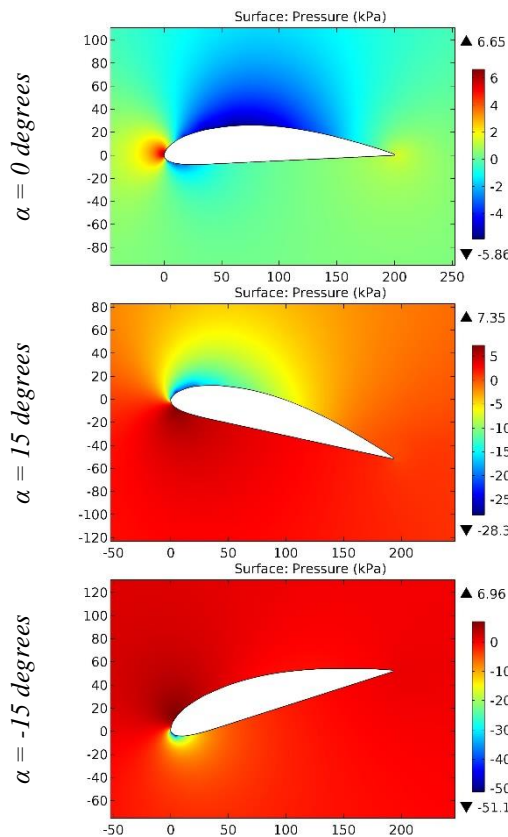


**Figure 89.** The pressure contours on the surfaces of the GOE 692 airfoil.

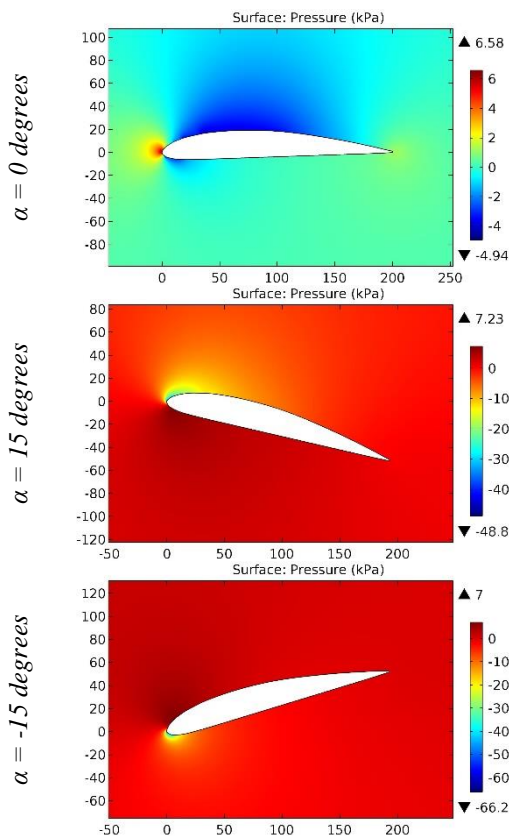


**Figure 90.** The pressure contours on the surfaces of the GOE 693 airfoil.

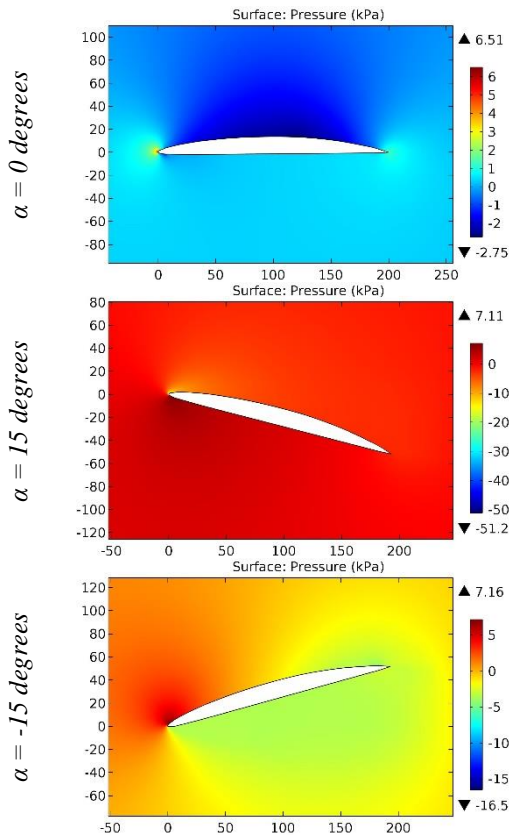


**Figure 91.** The pressure contours on the surfaces of the GOE 6K airfoil.

ISRA (India)	= 6.317	SIS (USA)	= 0.912	ICV (Poland)	= 6.630
ISI (Dubai, UAE)	= 1.582	РИНЦ (Russia)	= 3.939	PIF (India)	= 1.940
GIF (Australia)	= 0.564	ESJI (KZ)	= 8.771	IBI (India)	= 4.260
JIF	= 1.500	SJIF (Morocco)	= 7.184	OAJI (USA)	= 0.350

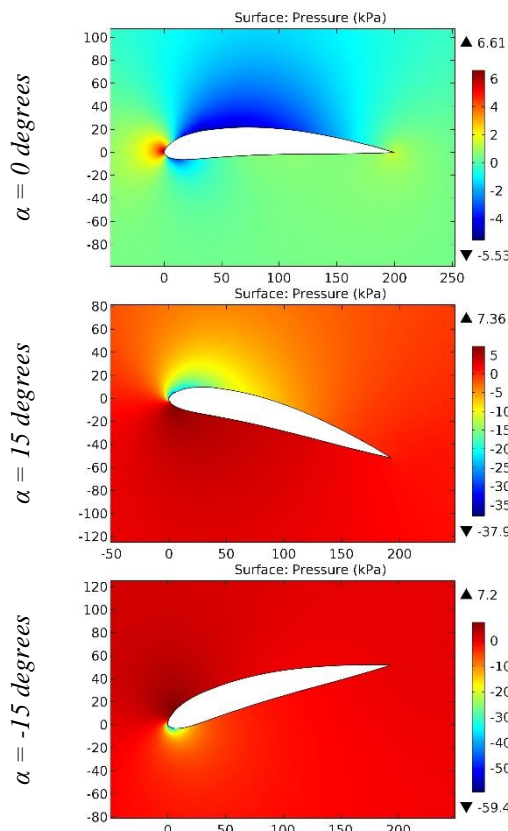


Figure 92. The pressure contours on the surfaces of the GOE 701 airfoil.

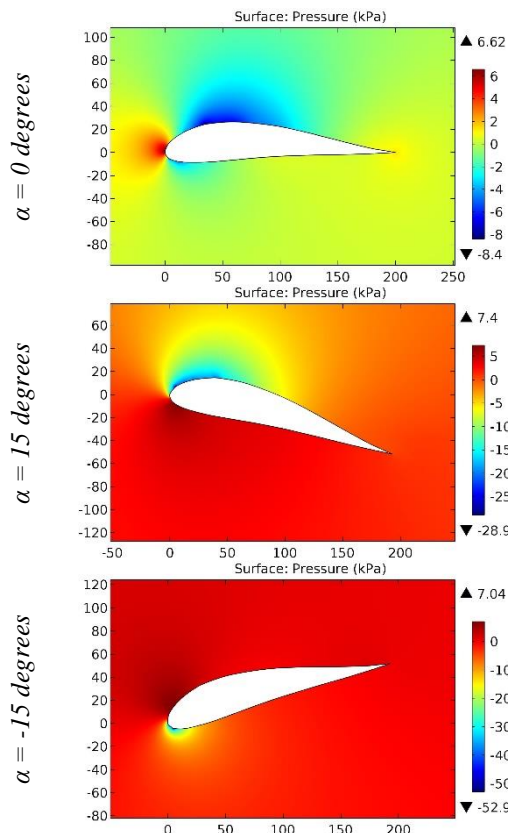


Figure 93. The pressure contours on the surfaces of the GOE 702 airfoil.

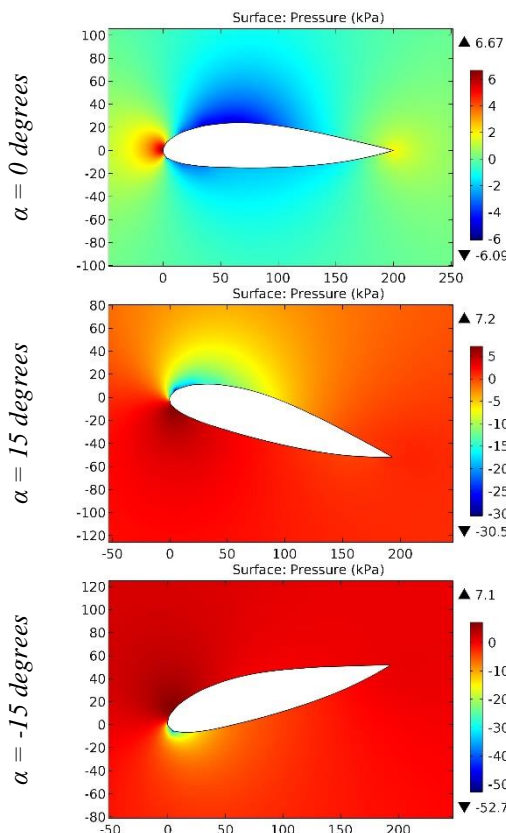


Figure 94. The pressure contours on the surfaces of the GOE 703 airfoil.

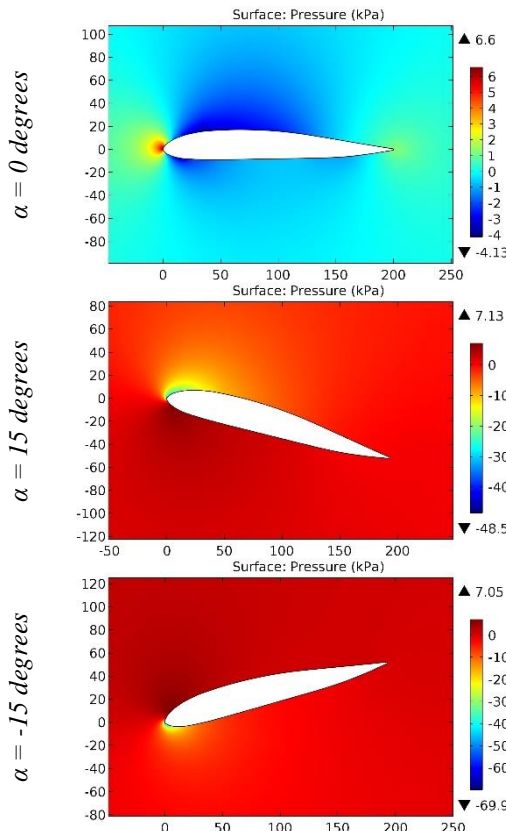


Figure 95. The pressure contours on the surfaces of the GOE 704 airfoil.

ISRA (India)	= 6.317	SIS (USA)	= 0.912	ICV (Poland)	= 6.630
ISI (Dubai, UAE)	= 1.582	РИНЦ (Russia)	= 3.939	PIF (India)	= 1.940
GIF (Australia)	= 0.564	ESJI (KZ)	= 8.771	IBI (India)	= 4.260
JIF	= 1.500	SJIF (Morocco)	= 7.184	OAJI (USA)	= 0.350

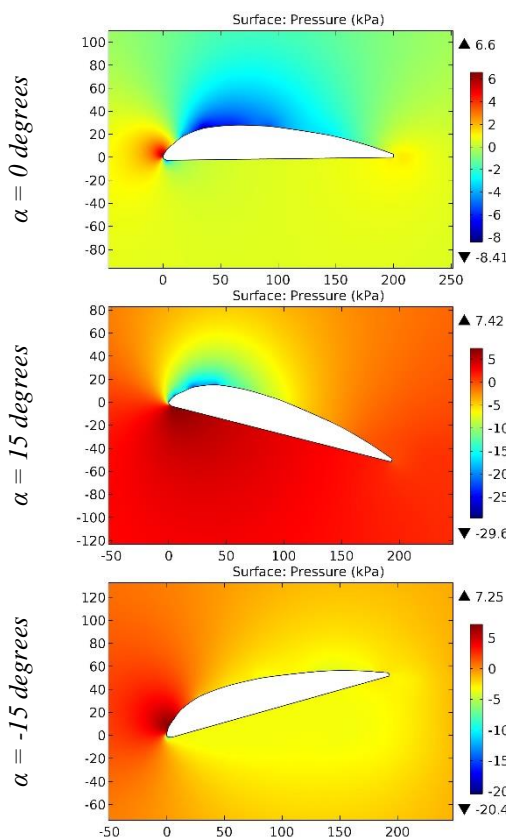


Figure 96. The pressure contours on the surfaces of the GOE 711 airfoil.

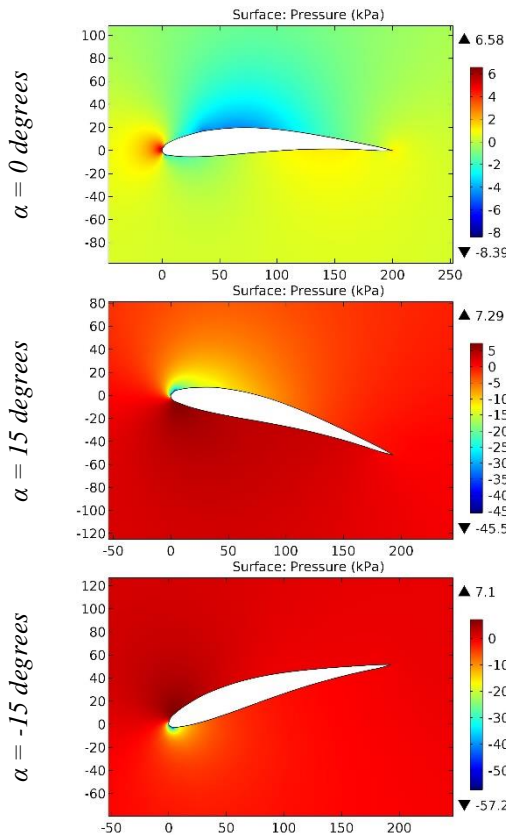
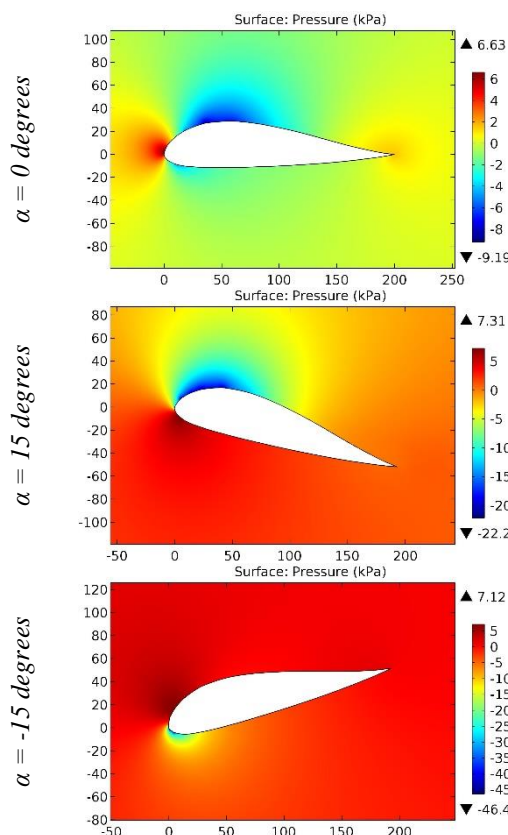
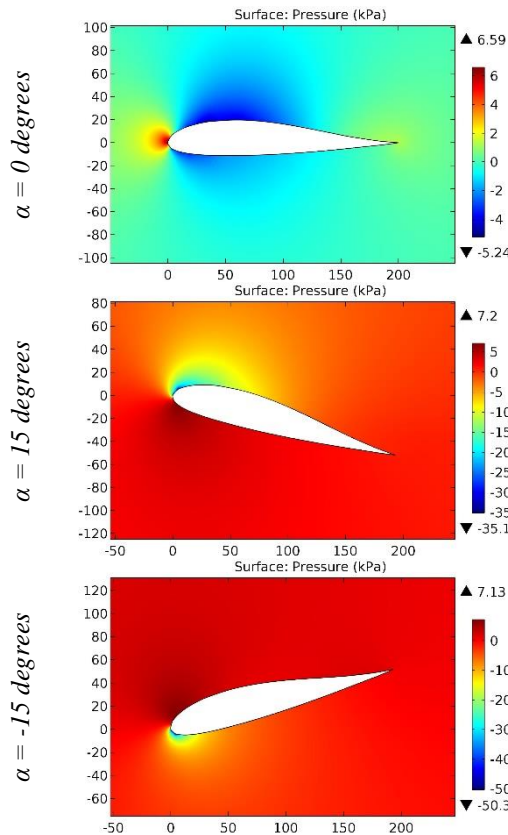


Figure 97. The pressure contours on the surfaces of the GOE 723 airfoil.

<b>ISRA (India)</b>	= <b>6.317</b>	<b>SIS (USA)</b>	= <b>0.912</b>	<b>ICV (Poland)</b>	= <b>6.630</b>
<b>ISI (Dubai, UAE)</b>	= <b>1.582</b>	<b>РИНЦ (Russia)</b>	= <b>3.939</b>	<b>PIF (India)</b>	= <b>1.940</b>
<b>GIF (Australia)</b>	= <b>0.564</b>	<b>ESJI (KZ)</b>	= <b>8.771</b>	<b>IBI (India)</b>	= <b>4.260</b>
<b>JIF</b>	= <b>1.500</b>	<b>SJIF (Morocco)</b>	= <b>7.184</b>	<b>OAJI (USA)</b>	= <b>0.350</b>



**Figure 98.** The pressure contours on the surfaces of the GOE 735 airfoil.



**Figure 99.** The pressure contours on the surfaces of the GOE 738 airfoil.

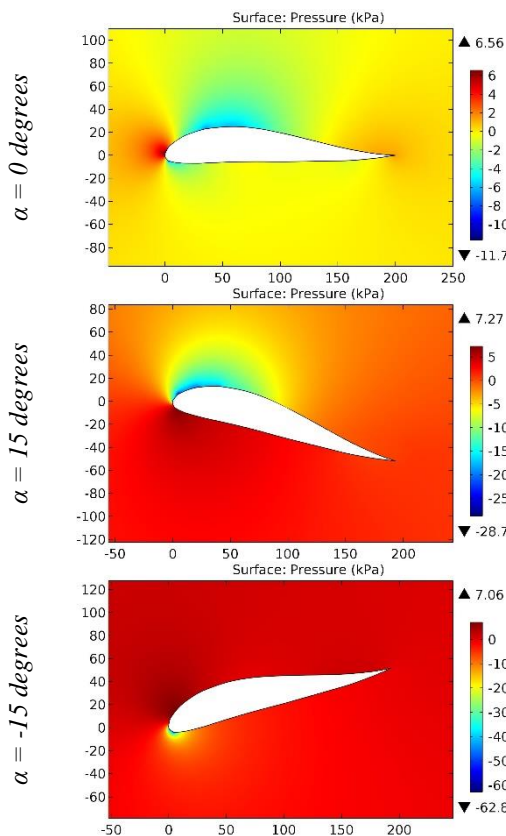


**Figure 100.** The pressure contours on the surfaces of the GOE 741 airfoil.

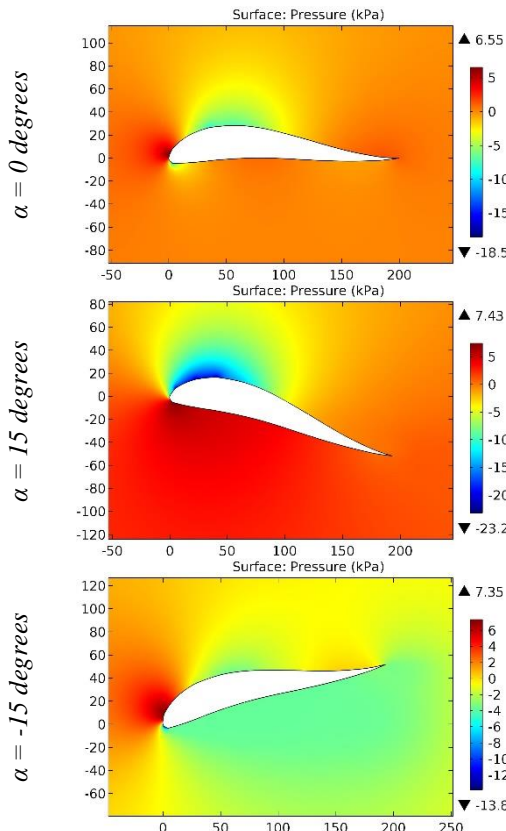


**Figure 101.** The pressure contours on the surfaces of the GOE 744 airfoil.

**Impact Factor:**

ISRA (India)	= 6.317	SIS (USA)	= 0.912	ICV (Poland)	= 6.630
ISI (Dubai, UAE)	= 1.582	РИНЦ (Russia)	= 3.939	PIF (India)	= 1.940
GIF (Australia)	= 0.564	ESJI (KZ)	= 8.771	IBI (India)	= 4.260
JIF	= 1.500	SJIF (Morocco)	= 7.184	OAJI (USA)	= 0.350

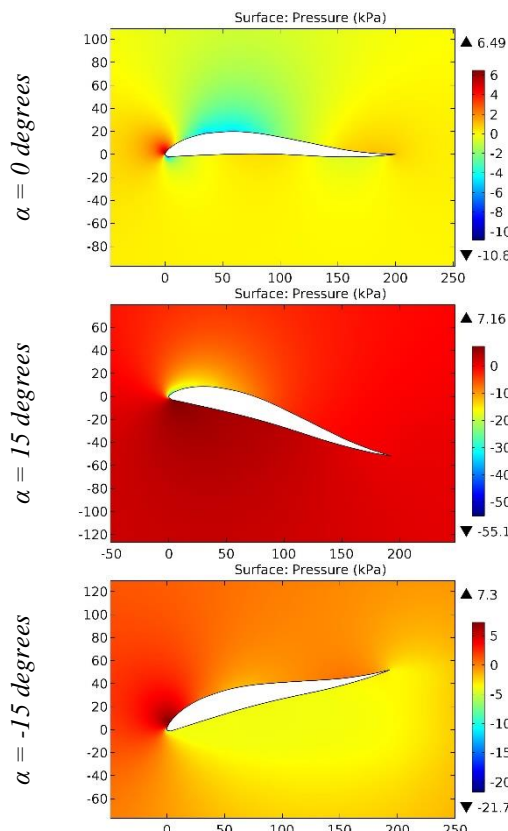


Figure 102. The pressure contours on the surfaces of the GOE 746 airfoil.

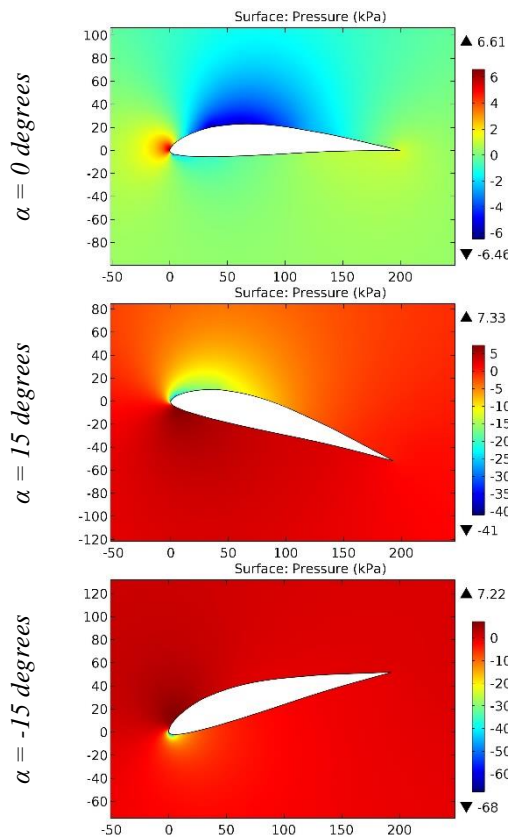


Figure 103. The pressure contours on the surfaces of the GOE 758 airfoil.

**Impact Factor:**

ISRA (India)	= 6.317	SIS (USA)	= 0.912	ICV (Poland)	= 6.630
ISI (Dubai, UAE)	= 1.582	РИНЦ (Russia)	= 3.939	PIF (India)	= 1.940
GIF (Australia)	= 0.564	ESJI (KZ)	= 8.771	IBI (India)	= 4.260
JIF	= 1.500	SJIF (Morocco)	= 7.184	OAJI (USA)	= 0.350

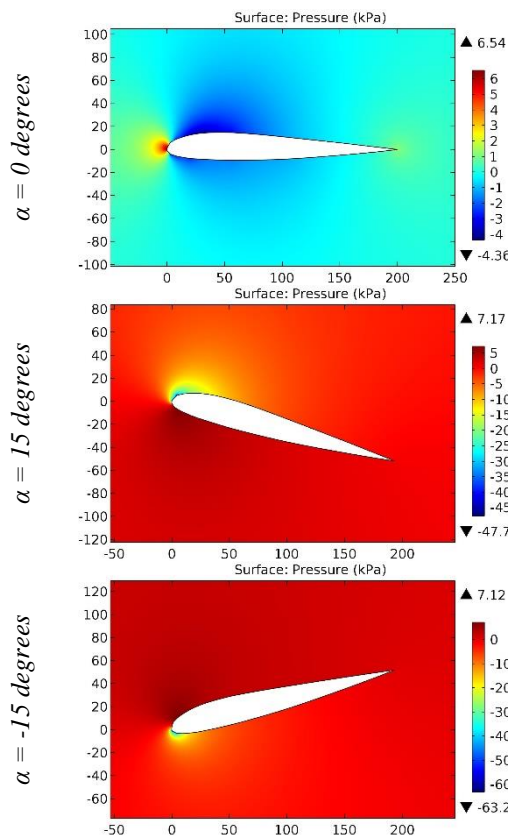


Figure 104. The pressure contours on the surfaces of the GOE 766 airfoil.

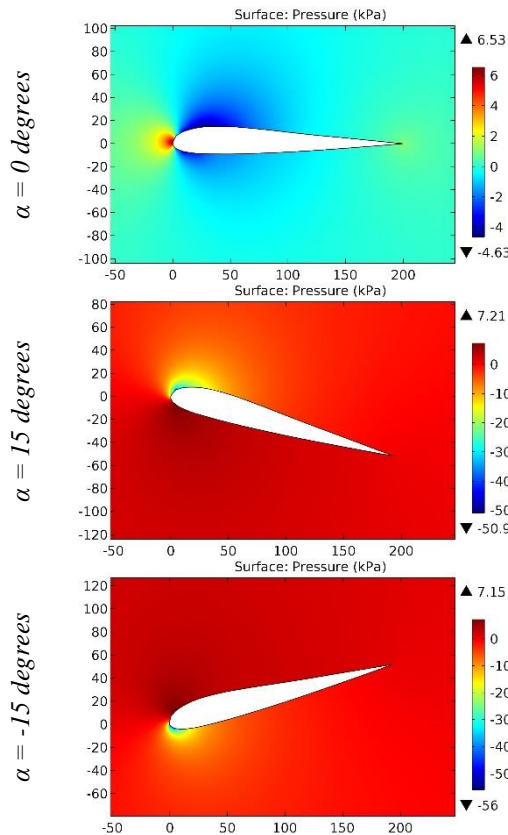
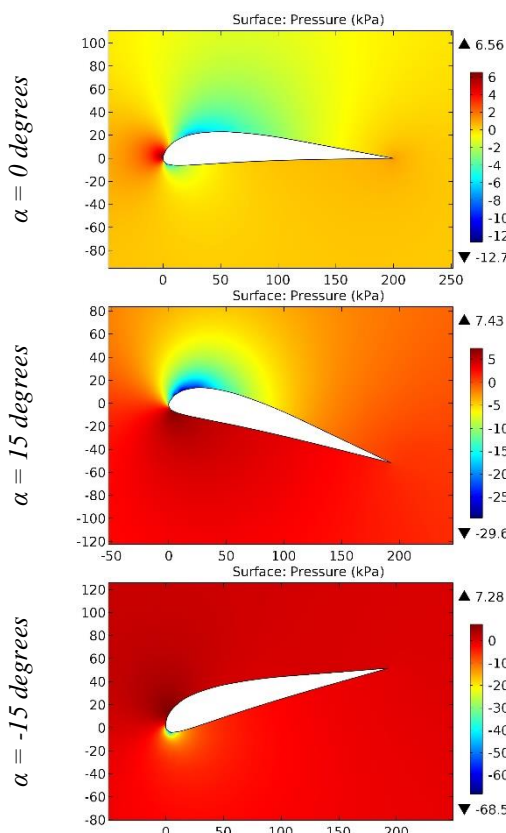
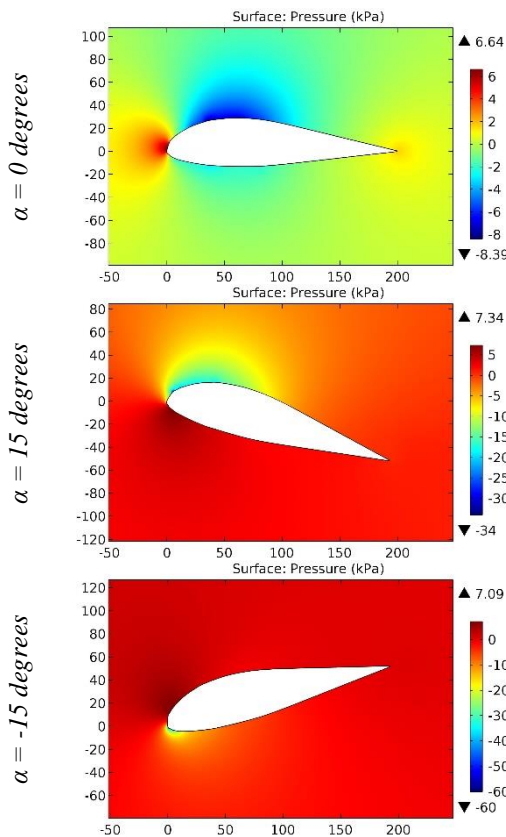


Figure 105. The pressure contours on the surfaces of the GOE 767 airfoil.

ISRA (India) = 6.317	SIS (USA) = 0.912	ICV (Poland) = 6.630
ISI (Dubai, UAE) = 1.582	РИНЦ (Russia) = 3.939	PIF (India) = 1.940
GIF (Australia) = 0.564	ESJI (KZ) = 8.771	IBI (India) = 4.260
JIF = 1.500	SJIF (Morocco) = 7.184	OAJI (USA) = 0.350



**Figure 106.** The pressure contours on the surfaces of the GOE 769 airfoil.



**Figure 107.** The pressure contours on the surfaces of the GOE 770 airfoil.

ISRA (India)	= 6.317	SIS (USA)	= 0.912	ICV (Poland)	= 6.630
ISI (Dubai, UAE)	= 1.582	РИНЦ (Russia)	= 3.939	PIF (India)	= 1.940
GIF (Australia)	= 0.564	ESJI (KZ)	= 8.771	IBI (India)	= 4.260
JIF	= 1.500	SJIF (Morocco)	= 7.184	OAJI (USA)	= 0.350

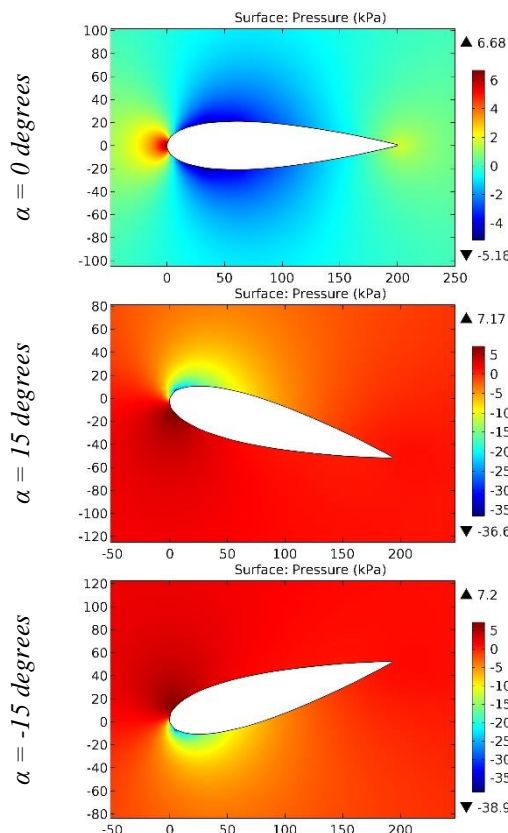


**Figure 108.** The pressure contours on the surfaces of the GOE 775 airfoil.

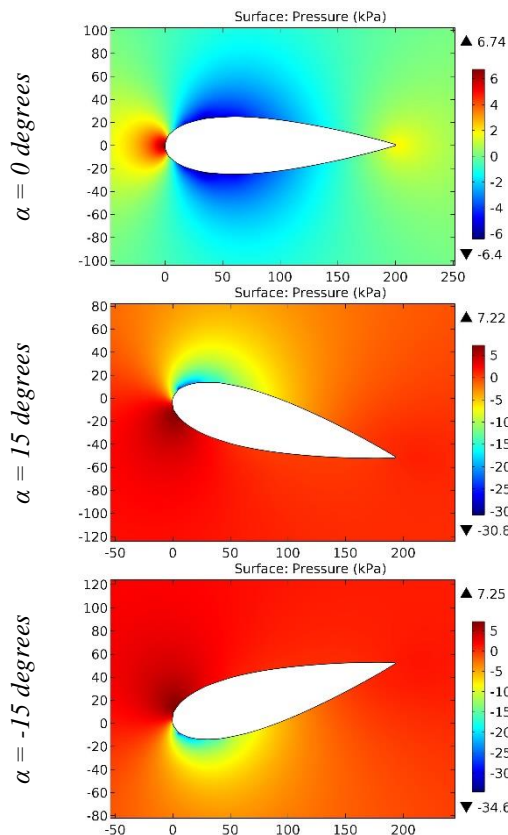


**Figure 109.** The pressure contours on the surfaces of the GOE 776 airfoil.

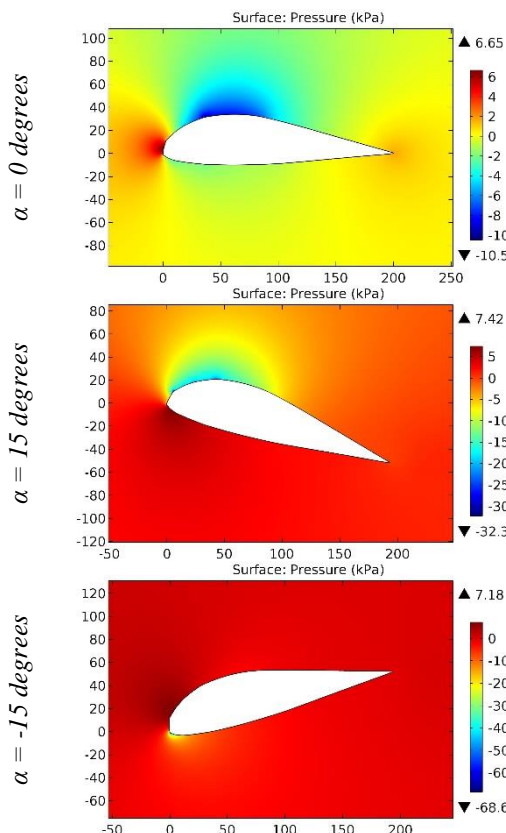


**Figure 110.** The pressure contours on the surfaces of the GOE 777 airfoil.

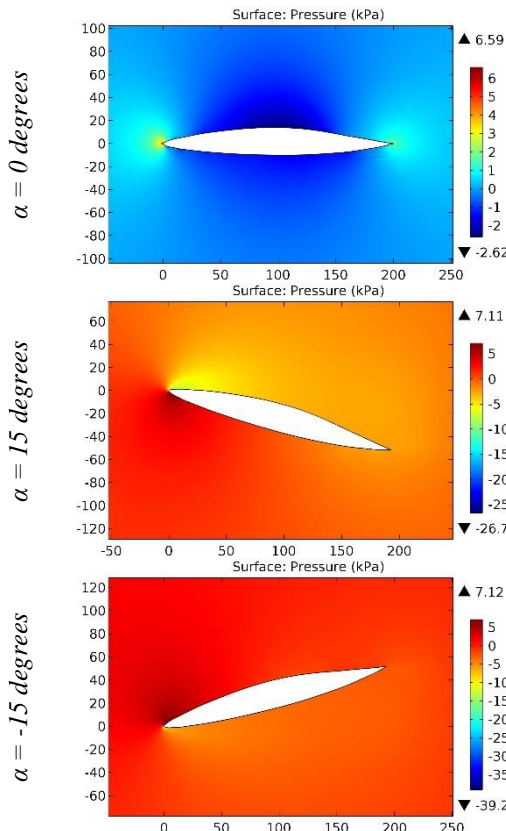


**Figure 111.** The pressure contours on the surfaces of the GOE 780 airfoil.

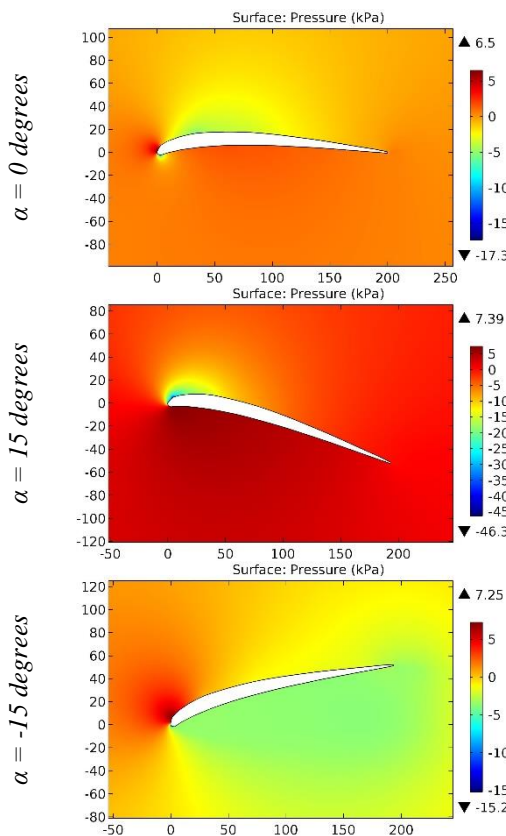


**Figure 112.** The pressure contours on the surfaces of the GOE 79 (PFALZ 11) airfoil.

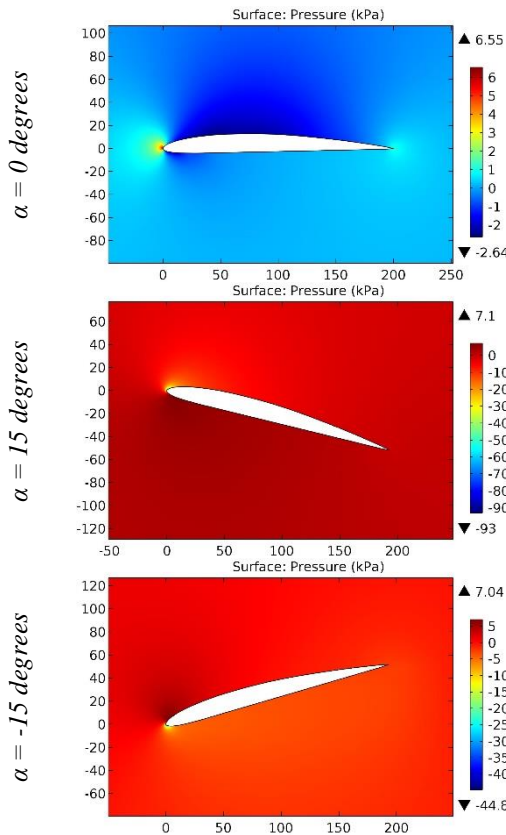


**Figure 113.** The pressure contours on the surfaces of the GOE 795 airfoil.

ISRA (India)	= 6.317	SIS (USA)	= 0.912	ICV (Poland)	= 6.630
ISI (Dubai, UAE)	= 1.582	РИНЦ (Russia)	= 3.939	PIF (India)	= 1.940
GIF (Australia)	= 0.564	ESJI (KZ)	= 8.771	IBI (India)	= 4.260
JIF	= 1.500	SJIF (Morocco)	= 7.184	OAJI (USA)	= 0.350

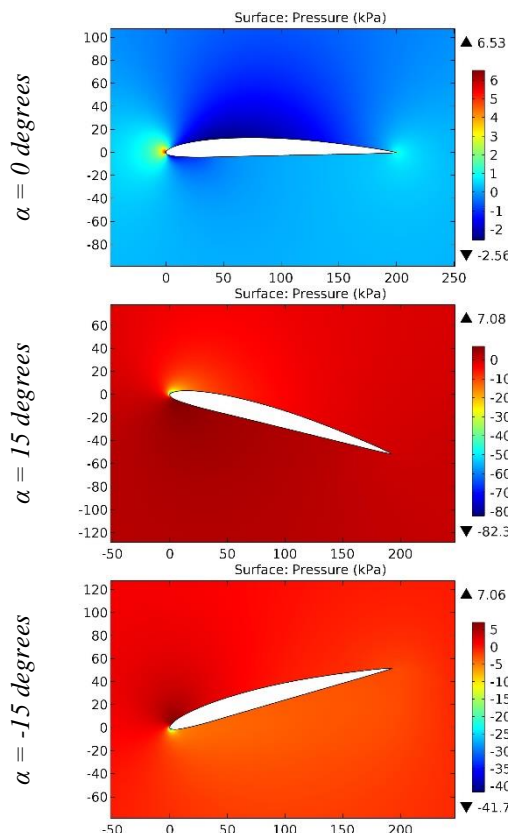


**Figure 114.** The pressure contours on the surfaces of the GOE 795 smoothed airfoil.

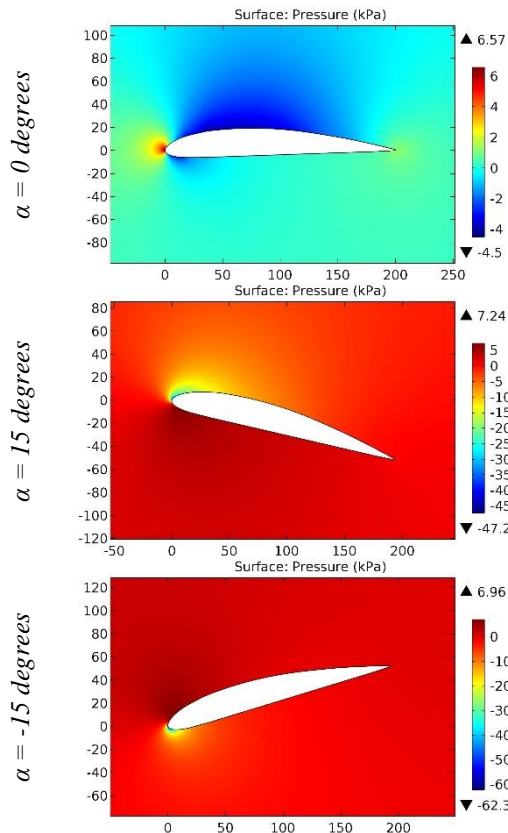


**Figure 115.** The pressure contours on the surfaces of the GOE 796 airfoil.

ISRA (India) = 6.317	SIS (USA) = 0.912	ICV (Poland) = 6.630
ISI (Dubai, UAE) = 1.582	РИНЦ (Russia) = 3.939	PIF (India) = 1.940
GIF (Australia) = 0.564	ESJI (KZ) = 8.771	IBI (India) = 4.260
JIF = 1.500	SJIF (Morocco) = 7.184	OAJI (USA) = 0.350

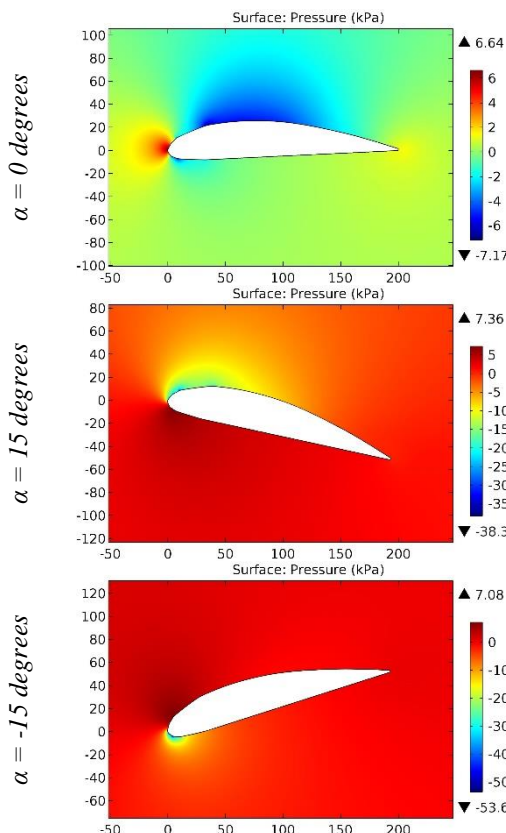


**Figure 116.** The pressure contours on the surfaces of the GOE 797 airfoil.

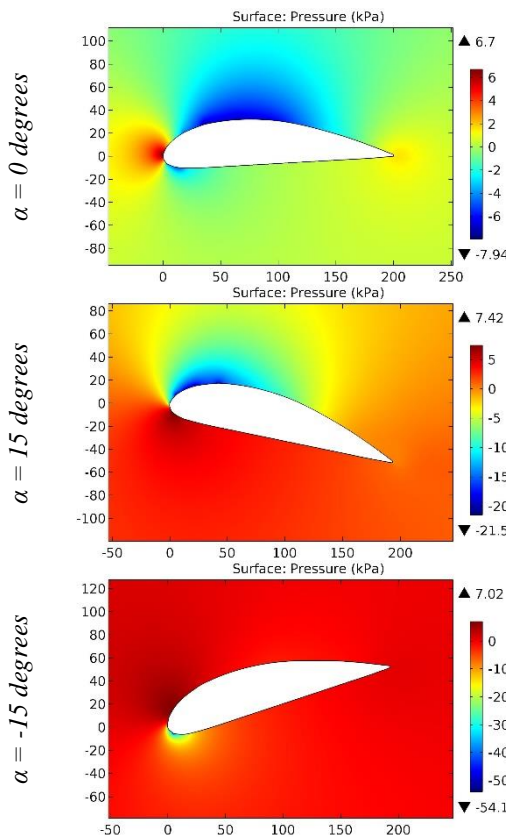


**Figure 117.** The pressure contours on the surfaces of the GOE 798 airfoil.

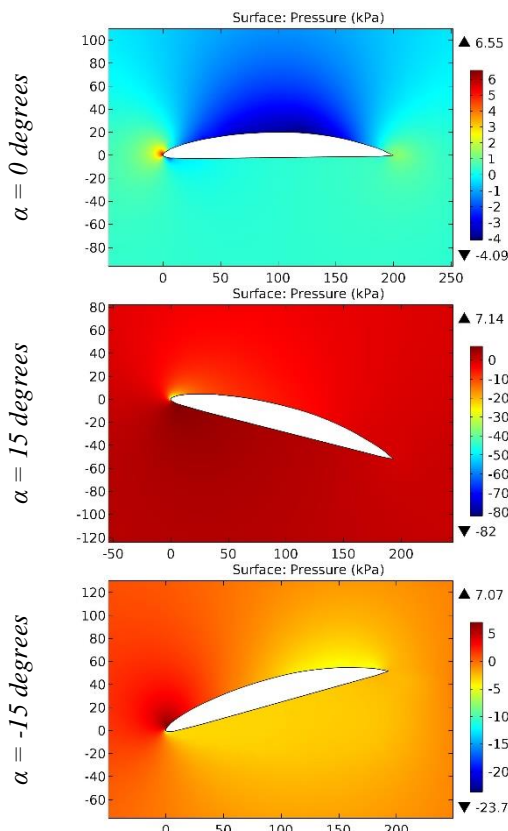


Figure 118. The pressure contours on the surfaces of the GOE 7K airfoil.

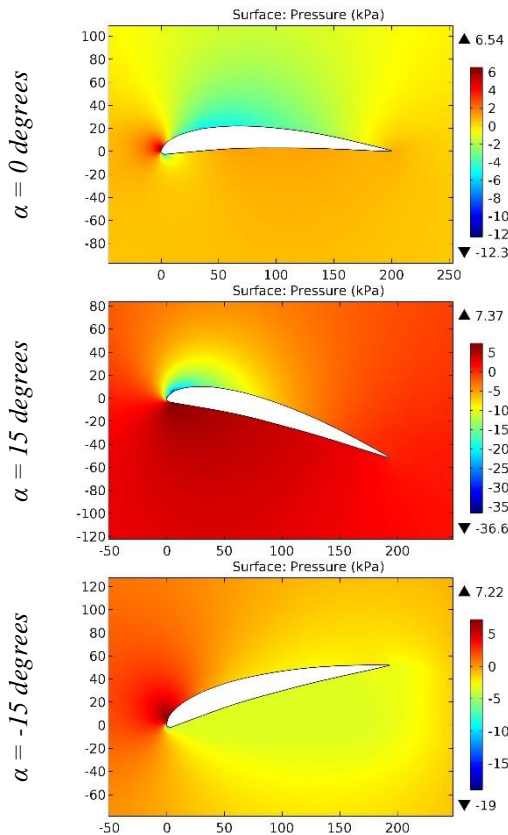
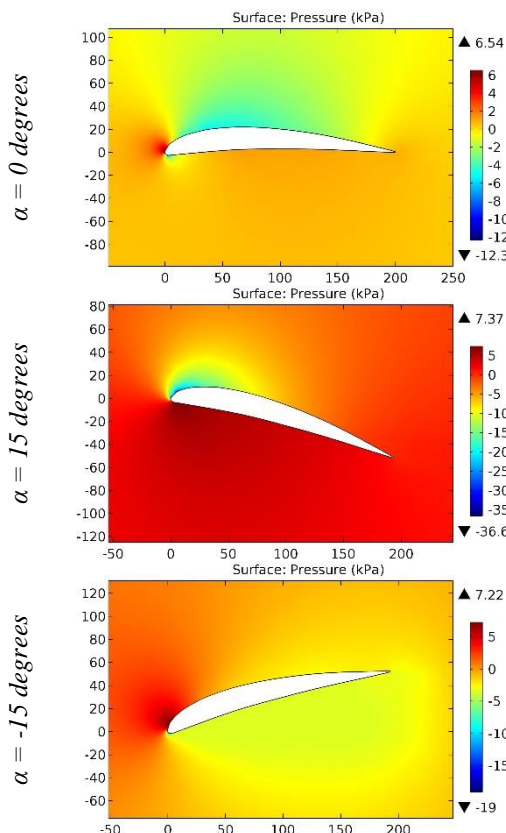
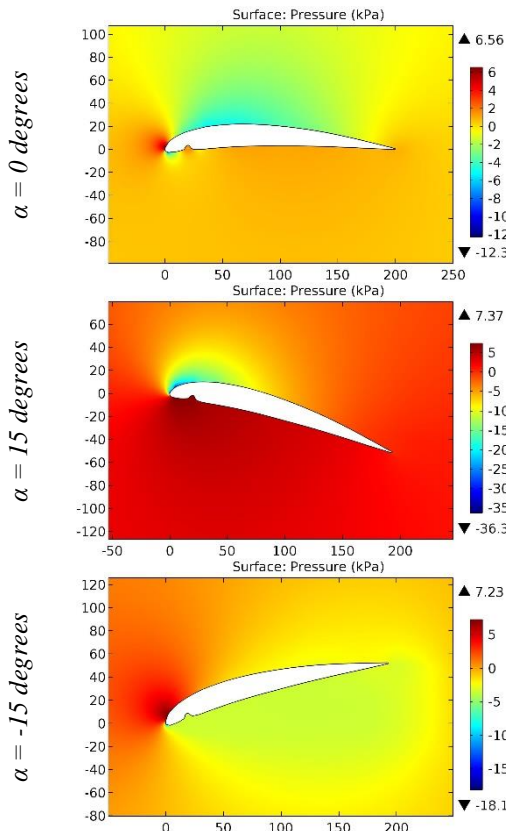


Figure 119. The pressure contours on the surfaces of the GOE 801 (MVA 301) airfoil.



**Figure 120.** The pressure contours on the surfaces of the GOE 802 airfoil.



**Figure 121.** The pressure contours on the surfaces of the GOE 802 A airfoil.

ISRA (India) = 6.317	SIS (USA) = 0.912	ICV (Poland) = 6.630
ISI (Dubai, UAE) = 1.582	РИНЦ (Russia) = 3.939	PIF (India) = 1.940
GIF (Australia) = 0.564	ESJI (KZ) = 8.771	IBI (India) = 4.260
JIF = 1.500	SJIF (Morocco) = 7.184	OAJI (USA) = 0.350

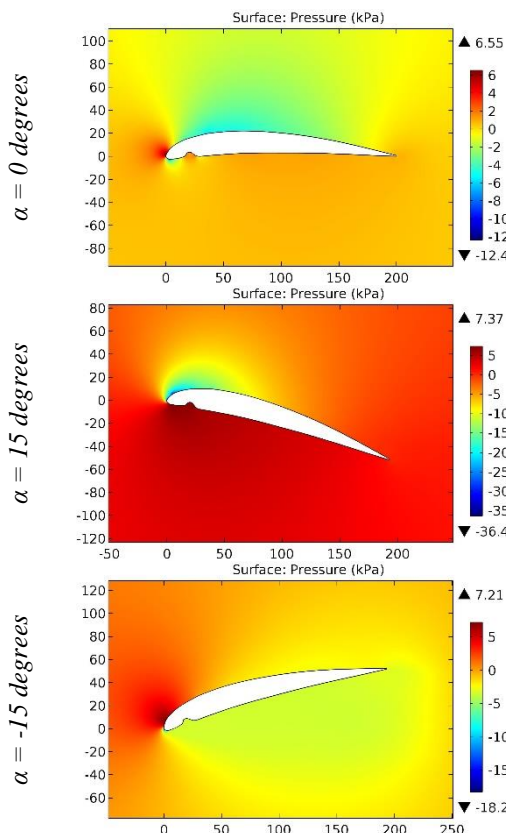


Figure 122. The pressure contours on the surfaces of the GOE 802 B airfoil.

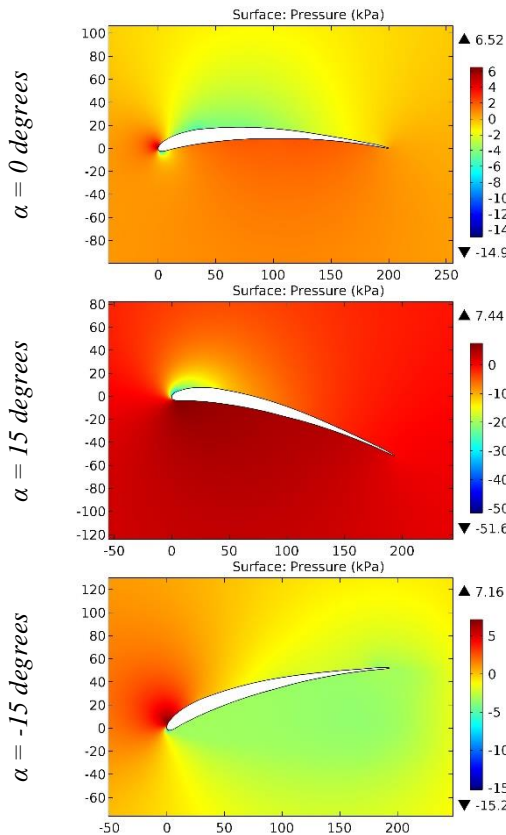


Figure 123. The pressure contours on the surfaces of the GOE 803 (HACKLINGER) airfoil.

## Impact Factor:

<b>ISRA (India)</b>	= <b>6.317</b>	<b>SIS (USA)</b>	= <b>0.912</b>	<b>ICV (Poland)</b>	= <b>6.630</b>
<b>ISI (Dubai, UAE)</b>	= <b>1.582</b>	<b>РИНЦ (Russia)</b>	= <b>3.939</b>	<b>PIF (India)</b>	= <b>1.940</b>
<b>GIF (Australia)</b>	= <b>0.564</b>	<b>ESJI (KZ)</b>	= <b>8.771</b>	<b>IBI (India)</b>	= <b>4.260</b>
<b>JIF</b>	= <b>1.500</b>	<b>SJIF (Morocco)</b>	= <b>7.184</b>	<b>OAJI (USA)</b>	= <b>0.350</b>

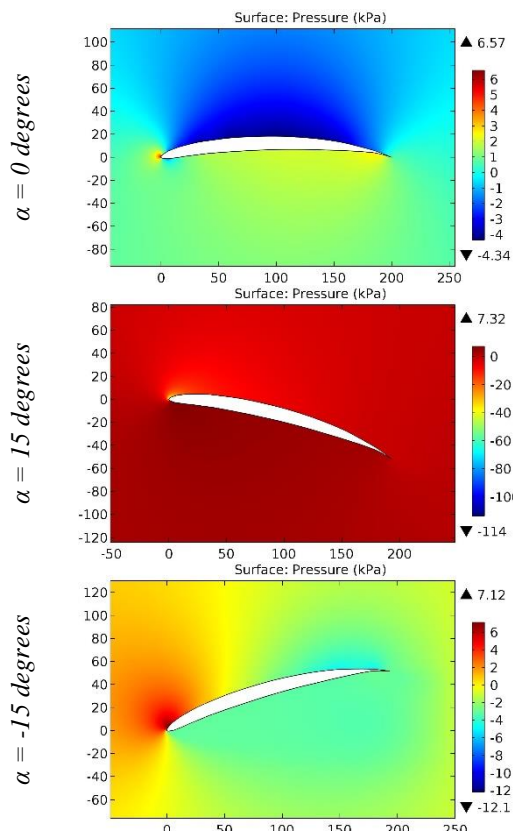


Figure 124. The pressure contours on the surfaces of the GOE 804 (EA 8) airfoil.

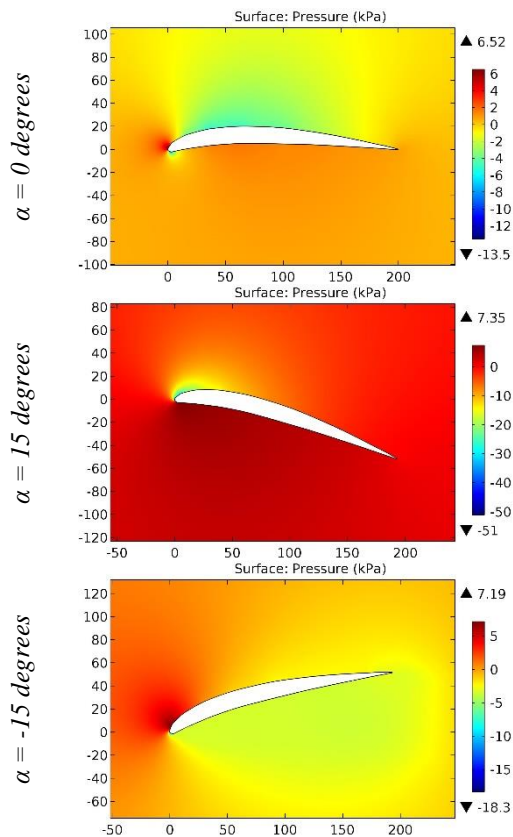
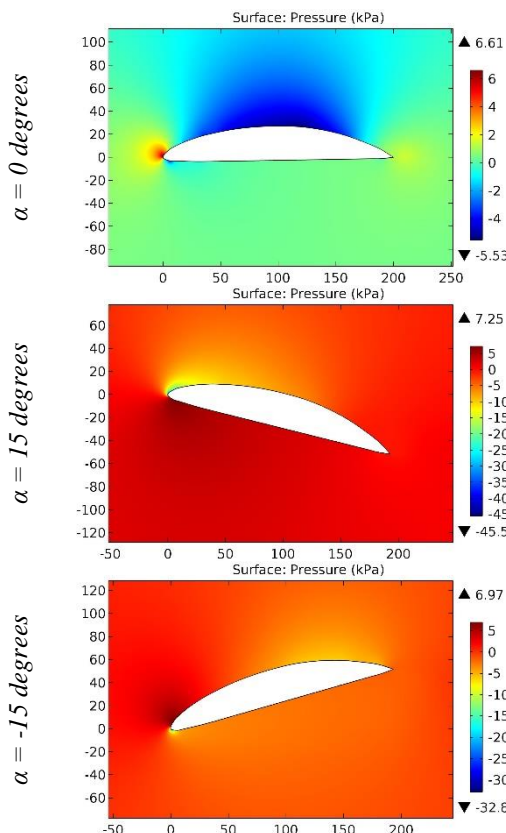
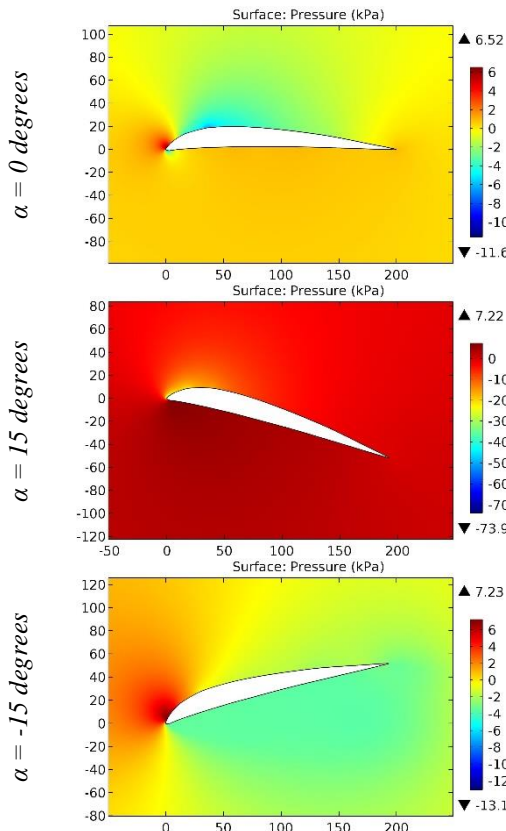


Figure 125. The pressure contours on the surfaces of the GOE 81 airfoil.

ISRA (India) = 6.317	SIS (USA) = 0.912	ICV (Poland) = 6.630
ISI (Dubai, UAE) = 1.582	РИНЦ (Russia) = 3.939	PIF (India) = 1.940
GIF (Australia) = 0.564	ESJI (KZ) = 8.771	IBI (India) = 4.260
JIF = 1.500	SJIF (Morocco) = 7.184	OAJI (USA) = 0.350



**Figure 126.** The pressure contours on the surfaces of the GOE 8K airfoil.



**Figure 127.** The pressure contours on the surfaces of the GOE 92 airfoil.

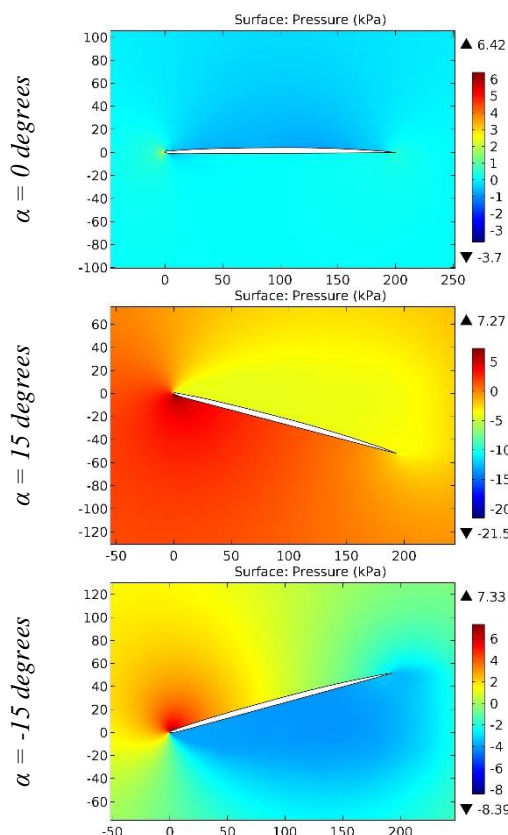


Figure 128. The pressure contours on the surfaces of the GOE 9K airfoil.

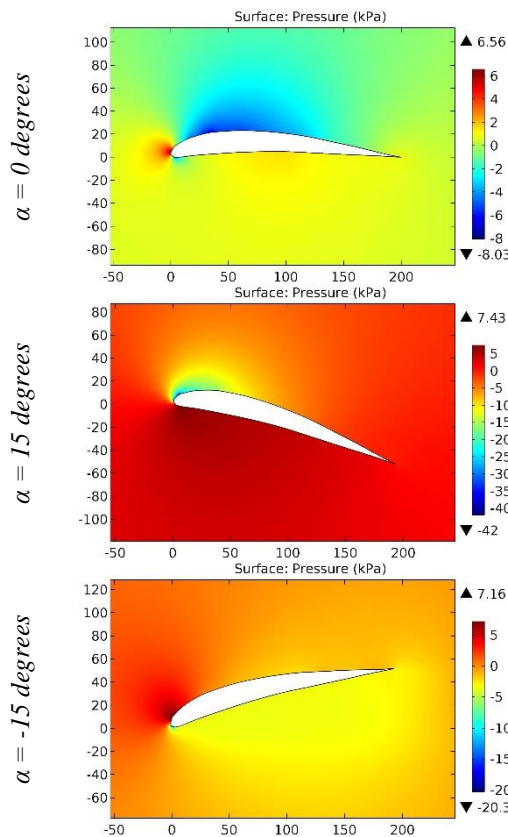


Figure 129. The pressure contours on the surfaces of the Goldberg G 5 airfoil.

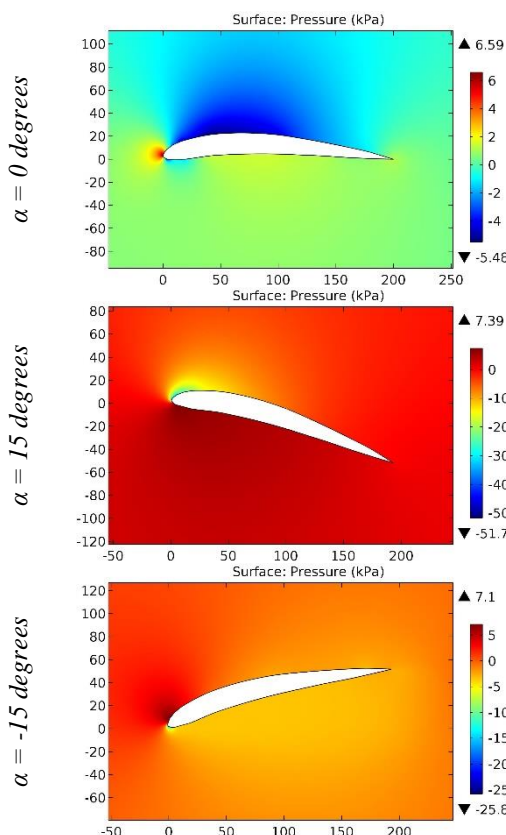


Figure 130. The pressure contours on the surfaces of the Goldberg Zipper airfoil.

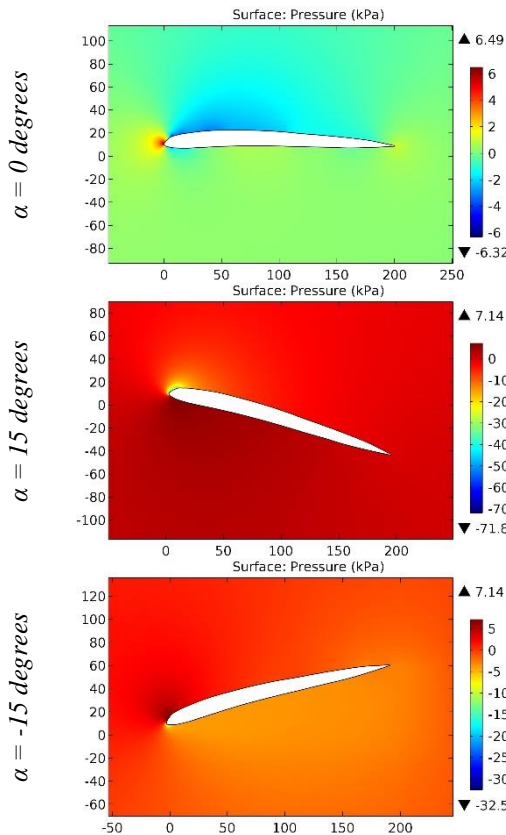
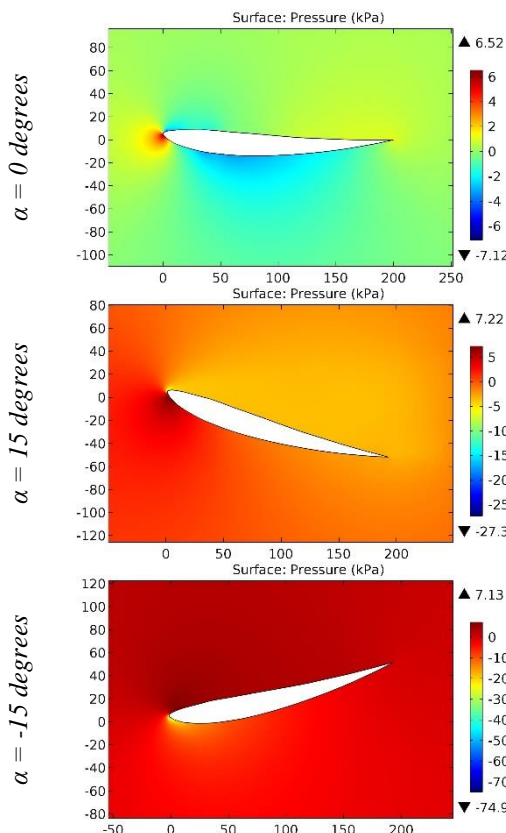
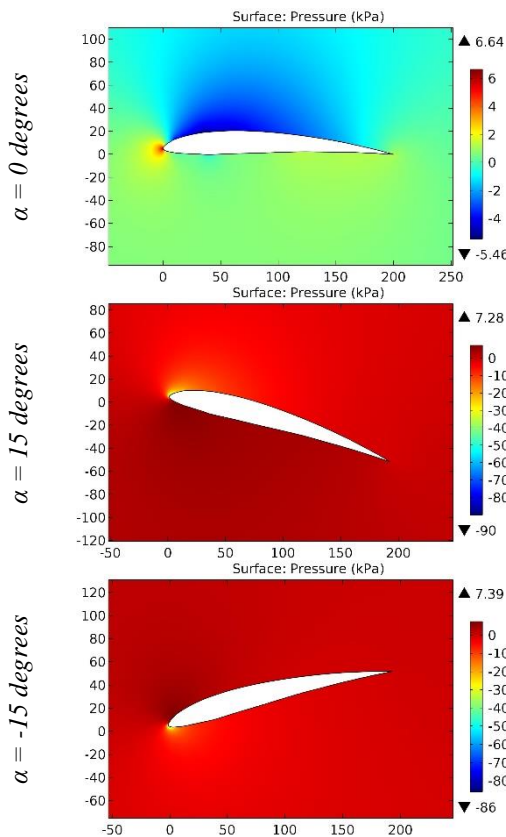


Figure 131. The pressure contours on the surfaces of the GOLDBRG6 airfoil.



**Figure 132.** The pressure contours on the surfaces of the GOO602 airfoil.



**Figure 133.** The pressure contours on the surfaces of the GOO620M airfoil.

ISRA (India) = 6.317	SIS (USA) = 0.912	ICV (Poland) = 6.630
ISI (Dubai, UAE) = 1.582	РИНЦ (Russia) = 3.939	PIF (India) = 1.940
GIF (Australia) = 0.564	ESJI (KZ) = 8.771	IBI (India) = 4.260
JIF = 1.500	SJIF (Morocco) = 7.184	OAJI (USA) = 0.350

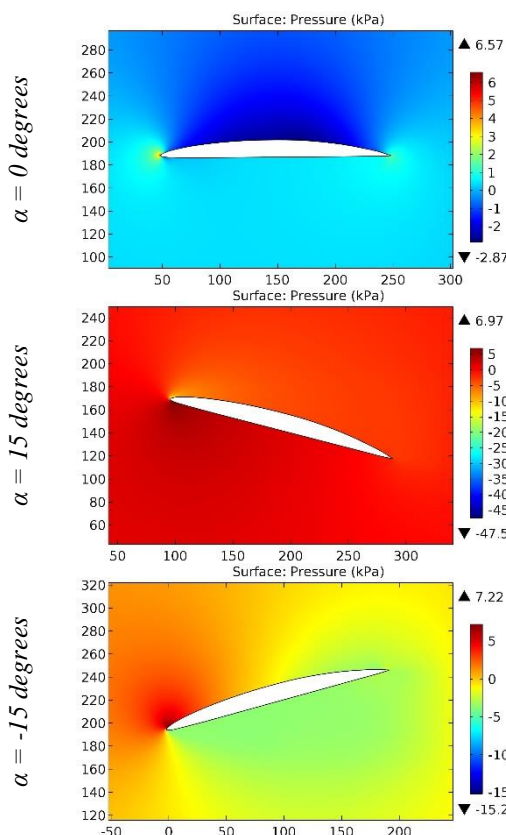


**Figure 134.** The pressure contours on the surfaces of the Gottingen 6K airfoil.

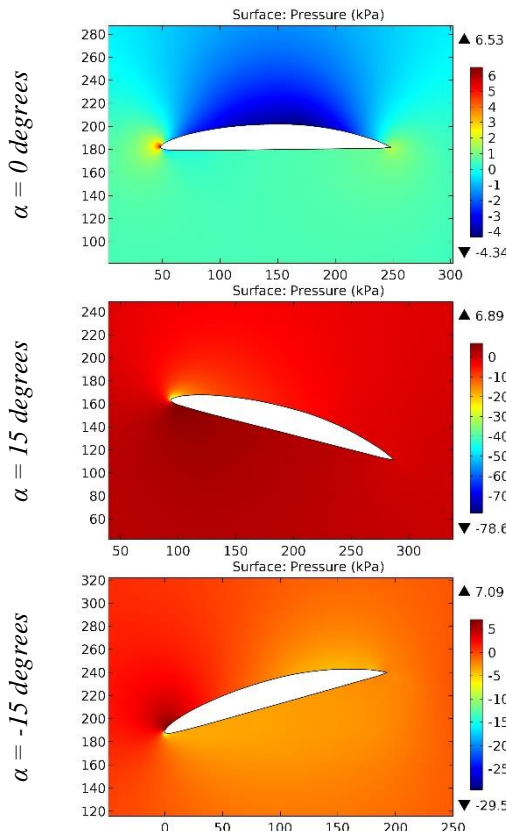


**Figure 135.** The pressure contours on the surfaces of the Gottingen 7K airfoil.

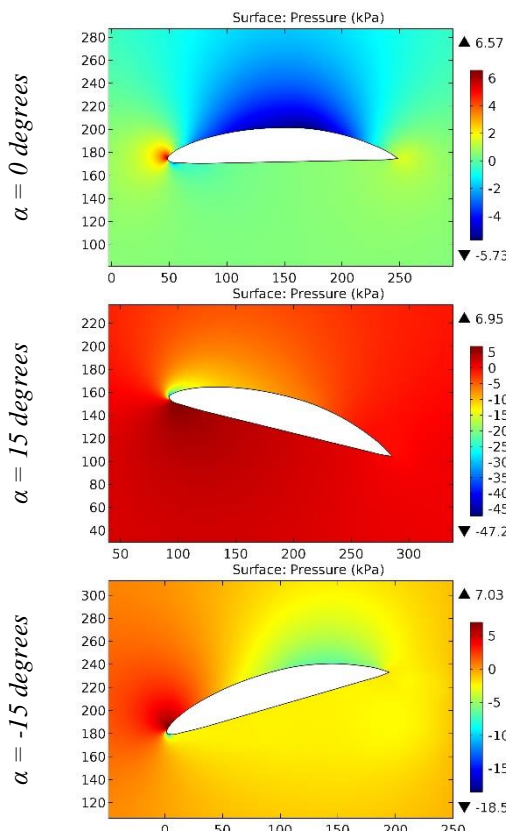


**Figure 136.** The pressure contours on the surfaces of the Gottingen 8K airfoil.

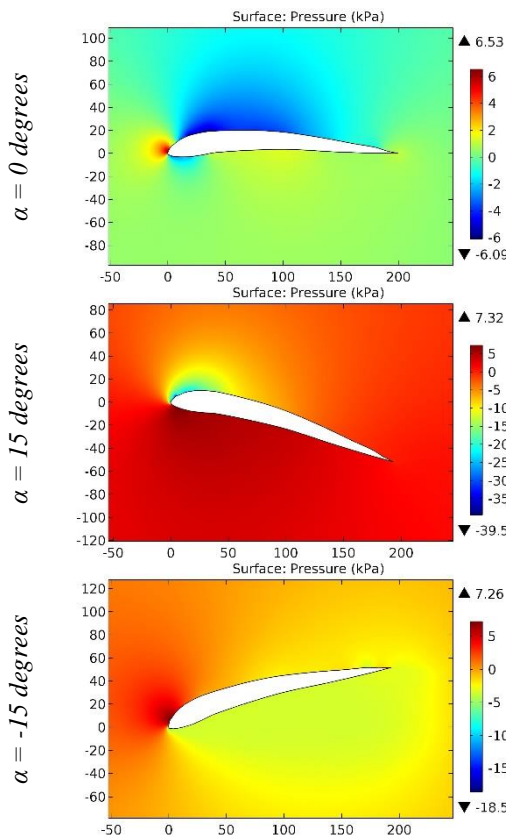


**Figure 137.** The pressure contours on the surfaces of the Grant G10 airfoil.

ISRA (India)	= 6.317	SIS (USA)	= 0.912	ICV (Poland)	= 6.630
ISI (Dubai, UAE)	= 1.582	РИНЦ (Russia)	= 3.939	PIF (India)	= 1.940
GIF (Australia)	= 0.564	ESJI (KZ)	= 8.771	IBI (India)	= 4.260
JIF	= 1.500	SJIF (Morocco)	= 7.184	OAJI (USA)	= 0.350

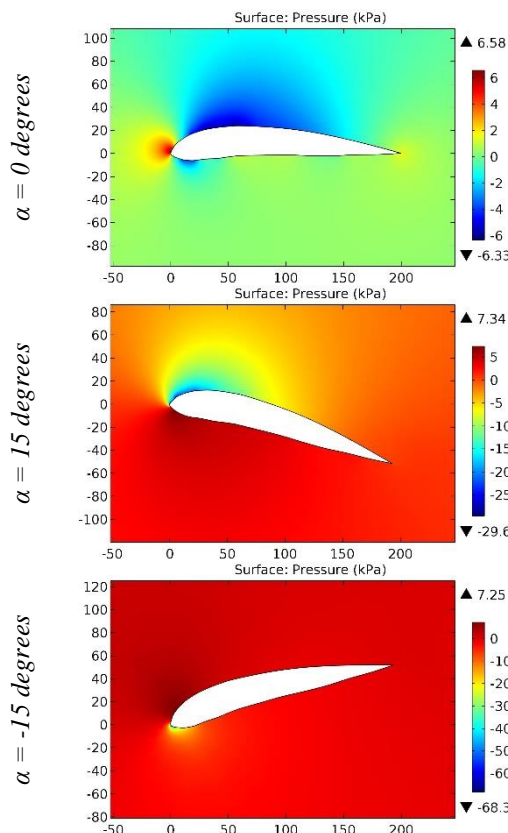


Figure 138. The pressure contours on the surfaces of the Grant X airfoil.

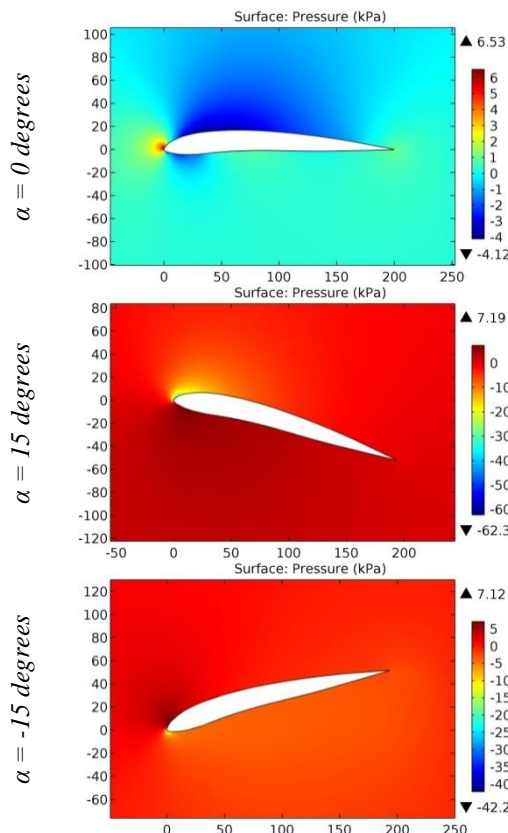
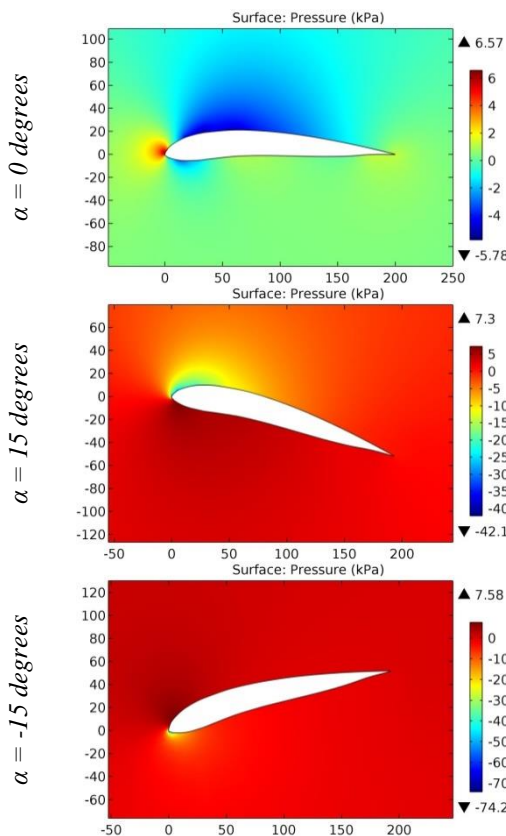
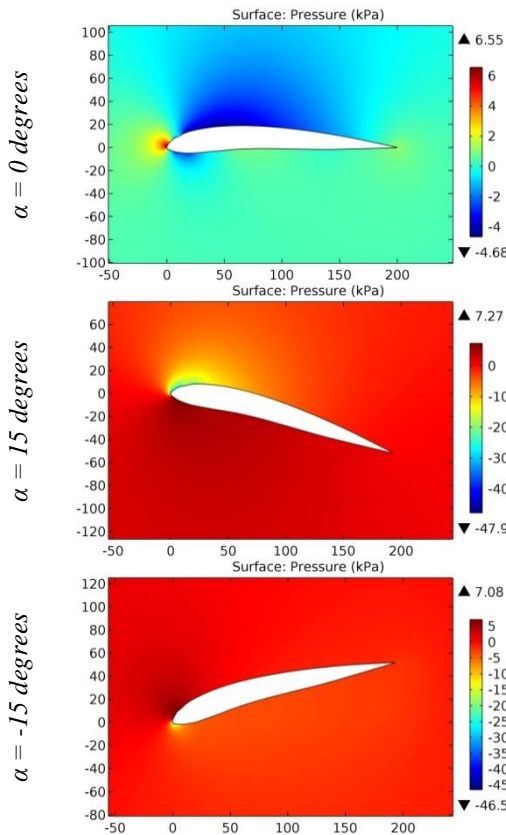


Figure 139. The pressure contours on the surfaces of the Grant X-10 airfoil.



**Figure 140.** The pressure contours on the surfaces of the Grant X-8 airfoil.



**Figure 141.** The pressure contours on the surfaces of the Grant X-9 airfoil.

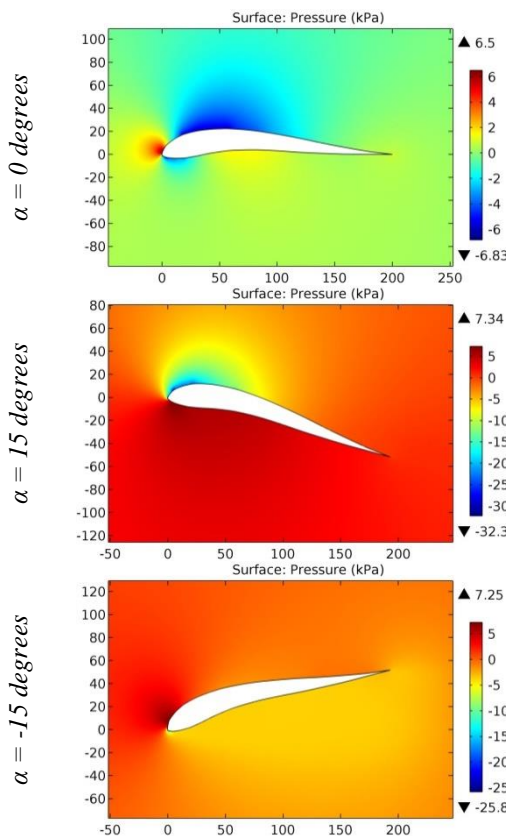


Figure 142. The pressure contours on the surfaces of the GRANTG9 airfoil.

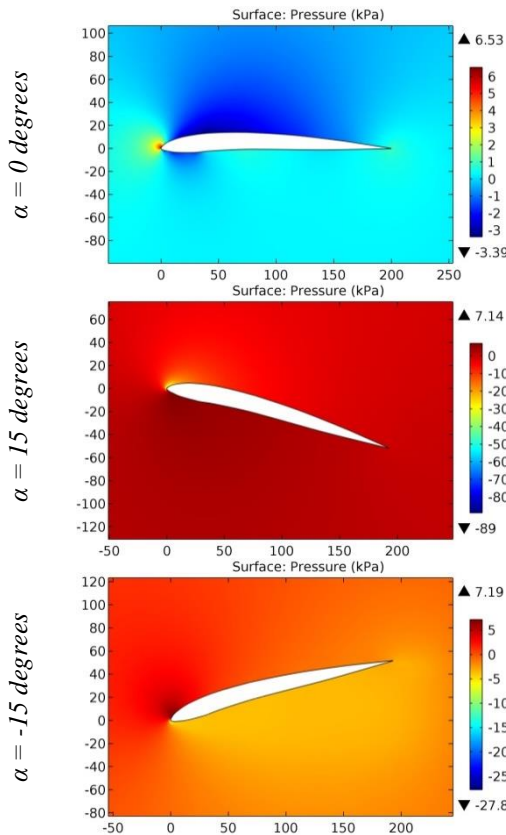
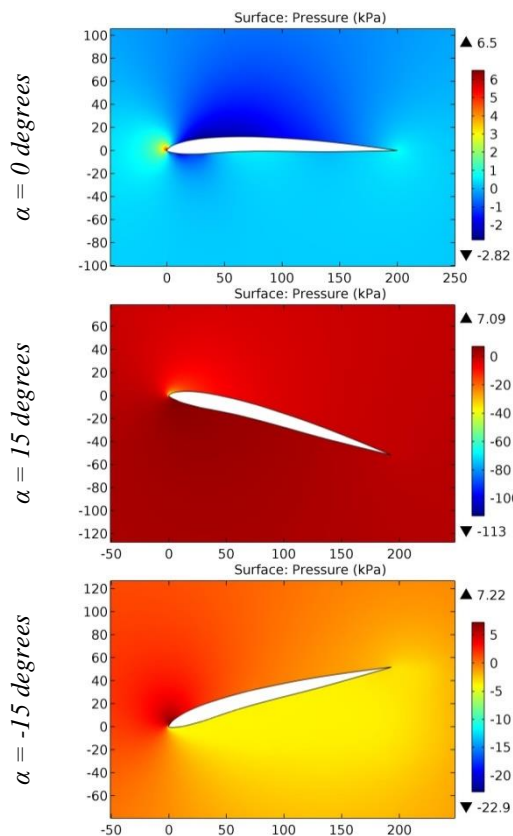
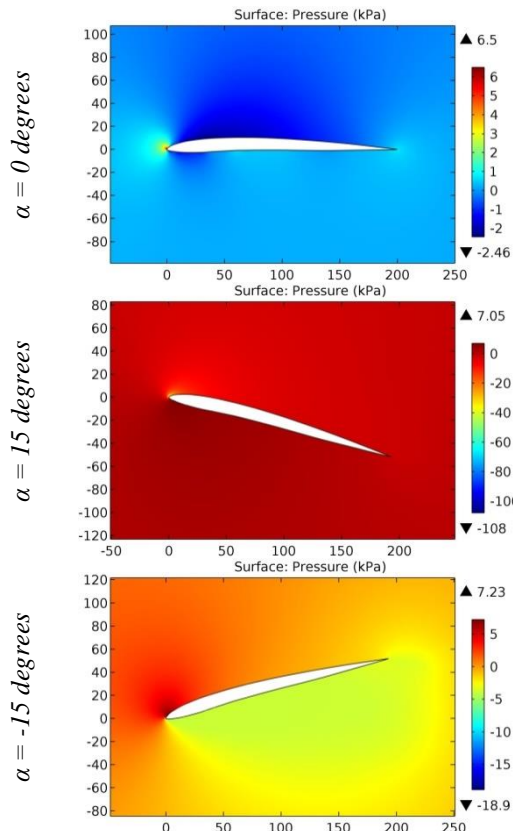


Figure 143. The pressure contours on the surfaces of the GRANTX12 airfoil.

ISRA (India)	= 6.317	SIS (USA)	= 0.912	ICV (Poland)	= 6.630
ISI (Dubai, UAE)	= 1.582	РИНЦ (Russia)	= 3.939	PIF (India)	= 1.940
GIF (Australia)	= 0.564	ESJI (KZ)	= 8.771	IBI (India)	= 4.260
JIF	= 1.500	SJIF (Morocco)	= 7.184	OAJI (USA)	= 0.350



**Figure 144.** The pressure contours on the surfaces of the GRANTX14 airfoil.



**Figure 145.** The pressure contours on the surfaces of the GRANTX16 airfoil.

ISRA (India)	= 6.317	SIS (USA)	= 0.912	ICV (Poland)	= 6.630
ISI (Dubai, UAE)	= 1.582	РИНЦ (Russia)	= 3.939	PIF (India)	= 1.940
GIF (Australia)	= 0.564	ESJI (KZ)	= 8.771	IBI (India)	= 4.260
JIF	= 1.500	SJIF (Morocco)	= 7.184	OAJI (USA)	= 0.350

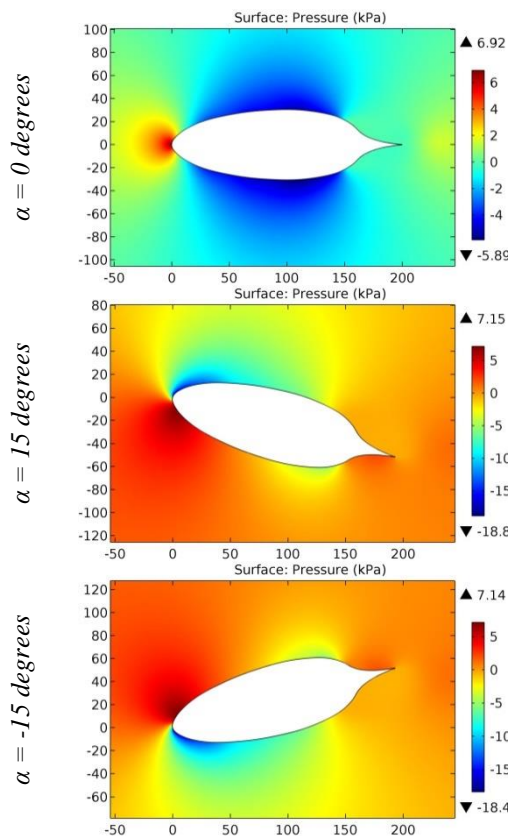


**Figure 146.** The pressure contours on the surfaces of the Griffith 30% thick symmetrical suction airfoil.

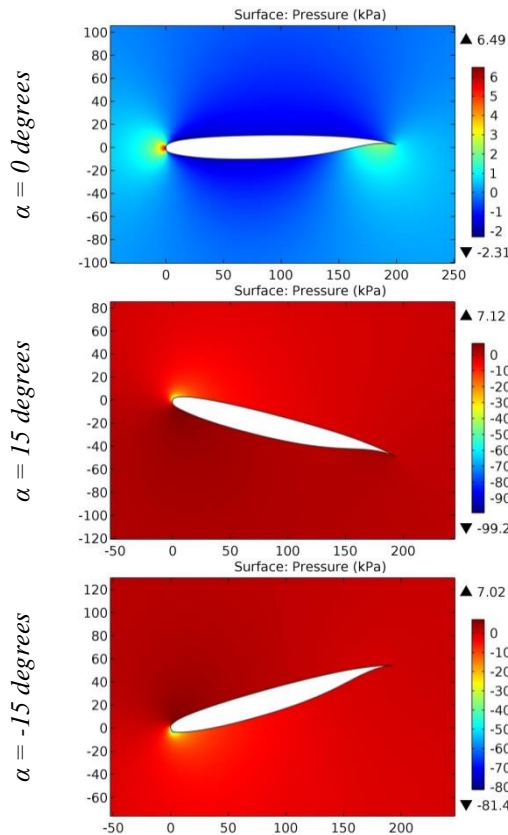


**Figure 147.** The pressure contours on the surfaces of the GRUMMAN K-2 airfoil.

<b>ISRA (India)</b>	= <b>6.317</b>	<b>SIS (USA)</b>	= <b>0.912</b>	<b>ICV (Poland)</b>	= <b>6.630</b>
<b>ISI (Dubai, UAE)</b>	= <b>1.582</b>	<b>РИНЦ (Russia)</b>	= <b>3.939</b>	<b>PIF (India)</b>	= <b>1.940</b>
<b>GIF (Australia)</b>	= <b>0.564</b>	<b>ESJI (KZ)</b>	= <b>8.771</b>	<b>IBI (India)</b>	= <b>4.260</b>
<b>JIF</b>	= <b>1.500</b>	<b>SJIF (Morocco)</b>	= <b>7.184</b>	<b>OAJI (USA)</b>	= <b>0.350</b>

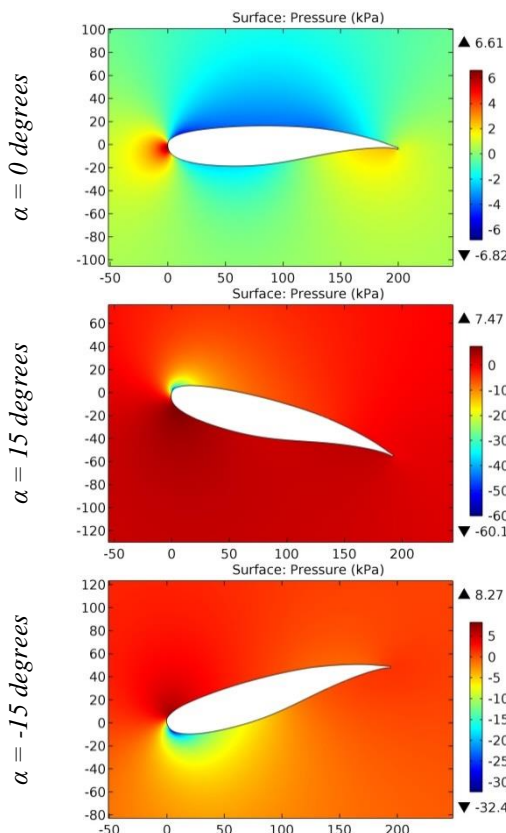


**Figure 148. The pressure contours on the surfaces of the GRUMMAN K-3 airfoil.**

The geometric shape of the GOE 531 airfoil makes it possible to reduce the drag on the leading edge during maneuvers compared to the horizontal flight of the airplane.

Comparing the GOE602 and GOE602M airfoils, it can be noted that in the first case, the drag is less due to the smoothed convex bottom surface.

The groove on the bottom surface of the GOE 802 A and GOE 802 B airfoils slightly reduces pressure on the surfaces, compared to the GOE 802 airfoil, which is produced without the groove.

The GOE 5K and GOE 9K supersonic airfoils at the negative and zero angles of attack ensure the formation of negative pressures of the small values on the surfaces.

The maximum increase in pressure on the leading edge occurs at the angle of attack of 15 degrees for the following airfoils: GOE 529, GOE 531, GOE 532, GOE 54, GOE 55, GOE 559, GOE 561, GOE 562, GOE 564, GOE 565, GOE 566, GOE 57, GOE 571, GOE 572, GOE 573, GOE 574, GOE 585, GOE 587, GOE 590, GOE 591, GOE 592, GOE 595, GOE 596, GOE 5K, GOE 602, GOE 602 MOD, GOE 610 B, GOE 610-B MOD, GOE 611, GOE 613, GOE 622, GOE 63, GOE 630, GOE 670, GOE 673, GOE 682, GOE 6K, GOE 711, GOE 744, GOE 746,

GOE 79 (PFALZ 11), GOE 795, GOE 795 smoothed, GOE 7K, GOE 801 (MVA 301), GOE 802, GOE 802 A, GOE 802 B, GOE 803 (HACKLINGER), GOE 804 (EA 8), GOE 81, GOE 8K, GOE 92, GOE 9K, Goldberg G 5, Goldberg Zipper, GOLDBRG6, GOO620M, Gottingen 6K, Gottingen 7K, Gottingen 8K, Grant G10, Grant X-10, Grant X-9, GRANTG9, GRANTX12, GRANTX14, GRANTX16, Griffith 30% thick symmetrical suction airfoil, GRUMMAN K-2 and GRUMMAN K-3. The maximum increase in pressure on the leading edge occurs at the angle of attack of -15 degrees for the other airfoils.

### Conclusion

The convex-concave airfoils have the greater lift, since the difference between positive and negative pressures on the upper and lower surfaces is several times greater than that of the airfoils with the other geometric shapes in the cross section. On the other hand, the high drag on the leading edge is not created on these airfoils during flight of the airplane.

The GOE 804 (EA 8) airfoil has the distinctive aerodynamic characteristics. The pressures values during climb and descent of the airplane change by almost 10 times.

## Impact Factor:

<b>ISRA (India)</b>	<b>= 6.317</b>	<b>SIS (USA)</b>	<b>= 0.912</b>	<b>ICV (Poland)</b>	<b>= 6.630</b>
<b>ISI (Dubai, UAE)</b>	<b>= 1.582</b>	<b>РИНЦ (Russia)</b>	<b>= 3.939</b>	<b>PIF (India)</b>	<b>= 1.940</b>
<b>GIF (Australia)</b>	<b>= 0.564</b>	<b>ESJI (KZ)</b>	<b>= 8.771</b>	<b>IBI (India)</b>	<b>= 4.260</b>
<b>JIF</b>	<b>= 1.500</b>	<b>SJIF (Morocco)</b>	<b>= 7.184</b>	<b>OAJI (USA)</b>	<b>= 0.350</b>

## References:

1. Anderson, J. D. (2010). Fundamentals of Aerodynamics. *McGraw-Hill, Fifth edition.*
2. Shevell, R. S. (1989). Fundamentals of Flight. *Prentice Hall, Second edition.*
3. Houghton, E. L., & Carpenter, P. W. (2003). Aerodynamics for Engineering Students. *Fifth edition, Elsevier.*
4. Lan, E. C. T., & Roskam, J. (2003). Airplane Aerodynamics and Performance. *DAR Corp.*
5. Sadraey, M. (2009). Aircraft Performance Analysis. *VDM Verlag Dr. Müller.*
6. Anderson, J. D. (1999). Aircraft Performance and Design. *McGraw-Hill.*
7. Roskam, J. (2007). Airplane Flight Dynamics and Automatic Flight Control, Part I. *DAR Corp.*
8. Etkin, B., & Reid, L. D. (1996). Dynamics of Flight, Stability and Control. *Third Edition, Wiley.*
9. Stevens, B. L., & Lewis, F. L. (2003). Aircraft Control and Simulation. *Second Edition, Wiley.*
10. Chemezov, D., et al. (2021). Pressure distribution on the surfaces of the NACA 0012 airfoil under conditions of changing the angle of attack. *ISJ Theoretical & Applied Science, 09 (101)*, 601-606.
11. Chemezov, D., et al. (2021). Stressed state of surfaces of the NACA 0012 airfoil at high angles of attack. *ISJ Theoretical & Applied Science, 10 (102)*, 601-604.
12. Chemezov, D., et al. (2021). Reference data of pressure distribution on the surfaces of airfoils having the names beginning with the letter A (the first part). *ISJ Theoretical & Applied Science, 10 (102)*, 943-958.
13. Chemezov, D., et al. (2021). Reference data of pressure distribution on the surfaces of airfoils having the names beginning with the letter A (the second part). *ISJ Theoretical & Applied Science, 11 (103)*, 656-675.
14. Chemezov, D., et al. (2021). Reference data of pressure distribution on the surfaces of airfoils having the names beginning with the letter B. *ISJ Theoretical & Applied Science, 11 (103)*, 1001-1076.
15. Chemezov, D., et al. (2021). Reference data of pressure distribution on the surfaces of airfoils having the names beginning with the letter C. *ISJ Theoretical & Applied Science, 12 (104)*, 814-844.
16. Chemezov, D., et al. (2021). Reference data of pressure distribution on the surfaces of airfoils having the names beginning with the letter D. *ISJ Theoretical & Applied Science, 12 (104)*, 1244-1274.
17. Chemezov, D., et al. (2022). Reference data of pressure distribution on the surfaces of airfoils (hydrofoils) having the names beginning with the letter E (the first part). *ISJ Theoretical & Applied Science, 01 (105)*, 501-569.
18. Chemezov, D., et al. (2022). Reference data of pressure distribution on the surfaces of airfoils (hydrofoils) having the names beginning with the letter E (the second part). *ISJ Theoretical & Applied Science, 01 (105)*, 601-671.
19. Chemezov, D., et al. (2022). Reference data of pressure distribution on the surfaces of airfoils having the names beginning with the letter F. *ISJ Theoretical & Applied Science, 02 (106)*, 101-135.
20. Chemezov, D., et al. (2022). Reference data of pressure distribution on the surfaces of airfoils having the names beginning with the letter G (the first part). *ISJ Theoretical & Applied Science, 03 (107)*, 701-784.
21. Chemezov, D., et al. (2022). Reference data of pressure distribution on the surfaces of airfoils having the names beginning with the letter G (the second part). *ISJ Theoretical & Applied Science, 03 (107)*, 901-984.